Network-Secure Consumer Bidding in Energy and Reserve Markets

Ahmad Attarha
January 2022

A thesis submitted for the degree of
Doctor of Philosophy of
The Australian National University

Declaration

Except where otherwise indicated, this thesis is my own original work.

Ahmad Attarha
August 25, 2022

Acknowledgments

The support and efforts of my supervisors, colleagues, friends and family made the completion of this PhD a possibility. Here, I would like to publicly thank and acknowledge them for all their kind support.

First and foremost, I would like to thank my primary supervisor Dr. Paul Scott. You provided me with invaluable guidance throughout this journey. I am truly grateful for all the time you invested, your patience, understanding and support during these years. It is a privilege to work with you. My next acknowledgement goes to Prof. Sylvie Thiébaux, the chair of my supervisory panel. Your support has always been encouraging and our discussions have helped me become a better researcher. I am truly grateful for all your amazing guidance. I would also thank my advisory supervisor Prof. Lachlan Blackhall for his technical knowledge and valuable suggestions.

Many thanks to Dr. José Iria for all the technical discussions and his interesting suggestions. I would also like to thank some of my friends and colleagues at the ANU, particularly: Mahdi Noori, Masoume Mahmoodi, Mark Burgess, James Russell, Dan Gordon, Yi Yung, Jim de Groot, Ian Shillito, Mina Mohammadian, Wilhiam de Carvalho, Nicholas Kuo, and Mukesh Tiwari.

Finally, I thank my mom and dad who taught me to follow my dreams and never give up.

Abstract

Electricity systems are undergoing a fundamental transformation from centralised generation to a distributed paradigm in which electricity is produced at a smaller scale by numerous distributed energy resources (DER). The replacement of centralised facilities by DER brings economic and environmental benefits. However, it also makes it challenging for the market operator to secure the system with sufficient frequency response in the absence of centralised facilities – dominant providers of such services – in the electricity markets.

Fortunately, the aggregate response of DER can fulfil systems' need for frequency reserve services. However, DER are operated within distribution networks whose technical limits are not accounted for within the wholesale market. This raises the question of how DER can participate in the energy and reserve markets while respecting the distribution network's constraints. To ensure network constraints, consumer and grid constraints / preferences should be modelled simultaneously within a large-scale optimisation problem. Yet, the need for scale, involvement of multiple stakeholders (grid operator and consumers) who possibly have conflicting interests, privacy concerns, and the uncertainty around consumer data and market prices make this extra challenging.

This thesis contributes to addressing these challenges by developing network-secure consumer bids that account for the distributed nature of the problem, consumer data and market price uncertainties. Note that when bidding in the market, consumers, and thus, the network operating point is not clear, as it depends on the dispatch in the energy market and whether a contingency occurs. Therefore, we ensure grid feasibility for operating envelopes that include any possible operating points of consumers.

We first use the alternating direction method of multipliers (ADMM) to enable network-secure consumer biding. Using ADMM, consumers optimise for their energy and reserve bids and communicate with the grid their required operating envelopes. The network then solves OPFs to see whether any constraint is violated and updates the ADMM parameters. Such communications continue until converging on a consensus solution. We learnt that our ADMM-based solution approach is able to maintain grid's constraints as long as consumers commit to their envelopes – a requirement that might not hold

due to uncertainty. Thus, we further improve our bidding approach by modelling uncertainties around solar PV and demand, using a piecewise affinely adjustable robust constrained optimisation (PWA-ARCO). We observed that not only is PWA-ARCO able to compensate for live uncertainty variabilities, but also it can improve the reliability of consumer bids, especially in reserve markets. We also extend our initial envelopes by enabling consumers to provide reactive power support for the grid.

We next enable consumers to bid (possibly) their entire flexibility by developing price-sensitive offers. Such offers include a bid curve chunked into several capacity bands, each being submitted at a different price. We identified that when the prices cannot be forecast accurately, the price-sensitive bidding approach can improve consumer benefit. To ensure network feasibility, instead of an iterative ADMM approach, we propose a more scalable one-shot policy in which the network curtails the part of the consumer bid that violates the network. Compared to ADMM, the one-shot policy significantly reduced the computation complexity at the cost of a slightly less optimum outcome.

Overall, this thesis investigates different techniques to provide network-secure energy and reserve market services out of residential DER. It expands the knowledge in the area of consumer bidding solutions, adjustable robust optimisation, and distributed optimisation. It also discovers a range of interesting future research topics, including distribution network modelling and uncertainty characterisation.

Nomenclature

Abbreviation

ADMM	Alternating direction method of multipliers
AEMO	Australian Energy Market Operator
ARCO	Adjustable robust constraint optimisation
C&CG	Column and constraint generation
CAISO	California independent system operator
CB	Capacitor bank
COP	Current operating plan
CPP	Connection point power
DER	Distributed energy resources
DLMP	Distribution locational marginal price
DRUC	Day-ahead reliability unit commitment
DSO	Distribution system operators
EMS	Energy management system
ERCOT	Electricity Reliability Council of Texas
EV	Electric vehicle
FCAS	Frequency Control Ancillary Service
IFM	Integrated forward market
ISO	Independent system operator
LMP	Locational marginal price
LP	Linear programming

MCP	Market clearing price
MILP	Mixed integer linear programming
MPC	Model predictive control
MPM	Market power mitigation
NAC	Network-aware coordination
NEM	Australian National Electricity Market
NEMDE	Australian National Electricity Market Dispatch Engine
OI	Operating interval
PDF	Probability distribution function
PWA	Piecewise affine
PWA-ARCO	Piecewsie affinely adjustable robust constraint optimisation
RMR	Reliability must-run requirement
RUC	Residual unit commitment
SCED	Security-constrained economic dispatch
TD	Trading day
ToU	Time-of-use
TSO	Transmission system operators
UFLS	Under frequency load shedding
VPP	Virtual power plant
VSC	Voltage source converters

Contents

Chapter 1

Introduction

Economic opportunities and environmental benefits have led to a significant uptake of distributed energy resources (DER) in distribution networks. In Australia, as of 31 January 2022, more than 3 million rooftop solar PV systems have been installed (nearly 30% of all homes in Australia)[1]. Battery storage integration has followed a similar increasing pattern. Currently, there are 140,000 home battery systems installed in Australia, totalling 2,657MWh [2]. DER embrace is a global phenomenon; almost all countries are undergoing the same transition. Figure 1.1 shows the installed PV capacity per capita for the top 12 solar-installer countries in 2019[3].

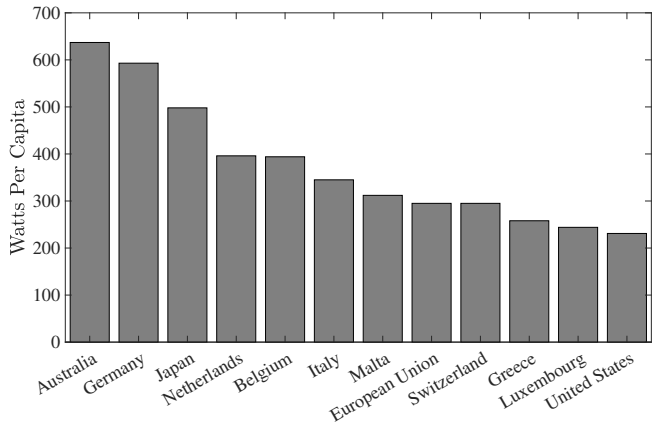

Figure 1.1: Installed PV capacity per capita

While the integration of DER is generally good news, it fundamentally changes the structure of our power systems. Large-scale transmission-level

[1] https://www.energy.gov.au/households/solar-pv-and-batteries

[2] https://electricalconnection.com.au/record-breaking-year-for-battery-energy-storage-in-australia/

[3] https://en.wikipedia.org/wiki/Solar_power_by_country#cite_note-iea-pvps-snapshot-2020-20

generation is being replaced by numerous small-scale distributed generations in the hands of consumers Iweh et al. [2021]; Haghifam et al. [2021]. Such a decentralisation makes it harder to meet power system reliability requirements, in particular, maintaining the frequency of our power system. The reason is that to maintain the frequency, system operators need to balance out supply and demand continuously – a task that becomes difficult to accomplish as the power generated / utilised by consumers is highly volatile and unpredictable. If the generation is more / less than demand, power system frequency rises / drops to be outside its acceptable range (50Hz $\pm$ 0.15 in Australia, China, Europe and 60Hz $\pm$ 0.3 in Canada, the USA Neidhöfer [2011]). When the frequency goes too far outside the range, generators and large motors will start disconnecting to protect themselves against damage. These disconnections can create more imbalance between demand and supply in the system, further affecting frequency, resulting in a full or partial blackout Yan et al. [2018].

To compensate for the mismatches between supply and demand, system operators secure the power system with enough reserves, which are activated in live operation to keep the frequency within the acceptable range. Prior to DER uptake, large-scale power stations were the main providers of frequency response services. However, DER embrace is making these power stations redundant Molina-Garcia et al. [2010]. Studies by Energy Networks Australia and the Australian Energy Market Operator (AEMO) AEMO and ENA [2018] suggest that rooftop PV will be sufficient to cover all load on low-demand days in some regions of Australia by early 2025. This happened for the first time much earlier than anticipated. On Sunday, October 11, 2020, solar power alone met 100% of demand for just over an hour in South Australia[4]. Therefore, if the system operators only count on grid-scale equipment for reserve services, they must either curtail a significant proportion of PV power to force enough conventional generators into these operating intervals – a sub-optimal solution which adds to the operation cost of our power system; or install new grid-scale equipment for the job – a sub-optimal solution which adds to the planning cost of power systems.

Fortunately, consumer-owned DER are quick-responding technologies, and their aggregate response can fulfil a large portion of the required frequency response. Unsurprisingly, the capability to provide reserve services will explode with the rise of electric vehicles. For example, 100% of cars to be sold in Norway are forecast to be electric by 2025 [5]. Even if connected with 3kW slow chargers, this still represents $\approx$ 6 GW capacity (almost one-fourth of peak load). Therefore, we believe consumer flexibility should be harnessed by

[4] https://reneweconomy.com.au/solar-meets-100-per-cent-of-south-australia-demand-for-first-time-78279/

[5] https://www.reuters.com/business/autos-transportation/electric-cars-take-two-thirds-norway-car-market-led-by-tesla-2022-01-03/

enabling consumer-owned DER to be bid into the wholesale markets. Given DER capability in providing reserves services alongside the emerging need of power systems for alternative frequency response providers, the focus of this thesis is to answer the following key question:

How can residential DER, installed and operated in distribution networks, participate in the wholesale energy and reserve markets?

In this thesis, we answer the above question from a steady-state perspective – the dynamic response of DER to frequency disturbance has been widely studied, e.g., in Amin et al. [2019], and is not the focus of this thesis. Without loss of generality, we also assume that a third party, e.g., an aggregator, controls consumer-owned DER to bid at scale or deliver market services based on market clearing outcome. Given these, we identified the following five challenges (C1 to C5) that we must address to provide a feasible answer to our key question:

C1 Computational Complexity: providing market services from thousands of DER rather than large-scale power stations is a challenging task. From the modelling perspective, each DER will translate into some variables and constraints. Thus, we end up with a large-scale optimisation problem that includes millions of variables and constraints Iria et al. [2020]. Solving such an optimisation problem to its (local-) optimum within the operation time frame is difficult.

C2 Distribution Network: our solution should be within network technical boundaries Mousavi and Wu [2021a]; Bahramara et al. [2017]. This is challenging from two angles: firstly, DER are mainly connected to / operated within distribution networks that are not included in the market clearing process. Secondly, aggregators do not have any information about network technical constraints Scott et al. [2019]. This can endanger power system security as the market operator will count on bids that cannot be delivered due to network shortcomings.

In addition, the bids to contingency reserves markets are capacities. Thus, the activation of these bids depends on whether or not a contingency occurs. If a contingency does occur, the DER response can still differ depending on the significance of the contingency. Thus, the operating point of the system is not only unknown but also highly unpredictable. This changes the conventional operation of distribution networks where all the setpoints are obtained, for a pre-defined operating point, based on an optimisation problem that determines DER operation.

C3 Multiple Stakeholders: DER are owned and operated by consumers with different constraints and preferences who might also have privacy con-

cerns Ross and Mathieu [2020]. Similarly, the network data is private to the distribution system operators (DSOs) Milford and Krause [2021]. Plus, DSOs work towards some operating targets which might conflict with those of consumers / aggregators. Obtaining bids that satisfy consumers and network technical limits whilst preserving the privacy of all parties when there is conflicting interest, adds to the complexity of this already challenging problem.

C4 Household Uncertainty: data uncertainty such as those associated with PV power output and residential demand can negatively affect consumers and the network Mousavi and Wu [2021b]. Consumer uncertainty can push the network out of its safe operating limits. The reason is that DER response to market prices creates synchronisations that drive the distribution network towards its limits. Thus, even a small change in the system (which can happen due to uncertainty) can violate the network limits, while modelling the uncertainty of numerous consumers is remarkably challenging. On the other hand, aggregators might not be able to deliver their energy and/or reserve bids due to uncertain realisations that are different from their forecasts. The market penalises aggregators for not delivering on their bids and even might expel them from the reserve markets where most of the benefit lies AEMO [2020].

C5 Market Price Uncertainty: aggregators decisions in electricity markets are directly influenced by market prices and not tariffs. Unlike tariffs, electricity prices are not known in advance of the operating interval, and aggregators need to use a price forecast to calculate their offers. Forecast errors can significantly affect aggregator benefit or even might lead to economic losses Gao et al. [2017a]; Sharma et al. [2017]; Ruibal and Mazumdar [2008].

In this thesis, we provide a complete answer to our key question while addressing the identified challenges. In the following, we explain our contributions.

1.1 Contribution

Sections 1.1.1, 1.1.2 and 1.1.3 summarise our contributions, which are detailed in Chapters 3, 4 and 5, respectively. Our first contribution 1.1.1 focuses on the first three challenges (C1 – C3). Contribution 1.1.2 builds on our first contribution 1.1.1 by additionally addressing the fourth challenge (C4), i.e., household uncertainty. Our third contribution 1.1.3 focuses on the last challenge (C5), i.e., market price uncertainty.

1.1.1 Obtaining Operating Envelopes Using Distributed Optimisation

Here, we focus on obtaining optimum bidding decisions for multiple markets coordinated with the grid. This ensures that DER dispatch in the energy market, together with any raise or lower reserve activation, is within the distribution network borders. Note that the grid capacity at each time depends on the combination of actions of all consumers Scott et al. [2016]. Therefore, such coordination is achieved by solving a large-scale optimisation problem that includes all consumers and network constraints. Privacy concerns and potentially conflicting interests of consumers and the grid make this problem extra difficult Wu et al. [2016].

To meet the above challenges, we propose a distributed approach based on the alternating direction method of multipliers (ADMM) Boyd et al. [2011] that decomposes the large-scale optimisation problem into pieces, each being solved separately while negotiating for network access. Not only does this make the coordination problem computationally accessible (i.e., addressing C1), but also it can preserve privacy, as each party solves their problem locally using their private data (i.e., addressing C3). Note that our approach also takes the interdependencies between multiple markets into account and ensures that any final operating point is within network boundaries Blackhall [2020]. Since such a final operating point is not known prior to real-time operation, when we solve the optimisation problem, we propose to solve the problem for an operating envelope rather than a single operating point. In this context, an operating envelope is an interval that includes any possible consumer operating point in response to the dispatch in the energy market plus any raise or lower reserve activation. In other words, we aim to ensure the grid feasibility for any possible outcome for consumers rather than a single point (i.e., addressing C2).

We also loosely address C4 (consumers' data uncertainty) by frequently running our approach, close to real-time, within a model predictive control (MPC) framework. This enables us to feed our optimisation problem with the latest uncertainty information and obtain more accurate results. We rigorously focus on C4 in our next contribution.

It is worth mentioning that our approach here is closely related to the literature stream in which distribution locational marginal prices (DLMPs) are used to obtain DER operation, in particular, network-aware coordination (NAC) Scott et al. [2016]. We provide a review of these approaches in Chapter 2. In summary, they often have a well-defined operating point to optimise over, e.g., defined by time-of-use (ToU) tariffs as in NAC. However, when it comes to bidding into the market, we do not know ahead of time what offers the market will accept or, in live operation, how frequency will fluctuate, requiring a response. Therefore, we work with operating envelopes rather than negotiating for one operating point, e.g., as in NAC.

The contribution of this section can be summarised as follows:

1. A distributed bidding approach that obtains the optimum share of DER in energy and reserve markets while being coordinated with the distribution network. Our approach ensures network's feasibility for an operating envelope that includes any possible DER outcome in response to energy dispatch and reserve activation.

1.1.2 Modelling Consumer Uncertainty and Enabling Network Support

In the previous section, we neglected data uncertainty, yet in practice, both solar PV and residential demand can change significantly in live operation. This could have two main drawbacks as follows:

- Consumers might not be able to commit to their operating envelopes due to uncertainty realisations different from the forecast used to obtain the envelopes. Deviations from the negotiated operating envelopes can violate the distribution network constraints Attarha et al. [2018a,c].
- The bids accepted in the electricity market can be different from what is delivered to the market. In most electricity markets, including the Australian National Electricity Market (NEM), participants can be significantly penalised for not delivering on their bids AEMO [2020].

Thus, here we go above an MPC implementation and rigorously model uncertainty. To do so, we extend our optimisation problem with controllers that enable consumers to honour their market commitments while sticking to their operating envelopes for any uncertain realisation within a polyhedral uncertainty set. We design our controllers in the context of adjustable robust constraint optimisation (ARCO) Ben-Tal et al. [2004]. Unlike the conventional ARCO in which the controller responses are limited to an affine function, we enable a more flexible response by using piecewise affine (PWA) functions. Unlike affinely ARCO, our PWA-ARCO enables a better response for uncertainty realisations away from the worst cases within the uncertainty set. During the distributed (ADMM-based) optimisation procedure, we optimise to obtain network-secure bids (similarly to Section 1.1.1) as well as parameters of our piecewise controllers. In live operation, when the uncertain parameters are revealed, these piecewise affine functions are enacted to keep the connection point power within the operating envelopes and honour the bids to the electricity market (i.e., addressing C4).

In our experiments of Section 1.1.1, we noticed that voltages are the most limiting factors in the network sub-problem Jabr [2019]; RA et al. [2022]; Abadi et al. [2020]. In other words, the network could allow greater throughput if the voltages are improved. Reactive power has the ability to improve the

voltage profile. In fact, for the same reason, capacitor banks (CBs) and voltage source converters (VSCs) Kasari and Bhattacharjee [2020] are commonly used in power systems. Similarly to CBs and VSCs, DER inverters can provide reactive power support for the network Zhu and Li [2016]; Mahmoodi et al. [2022]. Plus, unlike capacitor banks, DER can rapidly change their reactive power, making them suitable for real-time control De Carvalho et al. [2022]. This motivated us to design a piecewise affine P-Q controller for consumers to enable reactive power network support. The reactive power support could open up network capacity as it improves voltage profiles. Interestingly, we noticed that the reactive power support could also improve the convergence of our ADMM approach. This is because the reactive power support reduces the network disagreements with the consumers, so, we could converge on a consensus solution within fewer iterations.

In summary, the contributions of this section are:

1. Proposing a piecewise affinely ARCO consumer bidding approach which is less conservative than conventional affinely ARCO, leads to a higher value use of DER, and increases the reliability of DER bids.

2. Proposing a Q-P controller to enable consumers to negotiate their reactive power support with the grid. This increases the network throughput and, as we show empirically, can improve ADMM convergence.

1.1.3 Price-Sensitive Bidding Approach

This contribution is to take market price uncertainty, i.e., C5, into account. Note that so far, we assumed that the wholesale market price is constant, and thus, we decided on what dispatch aggregators wanted in advance and submitted bids that were accepted irrespective of the market-clearing price. This is achieved by submitting the generation and demand bids at the market floor and cap prices, respectively. Therefore, unless the market reaches its floor or cap price, these bids are fully dispatched regardless of the market-clearing price (MCP) Zhao et al. [2015]. Hence, we call them *price-insensitive* bid. However, the market price is volatile and can vary significantly from the forecast leading to economic loss for price-insensitive bidders.

To overcome the above issue, inspired by conventional generating units, we propose a *price-sensitive* bidding approach. Here consumers obtain flexible bids, consisting of several capacity bands across their feasible region at different prices. Similarly to a conventional generating unit, the final dispatch of such bids depends on the market clearing price, bringing the name "price-sensitive" to our approach. Price-sensitive bids allow consumers to fully exploit their DER capabilities and hedge the price uncertainty effect (i.e., addressing C5). Moreover, they provide more flexibility for the market operator that can be used to dispatch the whole power system more efficiently. The

reason is that, unlike price-insensitive bidding, the market is not constrained to dispatch DER at a predetermined operating point.

Although more efficient, bidding the available operating range of DER through different bid bands, rather than just a single price-insensitive bid band, generates new challenges. The main challenge is to obtain a feasible bid region that reflects the interdependencies between energy and reserve bids, as well as obtaining representative prices for different bid bands, while DER mainly have zero marginal cost. In addition, similarly to price-insensitive bids, we need to ensure network security for any bid band combination that can reach the market. Note that ensuring network limits via a distributed approach, e.g., ADMM as in sections 1.1.1 and 1.1.2, requires solving a more complicated problem at every iteration as consumers need to obtain multiple bid bands and prices. Therefore, here we opt for a simpler framework that, in terms of communication and computation, is equivalent to one iteration of the ADMM approach. In this approach, rather than an iterative procedure, the DSO curtails the part of the bids that violate the network constraints in one go. This reduces the computational efforts significantly while marginally increasing the operation cost. In our experiments, we were able to reduce the computation cost 166 times at the cost of a 2.5% reduction in consumer benefit.

To focus on different aspects of our price-sensitive bidding approach, we do not model consumer uncertainty, i.e., C4, in this section and only count on an MPC implementation similarly to 1.1.1 to loosely take such uncertainties into account. However, our piecewise affine controller in Section 1.1.2 is generally developed and could be incorporated into the consumer subproblem of the price-sensitive approach. We leave the investigation of such an extension to future work.

The contribution of this section can be summarised as follows:

1. A novel price-sensitive bidding approach for energy and reserve markets, which more accurately captures the flexibility and value of DER and enables DER dispatch to adjust to the uncertain realisation of market prices.

2. A new network optimisation layer that jointly conforms flexible energy and reserve bids within distribution network limits while encouraging competition between aggregators. This is done prior to bids reaching the market to avoid disruption to existing market structures, enabling the approach to be more readily taken up.

1.2 Summary

To summarise, the core research question in this thesis is how consumers can participate in the energy and reserve markets to harness their DER's potential while respecting the grid's technical limits. In reply to this question, we contribute to the knowledge in the following ways:

1. We develop two different energy management systems (EMSs), both of which co-optimise consumers in energy, raise and lower reserve markets and properly model the interdependencies between participation in each market. However, they differ in the type of bids they generate. One of them generates a single bid band according to the energy and reserve market price forecasts. The obtained bids are then submitted to the market at either market cap or floor prices. The other approach generates multiple capacity bands and prices to be submitted to the each market.

2. We study the effect of providing reactive power network support in both our bidding approaches. These reactive power supports, generated / consumed via smart inverters, can increase consumers' network access.

3. We propose a piecewise affinely adjustable robust constraint optimisation (PWA-ARCO) approach to model uncertainty around solar PV power and residential demand. Our PWA-ARCO approach is general and thus is neither limited to a bidding problem nor restricted by the bidding policy. However, to avoid complicating our price-sensitive bidding problem, we only illustrate its effectiveness in our price-insensitive bidding approach.

4. We investigate two different methods to ensure network feasibility. The first obtains network feasibility iteratively by negotiating between aggregators and the DSO using the distributed approach ADMM. While in the second one, the DSO curtails aggregator bids in one go without further negotiation or communication. We apply our ADMM-based approach to our price-insensitive approach while using the one-shot curtailment policy in our price-sensitive approach to reduce complexity.

1.3 Thesis Outline

This thesis is structured as follows:

Chapter 2 reviews the related works and provides the required background knowledge for this thesis in 6 different sections. Section 2.1 provides an overview of different electricity markets around the world. Section 2.2 reviews the related literature on the integration of DER into our power system. It more specifically focuses on market participation of DER, challenges

and the state-of-the-art solutions paving the way for market participation of consumer-owned DER. Section 2.3 provides an overview of the optimisation techniques used throughout this thesis. Section 2.4 explains the assumed communication setting between aggregators, consumers and the grid. Section 2.5 mathematically models an EMS and an OPF problem which are used in chapters 3, 4, and 5. Finally, Section 2.6 provides more details on NAC on which we build our approach in Chapter 3.

Chapter 3 introduces our price-insensitive bidding approach within dynamic operating envelopes. We develop aggregator and the DSO's subproblems separately that are linked through the ADMM approach to obtain network-secure bids.

Chapter 4 presents our PWA-ARCO solution approach to model solar PV and residential demand uncertainty. It also investigates the effect of providing reactive power network support in our bidding problem.

Chapter 5 presents our price-sensitive bidding approach. This chapter explains how we obtain the operating bid region for each consumer, how we chunk the obtained feasible region into bid bands and calculate the prices associated with each bid band. It also presents our one-shot bid curtailment approach, where we investigate two different network policies for curtailing consumers' bids. We also investigate the effect of providing reactive power support on the flexible bidding approach. Moreover, Chapter 5 provides comparisons to highlight the effectiveness of the price-insensitive bidding approach compared to the bidding approach in chapters 3 and 4; and investigates the effectiveness of our one-shot curtailment policy compared to iterative ADMM-based approaches introduced in chapters 3 and 4.

Chapter 6 concludes the findings of this thesis and discusses future developments.

Chapter 2

Background

This chapter consists of six sections which together provide the needed background material for this thesis. Section 2.1 gives an overview of electricity markets around the world and how they function. Section 2.2 provides a comprehensive review of the state-of-the-art research in the context of market participation of DER. Section 2.3 gives a summary of the optimisation techniques used throughout this thesis. Section 2.4 explains the communication setting between aggregators, consumers and the grid. Section 2.5 is allocated to DER and network modelling which will be used in chapters 3, 4 and 5. Section 2.6 provides more details on NAC on which we build our approach in Chapter 3.

2.1 Electricity Markets

An electricity market is a system that enables electricity to be sold, bought and traded. Buyers and sellers submit their bids and offer into a pool market which is being cleared by an independent entity known as the market operator.

Energy and power are two commodities traded within electricity markets. Energy is the electricity generated / consumed for a given period, measured in megawatt-hours (MWh). Power is the rate of energy transfer at any given time, measured in megawatts (MW). Power is mainly purchased to secure the power system with enough reserves. Reserves are activated to keep supply and demand equal and thus maintain the power system's nominal frequency. Reserves are part of an extended family named ancillary services. Ancillary services include any necessary assistance, such as voltage and frequency support, that enables our power system to operate within the required reliability targets.

Operators need different types of reserves to ensure security, this includes *regulation*, *spinning* and *non-spinning* reserves. Regulation reserves are continually used to compensate for minor changes in the demand / supply balance

(e.g., due to forecast error). Spinning reserve is the extra available capacity to increase / decrease the power output of generators (or loads) that are already connected to the power system. The non-spinning reserve is the extra generating capacity that is not currently connected to the system but can be brought online after a short delay Ela et al. [2011]. While spinning and non-spinning reserves are always ready to act, they are only used on the occasion of a contingency. Different markets might use different terminologies for these reserves. Figure 2.1 shows some different terminologies for reserve markets in Australia, North American Electric Reliability Corporation (NERC) and the Union for Coordination of Transmission of Electricity (UCTE).

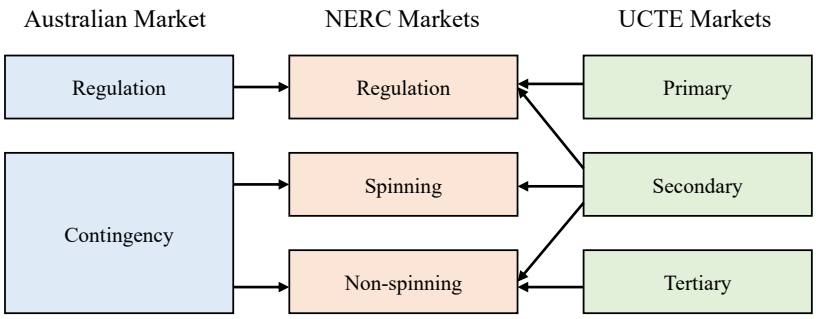

Figure 2.1: Different terminologies for reserves González et al. [2014]; Iria et al. [2019]

Participants can submit their bids at market cap / floor prices or a bid curve with different price bands. Market participants, who wish to submit their bids at either market cap or floor prices, decide in advance what dispatch they want and then submit the obtained offers to the market at either market cap (for demand offers) or floor price (for generation offers). This means that irrespective of the market-clearing price (MCP), as long as MCP does not reach its floor or cap, such offers will be accepted Arteaga and Zareipour [2019]. Hence, hereafter, we refer to these bids as *price-insensitive* bids. On the contrary, when a participant submits a bid stack at different prices, their accepted offers depend on the MCP. Thus, we call them *price-sensitive* throughout this thesis. Notice that participants can also submit their practical constraints (such as ramping or minimum-up / -downtime of the unit) alongside their bids to avoid unpractical dispatch outcomes Herrero et al. [2020]; AEMO [2020].

In this thesis, we assume that consumers are coordinated by a third party, e.g., an aggregator, to participate in the energy and reserve markets within the Australian national electricity market (NEM). However, with minor changes, our approach can be used for other electricity markets. In the following, we first provide an overview of our target market, the NEM. We then provide a

general overview of some of the electricity markets around the world and discuss the similarities and differences with the NEM to provide some intuition on how our approaches will look in different markets.

2.1.1 Australian National Electricity Market (NEM)

The NEM is a five-minute real-time market which is operated by the Australian energy market operator (AEMO). Note that there is no day-ahead market in the NEM Riesz et al. [2015]. However, to run the real-time market smoothly, AEMO asks participants to submit their pre-dispatch bids (capacity and price) the day before the trading day (TD). As shown in Figure 2.2, the bid prices stay fixed for the next day, but the bid capacity can be adjusted by the participants in each 5-minute operating interval (OI).

Under the NEM frequency standards, AEMO must ensure that following a credible contingency event, the frequency deviation remains within the contingency band (e.g., 49.5 to 50.5 Hz) and returns to the normal operating threshold (e.g., 49.85 to 50.15 Hz) within 5 minutes[1]. To do so, AEMO uses *raise* and *lower* reserve markets to trade the required reserves in every 5-minute dispatch interval. Since these reserves are used to maintain frequency, they are called frequency control ancillary service (FCAS) in the NEM.

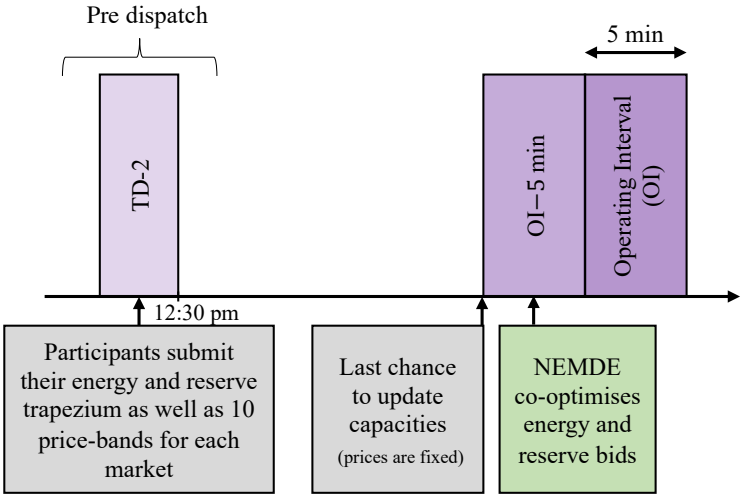

Figure 2.2: Market process in the NEM

Currently, the NEM includes 8 different FCAS markets: 2 regulation and 6 contingency FCAS markets. While the regulation FCAS includes a raise and a lower market, the contingency FCAS market is categorised into three main

[1] According to the event and / or location, contingency frequency band and the recovery time might differ AEMC [2017].

groups according to their response time: raise and lower 6-second, 60-second, and 5-minute FCAS markets Riesz et al. [2015]. In the NEM, energy and all FCAS markets are fully co-optimised on a single real-time platform known as NEMDE (national electricity market dispatch engine) [2]. NEMDE clears the Australian market every 5 minutes to obtain the energy and FCAS prices as well as the dispatch of the participants.

To bid in the NEM, participants must submit their energy-FCAS *trapezium* as well as up to 10 price bands for energy and each FCAS market. An example of an energy-and-FCAS trapezium submitted for a generator is shown in Figure 2.3. In this example, the raise FCAS capacity is first limited by the ramp rate of the unit (the flat top section); moving towards the maximum output of the unit on the energy axis (i.e., P^{max}), the capacity of the generating unit becomes more constraining than the ramp rate (i.e., $P + F \leq P^{max}$)[3].

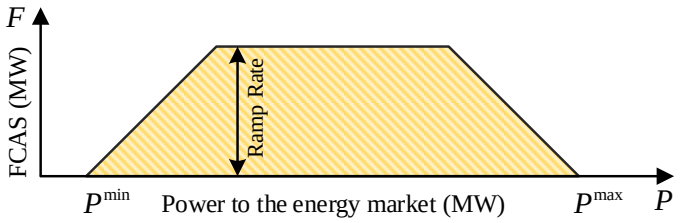

Figure 2.3: Energy-FCAS trapezium for a generating unit.

The NEM enables participants to break down their available capacity and submit them at up to 10 different prices (known as *price bands*). To participate in the market, a non-zero capacity should be allocated to at least one of these price bands. Given the capacities and price bands, NEMDE can dispatch the participants at any point of their trapezium (highlighted in yellow in Figure 2.3) to obtain the least-cost operating point. Co-optimising over participants' feasible regions helps AEMO to find the lowest overall operating costs.

Having NEM cleared, FCAS providers get paid their accepted bids regardless of whether or not a contingency actually occurs. In the case that a contingency does occur, they must respond up to their market-accepted capacity to correct the frequency deviation.

[2] https://aemo.com.au/en/energy-systems/market-it-systems/electricity-system-guides/nemde-queue-service

[3] https://www.aemo.com.au/Electricity/National-Electricity-Market-NEM/Security-and-reliability/-/media/2C771C82C8054929B16E4545216ACE03.ashx

2.1.2 California Independent System Operator (ISO)

The California ISO (CAISO) is responsible for the reliable operation of the high voltage grid in California. CAISO includes a day-ahead and a real-time market. Figure 2.4 shows how the CAISO works. The day-ahead market opens 7 days prior and closes at 10 am the day before the trading day (TD). It includes 3 sequential processes. First, a market power mitigation (MPM) test is performed. The bids that fail the test are revised to predetermined limits. Next, integrated forward market (IFM) co-optimises the energy and reserve market bids using a full network model. This obtains 100% of the required ancillary service based on the forecast conditions. And last, the residual unit commitment (RUC) process designates additional power plants that will be needed for the next day and must be ready to generate electricity. The results will be published at 1 pm on the day before the TD[4].

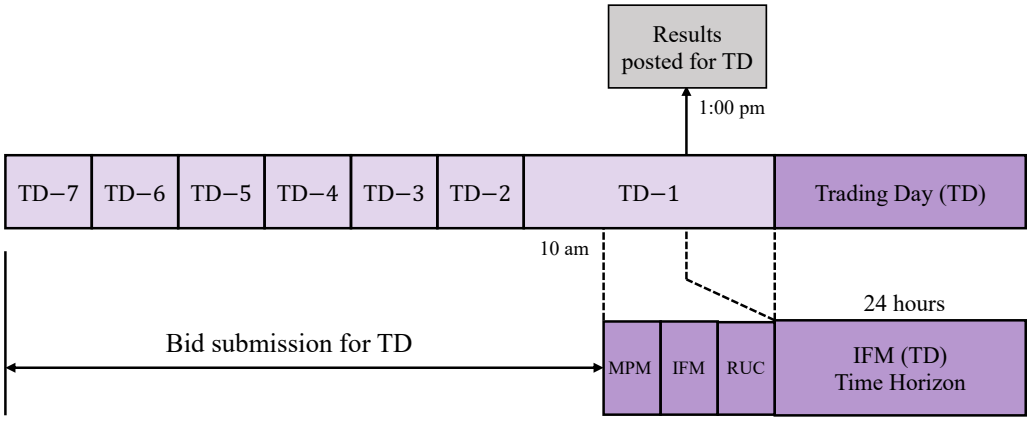

Figure 2.4: Day-ahead and real-time market process in the CAISO

The real-time market opens at 1 pm on the day before the TD and closes 75 minutes before the start of the trading hour. It provides the opportunity to meet the last few increments of demand not covered in the day-ahead schedules. If additional reserves are needed after the day-ahead market, they will be purchased through the real-time market. Energy and reserves bids are again co-optimised in the IFM in real-time every 5 minutes to obtain the optimum set of energy and reserve dispatches[5].

[4] `https://www.caiso.com/market/Pages/MarketProcesses.aspx`

[5] `https://bpmcm.caiso.com/Lists/PRR%20Details/Attachments/532/Market%20Operations%20BPM%20MPM%20Enh%20PRR.pdf`

2.1.3 Electricity Reliability Council of Texas (ERCOT)

The Electricity Reliability Council of Texas (ERCOT) was established in its current form as a power market operator in 2001 within the state of Texas. The ERCOT includes 4 ancillary services, namely regulation-up, regulation-down, responsive reserve, and non-spinning reserves Tsai [2021]. Responsive reserves are similar to spinning reserves in the CAISO, and their job is to restore the frequency of the ERCOT within the first few minutes of an event that causes a significant deviation from the standard frequency. Figure 2.5 shows how ERCOT works.

At 6 am, while ERCOT publishes the system condition forecast and reserve obligations, the participants submit their black start resources and reliability must-run (RMR) requirements. All the energy and reserve bids are submitted by 10 am a day before TD. The bids can include a start-up offer, minimum energy offer and energy curve offer with up to 10 price bands. Then the day-ahead market co-optimises all reserve markets together with the energy market to find the output. The results will be published at 1:30 pm. The participants can then update their current operating plan (COP) until 2:30. This provides accurate information about resources from a planning perspective and provides input for day-ahead reliability unit commitment (DRUC).

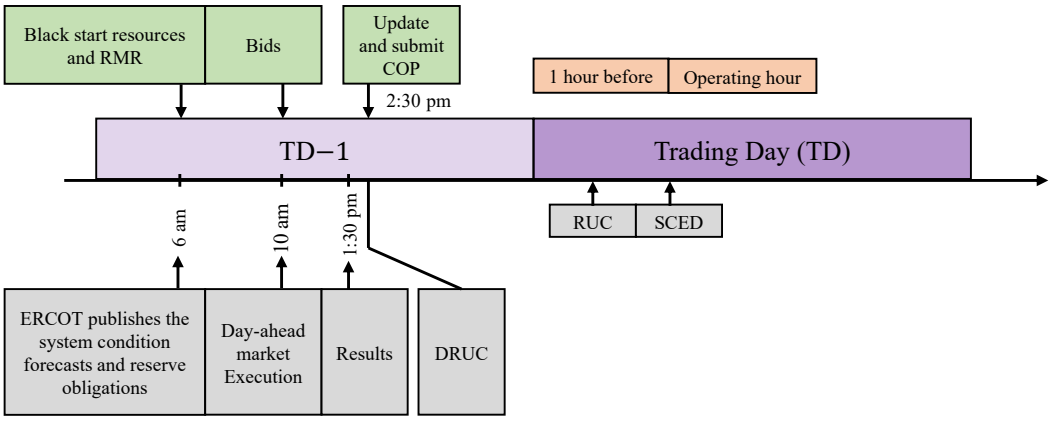

Figure 2.5: Day-ahead and real-time market process in ERCOT

The ERCOT implemented a real-time operating reserve demand curve methodology in 2014. Through this process, the value of available reserves in the real-time market is calculated and added to the real-time locational marginal price. This process is known as price adders in the ERCOT. The added prices are based on the determined value of lost load in the system and the probability that load would have to be shed, given the realised reserve levels. Price adders are calculated for both online (synchronised) and

offline (unsynchronised) reserves and are intended to approximate the co-optimisation of energy and reserves in real time.

An hour before the operating period, a reliability unit commitment is solved, and in real-time operations, security-constrained economic dispatch (SCED) is conducted every five minutes, and two price adders are calculated on the basis of the reserve levels that are realised during each settlement period—currently every 15-minute interval. One adder is calculated based on the realised level of online reserves and the other is calculated based on the sum of the realised levels of online and offline reserves. These adders are then added to the LMP-based energy price that is paid to generating entities and charged to load-serving entities in each settlement period. If the responsive reserve level falls below a 2000 MW minimum contingency in any period, ERCOT will set the price adder to the administratively determined value of lost load in the system, which is currently $9000/MWh.

2.1.4 European Market

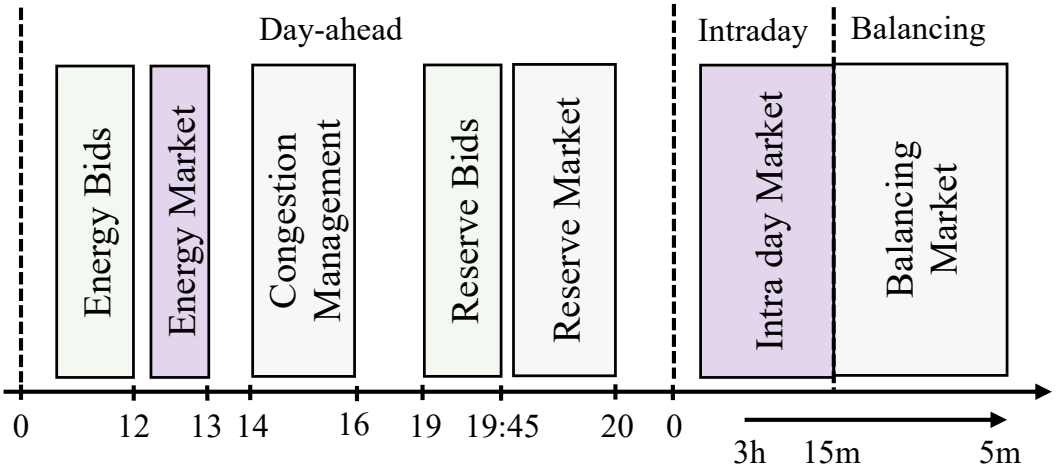

Figure 2.6: Market process in EUROPE

The European market also includes a day-ahead and a real-time market. Different types of bids are possible: a price-insensitive bid at either market cap or floor price; a price-sensitive bid where a stepwise curve is submitted (i.e., different quantities for different prices). The main European markets are Nord pool, EPEX, and MIBEL Iria et al. [2019]. Figure 2.6 shows the structure of a typical European market which includes a day-ahead, an intraday and a balancing market for defining prices and schedules in real-time. The energy bids for the day-ahead market are submitted at noon the day before TD. Once the energy market is cleared, the transmission system operator (TSO)

adds the physical bilateral contracts to the clearing offers and performs congestion management to generate viable daily schedules. Unlike the NEM, CAISO, and ERCOT, the energy and reserve markets are not co-optimised in the European markets, and as shown in Figure 2.6 they are cleared sequentially. The intraday and balancing markets allow bid adjustments before the real-time operation.

2.1.5 Comparisons Between the Markets

The CAISO, ERCOT, and European markets include both a day ahead and a real-time market. On the contrary, there is no day-ahead market in the NEM and energy and reserve transactions are done in a real-time market. While the CAISO, ERCOT and the NEM co-optimise energy and reserve markets, the European market follows a sequential policy in which the reserve market is cleared after the energy market. However, regardless of how the market clears, the participants might still want to co-optimise their bids to obtain the best share of bids to submit into energy and reserve markets. All markets accept either price-insensitive (bidding at the market cap or floor prices) or price-sensitive offers (bid curves with different prices). In the NEM, participants' technical limits form a trapezium[6]. In this thesis, we generate our bids to be submitted to the NEM. In every chapter, we provide some intuition on what our method will look like for different markets.

[6] `https://www.aemo.com.au/Electricity/National-Electricity-Market-NEM/Security-and-reliability/-/media/2C771C82C8054929B16E4545216ACE03.ashx`

2.2 Literature Review

We start this section with a general history describing how using demand-side flexibility evolved over time. This part covers a broad spectrum of research, including simple load shedding algorithms designed for grid-scale loads, as well as approaches suitable for current and future power systems in which the consumer-owned DER can provide valuable flexibility services. We then focus on the importance of the distribution network – as a means to connect consumers to the market; and review approaches that ensure the safe operation of the distribution network in the presence of consumer-owned DER. Finally, we touch on uncertainty around consumer data and review the state-of-the-art approaches to handling such uncertainties in power systems.

2.2.1 Demand Side Market Participation

Managing load (such as shifting peak power to off-peak to avoid unnecessary installation of generators) has been in place for a long time Morgan and Talukdar [1979]. However, it was not until 1980 when load participation in the frequency market attracted attention. In 1980 Schweppe et al. suggested using loads "to assist or even replace conventional turbine-governed systems and spinning reserve" Schweppe et al. [1980]. However, due to a lack of flexibility on the demand side, this support was limited to load shedding, which was used to resolve under-frequency issues, e.g., Berger and Schweppe [1989].

System operators use under-frequency load shedding (UFLS) as an effective way to maintain power system frequency. Different methods are suggested in the literature to provide under frequency reserve services using UFLS, such as Harrison [1980], Nirenberg et al. [1992] and Delfino et al. [2001]. These works keep reducing load as frequency continues to drop. UFLS plays a critical role in the way that our power systems work. When other responses fail to address frequency drop, UFLS, as a last resort, makes the difference between a complete system-wide blackout and more limited blackouts for lower priority loads.

Distributed energy resources have made demand response services go beyond UFLS as demand can respond more actively to generation / load variation Rahimi and Ipakchi [2010]. While grid-scale DER (such as wind farms Feltes et al. [2014], utility-scale batteries Dozein and Mancarella [2019]) have been participating in the wholesale market since the beginning, residential DER market participation has only become attractive in the last decade or so. This is triggered by a) improvements in controlling distributed resources in power systems and b) the emergence of aggregators. In the following, we briefly discuss each factor.

a) Regarding load control, Callaway and Hiskens [2010] proposes a direct

load control to enable distribution utilities / aggregators to deliver the desired response to electricity markets. The authors in Callaway [2011] show that the smaller loads (e.g. less than 10kW) with EMS can engage in active demand management to provide energy and frequency services within the wholesale market. Ma et al. [2011] proposes a decentralised control scheme based on non-cooperative games to coordinate charging plug-in electric vehicles. Meyn and Busic [2020] proposes a framework for residential / commercial loads enabling them to provide ancillary services to power systems.

b) Regarding load aggregation, an aggregator is a service provider that directly or indirectly manages groups of consumers / resources to trade pools of loads / generation as single products in the electricity markets. Iria et al. [2019]; Burger et al. [2016]. This makes the market participation of DER much simpler since consumers do not need to get involved with the complications around bidding and the markets. Plus, it will not change the current market clearing process as the market operators do not need to include thousands of individual consumers in the market clearing process.

In this thesis, we focus on the market participation of residential consumers through aggregators. We assume that there exists proper control and communication infrastructure so that aggregators can deliver on the market dispatch signal.

2.2.2 DER Bidding into electricity market

The literature on DER market participation can be categorised into two main groups, depending on the strategy consumers take to interact with the market: A) price-insensitive bidding and B) price-sensitive bidding. We next review state of the art in each category.

2.2.2.1 Price-Insensitive Bidding

A price-insensitive bidding approach is referred to a market engagement policy in which participants' offers are independent of the market price. Price-insensitive bidders decide on their market bids in advance and then submit their generation bids at the market floor price and their demand bids at the market cap price. This ensures that consumer generation / demand bids are accepted in the market. Such a bidding approach simplifies the problem to a scheduling one for which participants need an accurate price forecast. Price-insensitive bids can achieve reliable outcomes when prices are relatively stable and predictable. Yet, volatile market prices can negatively affect the price-

insensitive bidders. We categorise the price-insensitive bidding approaches into indirect and direct market participation, as explained in the following.

Indirect Market Participation (Retail Participation)

Under this category, consumers are not directly participating in the market. Here, a third party, i.e., a retailer, participates in the electricity market and sets tariffs (e.g., a time-of-use (ToU) and a feed-in tariff), according to which the end-users schedule their DER Scott et al. [2019]. Although the ToU tariff might somewhat reflect the overarching market, customers are not directly or immediately impacted by any influence they might have on the market prices.

When using tariffs, the benefit will be defined by off-peak, peak and feed-in prices. Therefore, consumers cannot benefit from the time-varying market prices. Instead, consumers may seek additional income by providing other services, such as voltage support, e.g., Jabr [2019], peak shaving / valley filling, e.g., Wang and Wang [2013].

The focus of this thesis is to explore a more direct DER market participation. Thus, we are neither interested in tariffs nor providing services other than those traded within the energy and reserve markets. This being said, in chapters 4 and 5, we use reactive power to provide voltage support. The reactive power support can open up network capacity, and as a result, consumers can participate in the market with fewer network limitations.

Direct Market Participation

A plethora of research works has focused on price-insensitive market participation of DER directly into energy (and frequency) markets, e.g., Attarha et al. [2018b,c]; Vayá and Andersson [2014]; Attarha et al. [2019]; Wang et al. [2018]; Yao et al. [2018]; Ottesen et al. [2018]; Iria et al. [2018, 2019]; Lee et al. [2016]; Zhu and Zhang [2019]; Ulbig et al. [2022]. Our approaches presented in chapters 3 and 4 also belong to this group of bidding approaches.

Price-insensitive market participation of DER has been studied in Attarha et al. [2018b], where a battery-PV pair is optimised to participate in the energy market. A two-stage optimisation is proposed in Attarha et al. [2018c] to obtain price-insensitive bids for a storage system paired with a wind farm that jointly participates in the energy market. Market participation of electric vehicles in the day-ahead energy market and residential DER in the real-time energy market are studied in Vayá and Andersson [2014] and Attarha et al. [2019] respectively.

As shown in Oudalov et al. [2006], the highest value of a battery is obtained when providing primary reserves. Although the analysis, done in Oudalov et al. [2006], is based on fixed contracts rather than direct market participation, it provides insights into the value of DER in providing reserves.

In addition, since DER are fast responding, they can efficiently provide different reserve services. However, Attarha et al. [2018b,c]; Vayá and Andersson [2014]; Attarha et al. [2019] are focusing solely on the energy market participation and thus ignoring a significant source of revenue. Plus, the experiments on Świerczyński et al. [2013] show that investing in battery storage for reserve is already financially viable. This will only become more profitable with the battery cost reduction making Attarha et al. [2018b,c]; Vayá and Andersson [2014]; Attarha et al. [2019] less attractive.

To make the most out of DER flexibility Yao et al. [2018]; Ottesen et al. [2018]; Iria et al. [2018, 2019]; Lee et al. [2016]; Zhu and Zhang [2019] co-participate in energy and reserve markets. As with price-insensitive bidding, these works co-optimise their DER according to price forecasts of multiple markets and obtain price-insensitive bids to submit into the market at either market cap or floor prices. The differences between these works lie in either the type of the DER or the reserve markets they bid into. For example, Yao et al. [2018] studies the aggregate response of electric vehicles (EVs) for frequency regulation services in the day-ahead market while Iria et al. [2018] and Iria et al. [2019] study the residential DER market participation respectively in tertiary and secondary reserve markets. Similar price-insensitive strategies that, in a broad sense, co-optimise DER in energy and reserve markets are proposed in Neyestani et al. [2016]; Vatandoust et al. [2018]; Good and Mancarella [2017].

Note that the distribution network, including its DER, can be viewed as a virtual power plant (VPP). A VPP is a cloud-based distributed power plant that aggregates the capacities of heterogeneous DER to enhance power generation and enable the trade of power in the electricity market. If the VPP includes the distribution network, it is closely comparable to our approach. In fact, such a VPP is equivalent to our setting, provided that one aggregator centrally manages all consumers and the distribution network at the same time. However, unlike VPP, our approach allows multiple aggregators to manage consumers in the same network, which is being operated by a DSO. We next review some works in the VPP paradigm that shares similarity with the core content of this thesis.

Yang et al. [2021] studies the ability of a VPP that includes different energy resources in providing demand response; Zhang et al. [2021b] proposes an optimal bidding model based on the time-of-use power prices; Zhang et al. [2021b] takes the wind and solar power uncertainty into account when making bidding decisions. Neglecting the network Chen et al. [2020] studies an optimal bidding strategy for VPP. The authors use information gap decision theory (IGDT) to deal with the uncertainties posed by load and day-ahead (DA) market clearing prices. Authors in Zhang et al. [2021a] investigate inverters' transient response of a VPP that aggregates DER. Mashhour and Moghaddas-Tafreshi [2010] studies the joint bidding of a VPP in the energy

and spinning reserve market under different market price scenarios. The authors take into account the distribution network constraints and centrally coordinate DER with the grid; Nezamabadi and Nazar [2016] includes the local grid to provide network-feasible bids for a VPP participating in energy, spinning reserve and reactive power markets.

Price-insensitive market participation of DER is not limited to residential DER and VPPs. Utility-scale DER (mainly a battery) have used this strategy to jointly bid in energy and reserve markets, such as Kazemi et al. [2017]; Oudalov et al. [2007]; Aghamohammadi and Abdolahinia [2014]; Xu et al. [2014, 2018]; Borsche et al. [2013]; Thorbergsson et al. [2013]; Mercier et al. [2009]. The participation of a battery storage system in reserve markets mainly leads to a MILP problem[7]. Solving the resulting MILP optimisation problem generates the charging / discharging schedules, together with the bids for each market. In summary, Kazemi et al. [2017] jointly optimises a battery storage system in day-ahead energy, spinning, and regulation reserve markets while modelling price and ancillary service deployment uncertainty using robust optimisation. We provide a brief review on robust optimisation in Section 2.3. Oudalov et al. [2007] calculates the minimum possible battery capacity that fulfils the technical requirements of the grid code for frequency reserve services based on the European market prices. Similarly, Aghamohammadi and Abdolahinia [2014] determines the optimal size of a battery storage system for primary frequency control in a Microgrid. A control strategy is proposed in Xu et al. [2014] to maintain batteries SoC within an optimal range and to slow down its ageing while providing frequency responses. An optimal bidding policy is given in Xu et al. [2018] to model the battery ageing when participating in the frequency regulation market. Borsche et al. [2013] investigates the power and energy capacity requirements for a storage system to provide frequency reserve services. Three different control strategies are given in Thorbergsson et al. [2013], and their benefits are compared when bidding into the Danish market. Finally, Mercier et al. [2009] obtains the optimum sizing and operation of a battery energy storage system used for spinning reserve in a small isolated power system.

Note that the schedules obtained using price-insensitive approaches are optimum as long as the MCP is similar to the forecast prices. This assumption will hold if the market power of DER is not significant. When there are numerous DER, their zero marginal cost can make the market prices too volatile to forecast accurately. Besides, a price-insensitive bidding approach can negatively affect both the market and aggregators. From the market perspective, price-insensitive bids always need to be settled. Therefore, the market is constrained to dispatch these DER bids at a predetermined operating point, despite the underlying flexibility of DER. From an aggregator's perspective,

[7] We provide a brief review on MILP optimisation approaches in Section 2.3.

the insensitivity of offers to the prices can negatively affect their profits. For instance, if a battery has been charged at $100, the discharge should occur for a price higher than $100. However, the aggregator might mistakenly forecast a high price and submit a discharge bid when the price realises to be less than $100.

To lessen the effect of the issue mentioned above, some utility-scale DER, Shafiee et al. [2017, 2016]; Arteaga and Zareipour [2019] first determine the effect of DER on the market prices and then use the obtained modified prices to schedule their DER. Similarly to the price-insensitive approaches, Shafiee et al. [2017, 2016]; Arteaga and Zareipour [2019] bid one capacity band to the electricity market (generation at zero and load at the market cap price). Not only are Shafiee et al. [2017, 2016]; Arteaga and Zareipour [2019] incapable of bidding a range of flexibility, but also they only consider the effect of their own DER on the electricity market prices. However, the price might change according to the behaviour of other participants (e.g., a generation company might trip, leading to a sudden price increase) – frequent real-world scenarios that Shafiee et al. [2017, 2016]; Arteaga and Zareipour [2019] do not take into account.

2.2.2.2 Price-Sensitive Bidding

Unlike price-insensitive bidders, price-sensitive bidders submit different capacities for different prices. If the MCP realises to be greater than or equal to price-sensitive offers, then their capacity will be accepted. This enables the price-sensitive bidders to hedge the market price uncertainty as their bids are sensitive to the price, and their final dispatch will be a function of MCP.

To the best of our knowledge, there is no bidding approach for residential DER that provides multiple capacity bands at different prices in the literature other than what we propose in Chapter 5. However, there are works that go above a price-insensitive bidding approach; for example, Nezamabadi and Nazar [2016] in which the authors calculate their bid price using quadratic cost function (fuel cost), and the time coupled work by Caramanis and Foster in Caramanis and Foster [2011] where they propose a new market clearing mechanism that takes DER time dependencies into account.

It is worth mentioning that for generators or grid-scale DER, bidding multiple capacity bands at different prices is a common practice. For instance, Weidlich et al. [2018] proposes a price-sensitive bidding approach to maximise generators' benefits. The authors in Weidlich et al. [2018] use the price forecast and the marginal cost to obtain the minimum market price at which they can increase their output by their ramp rate. If the price is lower than the calculated cost, they bid to reduce their output based on the ramp rate or until they reach their minimum operating point. For storage systems, like batteries and pump hydro units, they offer to choose a charging and discharg-

ing price in advance and bid for full charge or discharge if the price reaches these predetermined values.

Whether price-insensitive or -sensitive, the bids are finally cleared at the market price by the market operators. However, as mentioned before, residential DER are connected to / operated within distribution networks. Unlike transmission networks, to which big generators or utility-scale DER are connected, distribution network constraints are not included in the market clearing process. Therefore, consumer bids might violate the distribution network in the current market structure. This is shown in Ulbig et al. [2016] in which the authors investigate the effect of consumer-owned DER on the grid and show that consumer behaviour significantly violates the network without coordination. However, including thousands of consumers and distribution networks in the market clearing process over-complicates the problems. Alternatively, distribution network constraints can be ensured outside the market before consumer bids reach the market Ross and Mathieu [2020]. We next review approaches proposed to ensure distribution network security.

2.2.3 Network Inclusion

DER integration can affect distribution networks positively or negatively depending on their operation targets. If DER provide network support services, they can increase network capabilities and postpone network augmentation. However, when bidding into the market (the operation target we are interested in), the story is different. Responses of many DER to price spikes create synchronisations that might push the distribution network outside its limits Attarha et al. [2019]. A network violation can disconnect consumers from the market and create serious problems for the market. We explain this with an example in the following:

Imagine a scenario in which the distribution network is injecting into the transmission network and can increase the injection (provide raise frequency reserve service) through its DER. Now assume an event creates a frequency drop, and the distribution network is asked to add to the generation. In such a case, if a cable or a transformer is overloaded (a highly likely scenario when the network is neglected), the switches will disconnect the distribution network. Thus, not only can the raise reserve service not be delivered, but the initial injection is also disconnected. As a result, the frequency drops even further. Therefore, the inclusion of network constraints into a bidding approach is critical. Extensive research has been done around the secure operation of DER-penetrated distribution networks. The available solution approaches fall into one of the following categories: fixed export limits, operating envelopes, central OPF, and distributed OPF. We next provide a review of these approaches.

Fixed Export Limits

Fixed export limits have been incorporated in many real-world examples to avoid overvoltage that can occur due to rooftop PV grid injection. In Arizona, the USA, solar systems capacity cannot be greater than 125% of consumers' total connected load. In most Australian states, a fixed export limit of 5 kW is currently in place. Therefore, the excess PV power must either be consumed, e.g., to charge a battery, or be curtailed. In Germany, small-scale PV systems are not allowed to export more than 70% of their installed capacity Ricciardi et al. [2018]. Although simple, such fixed limits are overly conservative as they are obtained for a scenario with max generation and min demand throughout a year. In Chapter 3, we compare the effectiveness of our approach with such fixed export limits.

Notice that fixed export limits only consider the injection scenario. However, as battery storage systems and EVs are becoming more popular, limits for withdrawing power are also becoming important.

Operating Envelopes

Operating envelopes are convex sets that define the allowed real and reactive power transfers with the network at a given customer connection point or for an aggregate of customers in a region. Envelopes are calculated so that any joint combination of consumption or generation within the envelopes will not violate any network constraints Blackhall [2020]; Nazir and Almassalkhi [2019, 2021]. Since operating envelopes can guarantee network security locally, the market operator does not need to model thousands of DER (millions of variables and constraints) or network limits (non-linear and non-convex constraints) into their optimisation problems. While effective, obtaining representative operating envelopes is difficult.

References Blackhall [2020]; Petrou et al. [2020] suggest that distribution system operators (DSO) should calculate operating envelopes and allocate them to each consumer without considering their preferences, uncertainty or market participation. However, since some consumers might need less flexibility (e.g., due to self-consumption), such proposals can result in unrepresentative envelopes conservatively limiting market-participating consumers. Petrou et al. [2021] suggests obtaining envelopes that include consumers' preferences. The consumers in Petrou et al. [2021] firstly send their preferred connection point power to the DSO. The DSO then tries to minimise the squared distance between what a consumer needs and what the network can accept. Despite what operating envelopes intend, Petrou et al. [2021] is only valid as long as consumers operate at the requested operating points. The network constraints might be violated if consumers operate differently from what they initially requested. Plus, Petrou et al. [2021] requires full ob-

servability over consumer DER which in practice might not be available to the DSOs. In chapters 3 and 4 we obtain operating envelopes that do not face the above challenges and compare their effectiveness with the proposals mentioned above.

Authors in Markovic et al. [2016] proposed a combination of suitable grid tariffs and DSO adjustments to consumer injections. The authors first calculate suitable grid tariffs using which consumers optimise their DER. If the obtained injection values lead to a network violation, the network solves an optimisation problem to put limits on consumer injections. Consumers finally reschedule their DER given the DSO limits. The DSO optimisation and injection limits can be viewed as an operating envelope. However, when consumers participate in the market, their DER should be dispatched according to market prices, and thus, a well-defined tariff and operation point does not exist.

Operating envelopes have been proposed in Nazir and Almassalkhi [2019], and Nazir and Almassalkhi [2021] to obtain the hosting capacity and nodal DER injections in distribution networks, respectively. Nazir and Almassalkhi [2019] and Nazir and Almassalkhi [2021] obtain inner convex approximation of AC-power flow equations to provide AC admissible solution across the envelopes. The authors show that for excessive nodal power exchange, the network losses increase significantly and thus, the voltage decrease resulting from network losses outweighs the voltage increase resulting from DER injections. This can create holes in the feasible region leading to operating envelopes that are not AC admissible. While our network subproblem in this thesis can incorporate a similar convex inner approximation presented in Nazir and Almassalkhi [2019, 2021] or Lee et al. [2019], we directly work with non-convex equations, which we solve using the IPOPT solver. The reason is that the network operators do not tend to operate the network in points where the network losses are unreasonably high (the conditions needed for the holes mentioned in Nazir and Almassalkhi [2019] and Nazir and Almassalkhi [2021] to occur). We have provided a 2-bus system in Chapter 3 explaining the phenomenon Nazir and Almassalkhi mentioned in Nazir and Almassalkhi [2019, 2021]. We show that for distribution networks, where $R >> X$, the OPF becomes infeasible before any holes can be formed. We further discuss this in Section 3.3

Operating envelopes have also been calculated at the interconnection of TSO-DSO to provide the DSO with the available network-secure flexibility at the distribution network, e.g., in Nazir [2020]; Capitanescu [2018]. In the optimisation approaches presented in Nazir [2020]; Capitanescu [2018], the authors first calculate maximum and minimum real power that can be exchanged with the upstream network and then solve OPF for real-power inside the maximum and minimum power to calculate the associated reactive power. While similar approaches can be used in our network sup-problem to

calculate TSO-DSO operating region, our main focus is to obtain envelopes down at the level of consumers.

Centralised OPF

This is a different approach in which the DSO schedules all DER by solving a central OPF. For instance, Vatandoust et al. [2018] includes linear load flow equations and aggregates a large-scale battery and an EV fleet to bid into the day-ahead frequency regulation market. Similarly, Dall'Anese et al. [2017], Saint-Pierre and Mancarella [2016] and Souza et al. [2016] use optimal power flow to centrally dispatch DER to provide regulation service, do active distribution network management and participate in the energy market, respectively. In Nazir and Almassalkhi [2020], the authors use a convex inner approximation of the OPF problem and coordinate DER to minimise voltage deviations from the nominal values. However, running a central OPF when there are numerous consumers would lead to a large-scale, time-coupled, linear or non-linear[8] optimisation problem, which is computationally expensive for an online real-time setting. Also, Vatandoust et al. [2018]; Dall'Anese et al. [2017]; Saint-Pierre and Mancarella [2016]; Souza et al. [2016] require central access to all of the information of all the consumers, which is not practical and compromises consumers' privacy. In Chapter 3, we compare our solution approach, both in terms of solution quality and computational performance, with approaches that use a centralised OPF.

Distributed Solutions

To meet the challenges mentioned for a central OPF, distributed approaches have been suggested. The authors in Ross and Mathieu [2020] propose an $l1$ and $l2$ network safety index to obtain network-safe decisions without the need to have access to detailed information from behind-the-meter technologies. In Ross and Mathieu [2021]; Ross et al. [2019], the authors propose different control strategies for coordinating aggregators to provide network-aware services. These control strategies are either based on a blocking scheme in which the DSO blocks an aggregator's commands if they cause network issues as in Ross et al. [2019], or based on a mode-count control scheme Ross and Mathieu [2021] in which the on/off statues of TCLs are determined to avoid network violation.

Distributed optimisation, e.g., ADMM Boyd et al. [2011], has also been used to ensure network feasibility. ADMM has been used in various power system application including OPF Scott and Thiébaux [2015]; Tsai et al. [2017]; Yuan et al. [2016], congestion management Bai et al. [2017]; Huang et al. [2014], DER coordination Scott et al. [2019]; Attarha et al. [2019] and network

[8]Depending on the type of power flow equations, the resulting problem can be linear or non-linear

support Olivella-Rosell et al. [2018]; Shaloudegi et al. [2012]. ADMM method is explained later in Section 2.3.3. Our solution approach in chapters 3, 4 and 5 belongs to the category of distributed solutions. More specifically, we follow a similar ADMM-based approach in chapters 3 and 4, where we present our price-insensitive bidding approaches. However, in Chapter 5, where we introduce our price-sensitive bidding approach, we propose a new network-secure solution that is distributed in the sense that consumers and the network solve their problems independently. However, unlike iterative ADMM-based approaches in which consumers and the DSO negotiate until converging on the network-secure bids, in Chapter 5, we opt for a more scaleable one-shot policy which is equivalent to the computation complexity of a single ADMM iteration. In our one-shot policy, the consumers first obtain their preferred bids, neglecting any network limits, and send their bids to the DSO. Next, the DSO runs OPFs to shape consumer bids to be within network constraints in one shot. Since there is no iterative negotiation between consumers and the grid, we call this approach one-shot bid shaping.

In a deterministic setting, where all data is known and constant, the above approaches can ensure network feasibility. However, in reality, consumers' data, such as PV power and demand, are uncertain. Therefore, there is no guarantee that consumers can stick to their envelopes in approaches based on fixed export limits / operating envelopes; or commit to their negotiated connection point power in approaches based on central / distributed OPF. To avoid network infeasibilities, it is important to model uncertainty in these approaches. We next review common approaches to model data uncertainty in power system operation.

2.2.4 Uncertainty Characterisation

Uncertainty can not only lead to connection point powers (CPPs) being outside the envelope, or different from the negotiated CPPs but also can lead to bid deliveries being different from the ones submitted to the market. Delivering CPP different from what has been negotiated or outside the operating envelope defeats the purpose of network coordination. In other words, the network constraints might still be violated for uncertainty realisations different from the forecast. On the other hand, bid deliveries different from what has been offered to the market might significantly penalise consumers. So, uncertainty can negatively affect both feasibility and optimality, and thus, it is important to model uncertainty in our optimisation problems. The most common approaches in the literature to deal with uncertainty are reviewed in the following.

Model Predictive Control

The approaches based on online optimisation Scott et al. [2019]; Scott and Thiébaux [2015] coordinate DER using a model predictive control (MPC) framework. These approaches re-optimise frequently, close to real-time, using the latest and most accurate forecast information. In other words, they assume that the forecast is pretty accurate, close to operation and constant between two successive optimisations. This assumption holds, provided that the time step between two successive optimisations is small enough. Fortunately, in the NEM, participants are able to adjust their bids every 5 minutes. Therefore, we use an MPC implementation and re-optimise every 5 minutes to account for the latest uncertainty changes in our models in chapters 3, 4 and 5. Moreover, we introduce a piecewise affinely adjustable robust constrained optimisation (PWA-ARCO) approach in Chapter 4, which can be incorporated if the uncertainty realisation within a 5-minute operating interval (before the next optimisation) varies notably.

Stochastic Optimisation

Stochastic programming (SP) is used to account for a wide range of uncertainties, for example, wind power uncertainty in Wang et al. [2008, 2011]; Shiina and Birge [2004] and demand in Shiina and Birge [2004] within a unit commitment problem, the uncertainties in OPF Phan and Ghosh [2014] and demand response Wang et al. [2018]. In SP-based approaches, several scenarios are employed along with their associated probabilities to predict the possible future realisation of uncertainty. However, the scenarios used in SP can bias the solution away from the "true" PDF (probability distribution function). Thus, if the distribution of scenarios differs from the actual realisation, the resulting out-of-sample performance is often disappointing. Moreover, considering a large set of scenarios to enhance our prediction of uncertainty realisation renders the problem computationally intractable.

Robust Optimisation

Robust optimisation avoids having to consider large numbers of scenarios by finding and optimising according to a worst-case scenario. Three common approaches in robust optimisations are reviewed in the following.

1. *Adaptive Robust Optimisation:* This group of approaches mainly solves a two-stage optimisation problem. The second stage in such approaches is to find a worst-case scenario. The first stage then uses this worst-case scenario to optimise for robust planning variables, e.g., Attarha et al. [2018a]; Liu and Hsu [2018]; Giraldo et al. [2018]. Adaptive robust optimisation has been used in distributed approaches, including He et al.

[2017] where the decomposition is between a coupled electricity and gas network, and Gao et al. [2017b], and Mohiti et al. [2019] where the decomposition is between 3 interconnected microgrids.

These approaches often lead to a MILP problem that is mainly solved iteratively using column and constraint generation (C&CG) techniques. Since the decisions are made according to the worst-case scenario, which is very unlikely to occur in practice, these approaches often lead to over-conservative solutions.

2. *Affinely Adjustable Robust Optimisation:* Unlike the previous category, this group of approaches Jabr [2019]; Abadi et al. [2020]; Attarha et al. [2018b] make a part of the decision according to the forecast information (commonly known as non-adjustable), while another part of the decision waits for the realisation of uncertainty to take recourse actions (commonly known as adjustable).

   The ability to take recourse enables these approaches to be less conservative than adaptive robust optimisation approaches. In the DER context, this approach is more reasonable than a two-stage adaptive robust approach. The reason is that a two-stage robust approach ignores DER's fast-responding feature. Thus, it optimises them ahead of uncertainty realisations based on the worst possible outcome for the uncertain parameters. However, DER can easily adjust to the live operation changes. Therefore, adjustable robust approaches enable the response to tune itself based on the uncertainty realisation rather than being entirely made based on the worst case. Inspired by this, we propose a piecewise affinely adjustable solution approach called PWA-ARCO in Chapter 4 to model the uncertainty around PV power and demand within every 5-minute operating interval.

3. *Distributionally Robust Optimisation:* Distributionally robust optimisation (DRO) methods have been proposed in Babaei et al. [2019]; Zare et al. [2018]; Mieth and Dvorkin [2018] to improve the performance of RO, based on the distribution of the uncertain parameters. Unlike SP, the DRO methods do not require exact probability distributions of uncertainties. Instead, they construct an "ambiguity set," which is essentially a set of possible distributions that are consistent with the available samples de Klerk et al. [2020]; Li et al. [2019]. However, the authors in Poolla et al. [2020] have shown that using available techniques, such as Esfahani and Kuhn [2018], the number of constraints of the DRO problem increases with the number of samples, leading to high dimensionality. Hence, given the real-time market time frame (5 minutes in the NEM), these approaches are unlikely to scale. On the other hand, Babaei et al. [2019] uses the available data to tune the uncertainty set based on the

probability distribution function (PDF) of data . As stated in Babaei et al. [2019], if the PDF information cannot be extracted from the data, Babaei et al. [2019] works similarly to a conventional robust approach. In addition, Babaei et al. [2019]; Zare et al. [2018]; Mieth and Dvorkin [2018] either assume a linear recourse, as in Babaei et al. [2019] or ignore recourse capability, as in Zare et al. [2018]; Mieth and Dvorkin [2018].

2.3 Optimisation

Here, we provide background information on optimisation techniques used throughout this thesis. This will include linear programming (LP) Sierksma and Zwols [2015], mixed integer linear programming (MILP) Papadimitriou and Steiglitz [1998]; Chachuat [2019], distributed optimisation ADMM Boyd et al. [2011], and finally adjustable robust optimisation Ben-Tal et al. [2004].

2.3.1 Linear Programming

A linear program can be written in its most general form as follows Sierksma and Zwols [2015]:

$$\min_{x \in \mathbb{R}^n_+} c^\intercal x \tag{2.1}$$

$$\text{s.t. } Ax \leq b : \mu \geq 0 \tag{2.2}$$

$$x \geq 0 \tag{2.3}$$

where $A \in \mathbb{R}^{m \times n}$, $b \in \mathbb{R}^m$, and $c \in \mathbb{R}^n$. Also, $\mu \in \mathbb{R}^m_+$ is the vector of dual variables associated with constraints of our optimisation problem. The feasible region of (2.1)–(2.2) is a convex polyhedron – a set defined as the intersection of finitely many half spaces, each of which is defined by a linear inequality given by (2.2). The optimum solution to this problem will be located on one of the edges / vertices of the polyhedral feasible region. Notice that characteristics of many DER can be modelled using linear constraints. Therefore, LP will become useful when developing energy management systems.

Every LP has a dual problem. While equivalent, in some cases, the dual problem is easier to solve than the original primal problem Bertsimas and Tsitsiklis [1997]. Using the dual variable μ, the dual of (2.1)–(2.2) can be written as follows:

$$\max_{\mu \in \mathbb{R}^m_+} b^\intercal \mu \tag{2.4}$$

$$\text{s.t. } A^\intercal \mu \leq c : x \geq 0 \tag{2.5}$$

$$\mu \geq 0 \tag{2.6}$$

where the primal variable x is now the dual variable associated with the constraint (2.5) in the dual problem. We explain an example in which solving the dual problem is more useful than solving the primal problem in Section 2.3.4. We use LP and duality in Chapter 4 to provide a tractable formulation to immunise our decisions against consumer uncertainty.

2.3.2 Mixed Integer Linear Programming

Mixed integer linear programming (MILP) is a type of optimisation problem in which all or some of the decision variables are integers Papadimitriou and Steiglitz [1998]. We can write a MILP problem in its most general form as follows:

$$\min_{x \in \mathbb{R}^n, y \in \mathbb{Z}^n} c^\intercal x + d^\intercal y \tag{2.7}$$

$$\text{s.t. } Ax + By \leq b \tag{2.8}$$

where $A, B \in \mathbb{R}^{m \times n}$, $b \in \mathbb{R}^m$, and $c, d \in \mathbb{R}^n$. Notice that if we relax the integer variables, i.e., $y \in \mathbb{Z}^n \rightarrow y \in \mathbb{R}^n$, then the problem will change into an LP. However, this generally produces a lower bound to the objective function, and the solution might be infeasible Papadimitriou and Steiglitz [1998]. In case the solution of the resulting LP program is integer feasible, then we have found the optimum solution to the MILP problem.

There are effective approaches to solve MILP problems, such as *branch and bound* and *cutting plane* methods. In summary:

- Branch and bound (B&B) methods partition the feasible region into different branches. The best solution in a partition is optimal overall Papadimitriou and Steiglitz [1998].
- Cutting plane approach works with the binary relaxed MILP problem, i.e., the LP program. If the solution of the LP is not integer feasible, a new cut (which basically is a linear constraint) is added. The same process is repeated until the optimum solution of the resulting LP is integer feasible, and thus the optimum solution of the MILP problem is found Karlof [2005].

In this thesis, we count on solvers such as CPLEX Cplex [2009], and Gurobi Gurobi Optimization, LLC [2022] to solve the MILP problems. In this thesis, we mainly need to work with MILP when working with batteries to ensure that our model does not allow for simultaneous charge and discharge decisions (in chapters 3, 4, 5). Plus, in Chapter 4, when modelling our piecewise controllers, we use some theories from MILP to justify our approach.

2.3.3 Distributed Optimisation ADMM

The alternating direction method of multipliers (ADMM) breaks the central optimisation problem into several subproblems and solves it in a distributed fashion Boyd et al. [2011]. ADMM builds on the distributed optimisation dual ascent by improving its convergence properties based on the method of

multipliers. Consider the following problem:

$$\min_{x\in\mathbb{R}^n, z\in\mathbb{R}^m} f(x) + f'(z) \tag{2.9}$$

$$\text{s.t. } h(x) \leq 0 \tag{2.10}$$

$$h'(z) \leq 0 \tag{2.11}$$

$$Ax + Bz = d : \lambda \tag{2.12}$$

where $A \in \mathbb{R}^{c\times n}$, $B \in \mathbb{R}^{c\times m}$, $d \in \mathbb{R}^c$ and λ is the dual variable associated with constraint (2.12). If the equality constraint (2.12) is relaxed, the optimisation problems $\min_{x\in\mathbb{R}^n} f(x)$; s.t. $h(x) \leq 0$ and $\min_{z\in\mathbb{R}^m} f'(z)$; s.t. $h(z) \leq 0$ could be solved separately to obtain x and z. Assuming that the objective f and f' and constraint functions h and h' are convex, ADMM uses the dual variable λ to relax the coupling constraint (2.12). As with the method of multipliers, the augmented Lagrangian $\mathcal{L}$ is obtained as:

$$\mathcal{L} = f(x) + f'(z) + \lambda^\intercal(Ax + Bz - d) + (\rho/2)||Ax + Bz - d||_2^2 \tag{2.13}$$

where $\rho > 0$ is a penalty parameter. The ADMM approach consists of three steps at each iteration. An x minimisation subproblem in (2.14); a z minimisation subproblem in (2.15); and a dual variable update in (2.16).

$$x^{k+1} := \operatorname*{argmin}_x \mathcal{L}(x, z^k, \lambda^k)$$

$$\text{s.t.} \quad h(x) \leq 0 \tag{2.14}$$

$$z^{k+1} := \operatorname*{argmin}_z \mathcal{L}(x^{k+1}, z, \lambda^k)$$

$$\text{s.t.} \quad h'(z) \leq 0 \tag{2.15}$$

$$\lambda^{k+1} := \lambda^k + \rho(Ax^{k+1} + Bz^{k+1} - d) \tag{2.16}$$

The iterative approach (2.14)–(2.16) is terminated when the stopping criteria is met. In this thesis, in line with Boyd et al. [2011], we terminate the algorithm when primal and dual residuals are smaller than a threshold as follows:

$$\max\{R_p^{(k)}\} \leq \epsilon \quad \text{where} \quad R_p^{(k)} := x^{(k)} - z^{(k)} \tag{2.17}$$

$$\max\{R_d^{(k)}\} \leq \epsilon \quad \text{where} \quad R_d^{(k)} := \rho(z^{(k)} - z^{(k-1)}) \tag{2.18}$$

The primal residuals (2.17) represent the constraint violation at the current solution, and the dual residuals (2.18) the violation of the KKT stationarity constraint Boyd et al. [2011].

Remark. The theoretical convergence of the ADMM algorithm to the

global optimum often needs the problem to be convex. However, as shown by several research, e.g., Mhanna et al. [2019]; Scott et al. [2019]; Attarha et al. [2020]; Hong et al. [2016]; Wang et al. [2019]; Srikantha and Mallick [2020]; Zeng et al. [2022], ADMM often performs well for non-convex problems in practice. There is ongoing research to prove ADMM convergence for non-convex problems as in Hong et al. [2016]; Wang et al. [2019]; Sun and Sun [2021]. More recently, the authors in Srikantha and Mallick [2020] proved that the ADMM algorithm converges for the non-convex OPF problem in a radial distribution network. Similarly to Mhanna et al. [2019]; Scott et al. [2019]; Attarha et al. [2020]; Hong et al. [2016]; Srikantha and Mallick [2020], in this thesis, we also apply ADMM to the non-convex OPF problem (solving by the IPOPT solver) and have not faced any convergence issues. The IPOPT solver was found efficient in solving non-convex OPF problems, e.g., in Capitanescu [2018]. In addition, since the main source of non-convexity appears in the network subproblem, without loss of generality, one can even use a convex relaxation of the OPF within our model, such as the relaxation proposed in Farivar and Low [2013].

Notice that the ADMM approach enables us to solve a large-scale optimisation problem in a distributed fashion. In the context of power systems, as more distributed energy resources are being introduced to our electricity system, such distributed techniques become extremely useful to solve the resulting large-scale optimisation problems that need to be solved to obtain the optimum operating point of our decentralised power systems. We particularly used this technique in Chapter 3 and 4 in this thesis.

Remark. The ADMM approach modelled through (2.14)–(2.16) is a synchronous implementation. Meaning that each step needs to receive all the information from all subproblems before it solves its optimisation problem. In the context of power systems, the network subproblem needs to wait to receive the information from all aggregators before solving the network subprogram. In other words, if different aggregators have different delays (e.g., due to differences in processing speeds), we should wait for the slowest aggregator to complete their update before proceeding to the next iteration. The shortcoming of this approach is that the system moves forward only at the pace of the slowest aggregator. Asynchronous versions of ADMM are proposed to solve this issue, e.g., in Zhang and Kwok [2014]; Agarwal and Duchi [2011]. While in this thesis, we work with synchronous ADMM Boyd et al. [2011], without loss of generality, an asynchronous algorithm can also be implemented. However, we leave the detailed study of such an implementation to future work.

2.3.4 Affinely Adjustable Robust Optimisation

The parameters of a real-world optimisation problem are often not known exactly. However, in most power system applications, a forecast of parameters, as well as a bound within which the uncertainty realisation might vary are available. This information can make an uncertainty set. Let $\epsilon \in \mathbb{R}^l$ be the uncertain parameters modelled in the following polyhedral uncertainty set:

$$E \triangleq \left\{ \epsilon \in \mathbb{R}^l | W\epsilon \leq v \right\} \tag{2.19}$$

where $W \in \mathbb{R}^{k \times l}$ and $v \in \mathbb{R}^l$ are parameters of the polyhedral uncertainty set. Let us start with the constraints of an LP optimisation problem as follows:

$$\mathcal{B}x + \mathcal{C}\epsilon + d \leq 0 \tag{2.20}$$

where $\mathcal{B} \in \mathbb{R}^{m \times n}$, $\mathcal{C} \in \mathbb{R}^{m \times l}$, and $d \in \mathbb{R}^m$. A deterministic approach ensures that (2.20) is satisfied for $\bar{\epsilon}$ where $\bar{\epsilon}$ is the forecast scenario. On the contrary the robust optimisation of (2.20) will be as follows:

$$\mathcal{B}x + \mathcal{C}\epsilon + d \leq 0 \quad \forall \epsilon \in E \tag{2.21}$$

The for-all quantifier in (2.21) means that the constraint must be satisfied for any uncertainty realisation within the uncertainty set E. To allow real-time recourse, an AARCO approach allows the decision variables to be an affine function of uncertainty as:

$$x \rightarrow x(\epsilon) \triangleq A\epsilon + b \tag{2.22}$$

where $A \in \mathbb{R}^{n \times l}$ and $b \in \mathbb{R}^n$. Prior to real-time, we optimise to obtain A and b. In live operation, when the true value of ϵ is revealed, $x(\epsilon)$ will become fully known. This is in the spirit of a linear feedback controller, where the value of x can be constantly updated in response to the realisation of uncertainty.

We next substitute (2.22) into (2.21) and rewrite (2.21) in its equivalent robust form using a max protection function on a per-constraint basis Ben-Tal et al. [2004]. This results in:

$$\mathcal{B}b + \max_{\epsilon \in E} (\mathcal{B}A\epsilon + \mathcal{C}\epsilon) \leq d \tag{2.23}$$

$$W\epsilon \leq v : \mu \tag{2.24}$$

This generates a maximisation problem inside the constraint. Notice that the maximisation problem is an LP for any given $\mathcal{B}$, A and $\mathcal{C}$; ϵ is its decision variable with linear constraints $W\epsilon \leq v$ where μ represents its dual variable.

Using duality theory Ben-Tal et al. [2004], this maximisation can be transformed into a minimisation problem as follows:

$$\mathcal{B}b + \min_{\mu}(v^{\intercal}\mu) \leq d \tag{2.25a}$$

$$W^{\intercal}\mu \geq \mathcal{B}A + \mathcal{C} \tag{2.25b}$$

Notice that if constraint (2.25a) is satisfied for a value of $v^{\intercal}\mu$, then it will be satisfied for its minimum as well. Therefore we can drop the min operator. The resulting problem represents the constraint-wise robust counterpart of problem (2.23)–(2.24). As mentioned in Section 2.3.1, solving the dual problem here is more useful than solving the primal problem. Robust counterpart ensures that constraint (2.21) can be satisfied for any realisation of uncertainty within the uncertainty set E (i.e., the affine function $x(\epsilon)$ can be adjusted to compensate for all uncertainty realisations within E). Notice that here we only focus on the constraints. The epigraph form of the objective function can be written, and thus the robust objective can also be modelled as in (2.21). Alternatively, the objective may weigh up the outcome under a selection of scenarios or be optimised based on the expectation. We have used AARO optimisation in Chapter 4 to model the uncertainties associated with solar power and demand on the consumer side of the problem.

2.4 Aggregator, Consumers and Grid Interactions

Currently, small-scale resources cannot directly participate in the wholesale electricity market. Thus, in this thesis, we assume that aggregators are responsible for participating in the electricity market on behalf of consumers. An aggregator is a service provider that manages directly or indirectly groups of customers, e.g., consumers, in order to sell pools of loads and generators as single products in the electricity markets Iria et al. [2019]. In this thesis, we assume that there exists a contract between aggregators and consumers that allows aggregators to control consumer-owned DER for market services. In such a setting, aggregators equip their customers with a home energy management system (EMS) through which they can control DER. Consumers can get remunerated for their services depending on their agreement with aggregators. For instance, consumers might get a portion of the benefit made in the market or a discount on their electricity bills. In this thesis, we have not focused on the arrangements between aggregators and consumers.

Aggregators are also in charge of a) communicating with the DSO to ensure network feasibility and b) submitting the bids to the market. We have shown the required setting in Figure 2.7.

There are four main parties involved in our bidding problem: consumers, aggregators, the network, and the electricity market. DER information of each consumer is only available to the consumer or their aggregators; the network information is available to the DSO, and the market operator has any market-related data. However, since the network and consumer/aggregator problems are dependent, in each case, they communicate a limited amount of information. This could be as simple as the connection point power as in the approach of chapters 3, 4. Or the bid bands as in Chapter 5.

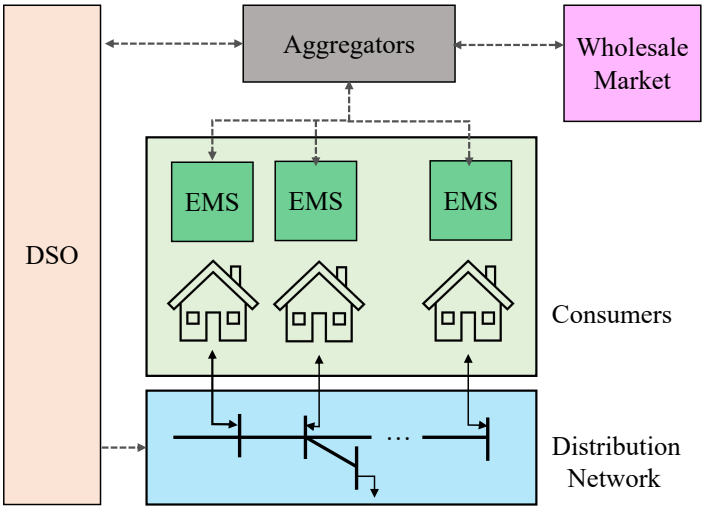

Figure 2.7: Aggregator interactions with consumers, DSO and the market

2.5 DER and Network Modelling

Here we provide a basic energy management system (EMS) and OPF models, which we use in chapters 3, 4 and 5 as a building block to construct our price-insensitive and price-sensitive bidding approaches.

2.5.1 Home Energy Management System

Throughout this thesis, we assume that consumers own a rooftop PV and a battery on top of their background load. In the following, we model the operational constraints of each DER in detail.

Solar PV

Using $t \in T$ for time, solar PV has a single variable p_t^{PV}, which can be curtailed down to zero from the forecast available solar p_t^F. This can be modelled as:

$$0 \leq p_t^{PV} \leq p_t^F \tag{2.26}$$

Battery Storage

A battery has variables for charge and discharge powers $p_t^{Ch}, p_t^{Dis} \in [0, R]$, and for the state of charge $E_t \in [E^{min}, E^{max}]$. These are linked with the state

of charge (SoC) at the previous time step through the equation:

$$E_t = E_{t-1} + \delta_t(\eta p_t^{Ch} - p_t^{Dis}/\eta) \tag{2.27}$$

where R is the battery charging / discharging rate, E^{min} and E^{max} respectively indicate the minimum and maximum battery state of charge, δ_t is the duration of each time step in hours, and η is the battery efficiency where η^2 gives the round-trip efficiency. Simultaneous charge / discharge decisions are avoided by including a binary variable u_t and the following constraints:

$$p_t^{Ch} \leq R u_t \tag{2.28}$$

$$p_t^{Dis} \leq R(1 - u_t) \tag{2.29}$$

Combined Power

The combined household power p_t is then:

$$p_t = p_t^{Dis} - p_t^{Ch} + p_t^{PV} - p_t^{U} \tag{2.30}$$

where we have included a parameter for the forecast household uncontrollable load $p_t^U \in \mathbb{R}$.

Objective function

In this thesis, we have assumed that consumers do not have any specific objective function other than minimising their cost (maximising the benefit in the market), which happens by the aggregator and is explained in each chapter. However, if there is an additional objective in a consumer sub-problem, it can be included in our model. We further explain this in sections 3.5, 4.5, and 5.3.1.

2.5.2 Network Model

Here, we model the distribution network constraints using the distflow equations Farivar and Low [2013]. Figure 2.8 summarises the notations. We use $i, j, k \in N$ for nodes in a tree network; p_n and q_n represent the real and reactive power of consumer $n \in C$. F_i^P, F_i^Q and I_i are the active power, reactive power and the squared current flowing into node i from the parent node k, where the line has resistance r_i, reactance x_i and impedance z_i. D_i represents the children nodes of node i; and C_i is the set of consumers at node i. Finally, V_i represents the squared voltage at node i. The network constraints can be written as:

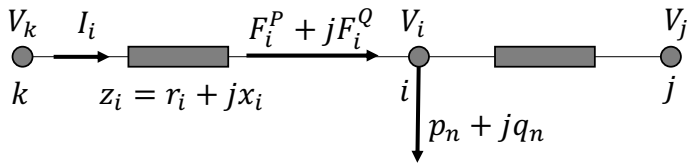

Figure 2.8: Distribution network notation

$$F_i^P - r_i I_i + \sum_{n \in C_i} p_n = \sum_{j \in D_i} F_j^P \quad \forall i \in N \tag{2.31}$$

$$F_i^Q - x_i I_i + \sum_{n \in C_i} q_n = \sum_{j \in D_i} F_j^Q \quad \forall i \in N \tag{2.32}$$

$$V_i = V_k - 2\left(r_i F_i^P + x_i F_i^Q\right) + z_i^2 I_i \quad \forall i \in N \tag{2.33}$$

$$v_{min}^2 \leq V_i \leq v_{max}^2 \quad \forall i \in N \tag{2.34}$$

$$F_i^{P2} + F_i^{Q2} = V_i I_i \quad \forall i \in N \tag{2.35}$$

$$0 \leq I_i \leq i_i^{max2} \quad \forall i \in N \tag{2.36}$$

Active and reactive power flow equations are given through (2.31)–(2.32); The voltage of each node is calculated through (2.33) and is enforced to be within its safe limits (v_{min}^2 and v_{max}^2) through (2.34). The complex power, flowing in each line, is given in (2.35) and finally, (2.36) limits the current of each line to the maximum line capacity i_i^{max2}.

Remark. As suggested in Farivar and Low [2013], the Conic relaxed convexification of the network subproblem (2.31)–(2.36) can be obtained by replacing "=" with "≤" in (2.35). However, the OPF result of such a relaxed problem is exact only if there is no upper bound limit on the voltages. In other words, when the voltage upper-bound limit is binding, the obtained results of such a relaxation do not lie within the feasible region. To avoid such an infeasible solution, in this thesis, we use the exact non-convex model (2.31)–(2.36) for our network sub-problem. As we show in chapters 3, 4 and 5, such a network model can be efficiently solved by the IPOPT solver.

2.6 Network Aware Coordination (NAC)

Since the approach presented in Chapter 3 builds on network-aware coordination (NAC) Scott et al. [2019], here we provide a more thorough review which we refer to in later chapters. NAC was used in a real-world trial to coordinate 31 residential batteries on a constraint feeder. The batteries are coordinated to reduce the need for the expensive diesel generator during periods of high feeder demand. The batteries in NAC were not used to provide frequency reserve services; they were scheduled using ToU tariffs within the ADMM approach (2.14)–(2.16) to reduce total operation cost. In the following, we provide a more detailed description of NAC.

In the first phase of the ADMM approach (2.14), every consumer schedules their resources accordingly to the ToU tariffs and DLMPs coming from the network subproblem. In the second phase (2.15), the network operator solves an optimal power flow problem to obtain network-feasible results. If no network is violated (e.g., operation at off-peak periods) at the convergence of the ADMM approach, the dual variables (DLMPs) obtained by (2.16) will be zero. However, during peak periods when the network is overloaded, the dual values in (2.16) get non-zero values. As a result, depending on the combination of tariff price and λ (please see equation (2.13)), consumers change their charge and discharge decision which avoids network violation. At the convergence of ADMM, the DLMPs represent the values for which network constraints are not violated.

Chapter 3

Network-Secure Energy and Reserve Bidding

3.1 Introduction

In this chapter, we study a price-insensitive bidding approach that enables aggregators to calculate consumer bids for energy, raise, and lower reserve markets while addressing the challenges we identified in Chapter 1. The particular challenge we address in this chapter is to ensure that DER bids are network-secure, meaning that aggregators do not overload the distribution network.

Alongside research, regulations are changing in favour of DER to enable them to provide reserve services. For example, Energy Networks Australia and AEMO agreed to commit to the Open Energy Networks Project (OpEN) in 2018 – a project which provides greater market access to energy and reserve services for distribution-level DER. Such market interactions should not create any network issues. For this to be accomplished, aggregators need to account for network constraints when making bidding decisions – a task which is not straightforward as the network and DER are owned and operated by different stakeholders (the DSO, consumers and aggregators). Other than the privacy concerns of each stakeholder, they might have conflicting operating targets making this coordination more difficult.

As explained in Section 2.2.3, the literature mainly counts on either operating envelopes or solving centralised / distributed OPFs to guarantee network constraints. Notice that these approaches are for a wide range of applications and not necessarily a bidding problem. In summary:

- Envelopes provide a pure local solution to the problem as they guarantee that no network constraint will be violated if consumers stick to their envelopes locally. However, current proposals recommend that distribution system operators (DSOs) should repeatedly calculate op-

erating envelopes and allocate them to each DER without considering consumer preferences, uncertainty or market participation (see Section 2.2.3). Since some consumers might need less flexibility (e.g., due to self-consumption), such proposals can result in envelopes conservatively limiting market-participating consumers.

- Centralised approaches provide a (near) global-optimum solution by solving a system-wide OPF problem. Centralised methods ignore the distributed nature of the problem and assume that a DSO can control and schedule all DER centrally. However, even if the DSO had full observability on all consumers, modelling numerous consumers within the grid leads to a large-scale, non-linear and non-convex optimisation problem. Due to DER state variables, such an optimisation problem is potentially time coupled. Thus, it is unlikely that these approaches scale to real-world problems, especially within a time frame required for real-time market operation, e.g., 5 minutes in the NEM.
- A distributed approach breaks the large-scale central problem into smaller pieces, each being solved independently while communicating some information about their common variables. Similarly to a centralised technique, a distributed method is able to obtain (near) global-optimum results, yet, it preserves some level of privacy for the consumers. Plus, a distributed approach shares the computational burden amongst multiple agents and, if implemented in parallel, can significantly reduce the run time.

Based on the above comparisons between the available approaches, a distributed setting seems to be the most effective strategy for our bidding problem. It allows us to break the problem down at the level of every consumer, resulting in a DSO subproblem and many consumer subproblems, each of which can be solved independently using their private information. As explained in Section 2.4, we assume that aggregators are in charge of solving consumer optimisation problems. To avoid working with any particular number of aggregators, here, without loss of generality, we assume that every consumer is an aggregator. Thus, we interchangeably use the terms aggregator and consumer to refer to the consumer sub-problem throughout this chapter. Notice that even if there is one single aggregator managing all consumers, the problem of every consumer can still be solved independently, either locally at consumer EMS or on the cloud, as there are no coupling constraints between consumer problems. This setting is introduced in NAC Scott et al. [2019] in which consumers optimise their DER based on a retail ToU tariff while coordinating with the grid using the distributed approach ADMM. For more information on NAC, please refer to Section 2.6. Note that the problem we deal with in this thesis is significantly more challenging than the coordination

problem NAC was solving. Unlike the coordination in NAC, here, we do not have a well-defined operating point for solving a distributed OPF. The reason is that here the final operating point of consumers depends on the dispatch in the energy market and the activation of the raise or lower reserve market, which is random and hard to predict.

To overcome this issue, we extend NAC to enable the DSO and aggregators to negotiate operating envelopes for every consumer rather than negotiating consumer CPPs. Moreover, our solution approach builds on the literature of operating envelopes in two main ways. 1) It brings consumer preferences into envelopes as aggregators can now negotiate operating envelopes that reflect their customers' preferences rather than having the envelopes dictated to them by the DSO. 2) It brings a system-wide perspective to the local envelopes. Thus, similarly to a distributed approach, we can obtain (near) global-optimum results.

To ensure that our envelopes and bids account for uncertainty variabilities, such as those around solar PV power and demand, we implement our approach on a model predictive control (MPC) framework that moves forward in lock with the real-time market, i.e., 5 minutes in the NEM. This also allows aggregators to include consumers' latest battery state of charge (SoC) in every optimisation. Notice that battery SoC can change depending on whether or not a contingency occurs. If a contingency does occur, the significance of the desired response can also impact the battery SoC. In summary, every 5 minutes, aggregators use their customer's latest (the most accurate) uncertainty information and battery SoC to negotiate with the grid their operating envelopes and obtain the network-secure energy and reserve bids.

We organise this chapter as follows: we first provide an upfront description of our method in Section 3.2. We then present our decomposition and ADMM approach in Section 3.4. We next provide a simple two-node test system and discuss the conditions on which our solution approach might fail to provide a feasible answer in Section 3.3. We present our consumer bidding optimisation to obtain inflexible energy and reserve bids in Section 3.5. We continue this chapter by presenting the detailed network subproblem in Section 3.6. The model predictive control implementation of our approach is described in Section 3.7. In Section 3.8, we illustrate the effectiveness of our solution approach by comparing it with a network-free as well as three comparative approaches based on operating envelopes. Finally, we summarise our approach and findings in Section 3.9.

3.2 The General High Level Problem

Figure 3.1 shows a general scheme of our distributed bidding approach that is repeated at every MPC iteration. As can be seen in Figure 3.1, we decom-

pose the problem so that the DSO and every aggregator (here consumer) have their own subproblems. In a consumer subproblem ①, each consumer uses the wholesale market as well as the distribution locational marginal prices (DLMPs) to optimise their energy and reserve bids. DLMPs are the Lagrangian multipliers (dual variables) for the energy conservation constraint at each distribution node and are obtained within the ADMM approach. Notice that DLMPs are different from LMPs in the transmission network and are meant to ensure distribution network security. If consumer behaviours do not violate the network, DLMPs will be zero. However, in case of a network violation, DLMPs increase to encourage consumers to change their behaviour until no constraint is violated. Consumers then communicate to the grid their required operating envelope[1].

Next, the network subproblem ② solves two OPFs, each associated with one extreme of the envelope, to ensure the secure operation of the network. The reason why we only use two OPFs is to ensure network feasibility for the worst-case conditions in which consumers are simultaneously injecting / withdrawing power to / from the grid (we will elaborate more on this in the upcoming section). The consumer and DSO negotiate until they converge to (near-) optimum and network-secure bids, as well as operating envelopes that satisfy network limits. Finally, the obtained network-secure bids ③ are submitted to the wholesale market.

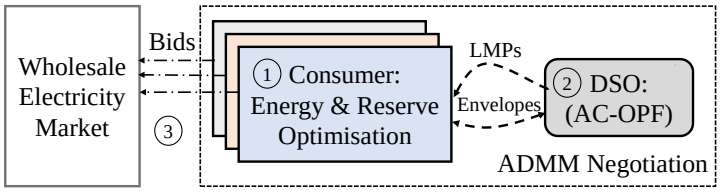

Figure 3.1: Overall network-secure bidding approach

In the following, we separately explain each part of the proposed approach. We start with a 2-node system in Section 3.3 and discuss the conditions under which our proposed approach provides a feasible solution. We next present (at high-level) our distributed approach in Section 3.4 and then thoroughly model the consumer and network subproblems of the proposed approach in sections 3.5 and 3.6, respectively.

[1]In this chapter, operating envelopes only cover consumers' connection points associated with their real power. We add the reactive power into our calculations in chapters 4 and 5.

3.3 Illustrative Example: A 2-Node Test System

In Section 3.2, we mentioned that we obtain the operating envelopes by solving two OPFs associated with the extreme cases where all consumers are simultaneously injecting / withdrawing power to / from the grid. However, since the OPF problem is non-convex, there might be cases where OPF gives a feasible solution at the extremes yet infeasible for some values within the envelope. Here, we use a simple 2-node test system, shown in Figure 3.2, to explain conditions under which using two OPFs for the operating envelope provides a feasible solution. To do so, we first provide an example of a case where solving OPFs for the extremes fails to provide feasible operating envelopes and explain how our assumptions avoid such cases. We then use more realistic conditions and study the infeasibilities within the envelopes (holes in the feasible region as explained in Nazir and Almassalkhi [2021]). We observed that for realistic impedance values (even when our assumptions are neglected), holes are not formed, and thus checking the extremes can provide safe operating envelopes.

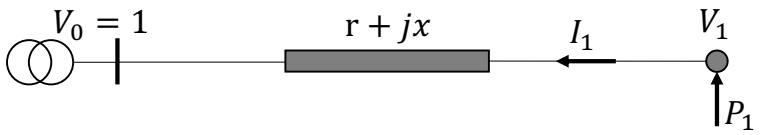

Figure 3.2: A 2-node test system

3.3.1 Extreme Case

Let us use impedance of $r = 0.55$ p.u. and $x = 1.33$ p.u. – values used in Nazir and Almassalkhi [2021]. Notice that such a $\frac{r}{x}$ ratio is not realistic in distribution networks where $\frac{r}{x} > 1$. Assuming zero reactive power and equations (2.31)–(2.35), we plot the voltage with respect to the real power injection at bus 1 in Figure 3.3.

According to Figure 3.3, the voltage at bus one initially increases as real power injection increases. This area is where the sensitivity of the voltage to real power injection is positive. However, from a point onward, the voltage starts dropping as more real power is injected. This is the area where the sensitivity of voltage to the real power injection is negative. From this point onward, the current and thus the losses in the system increase to a point where the voltage decrease associated with losses overcomes the voltage increase associated with real power injection. Notice that this figure is produced assuming that lines' thermal limits are not violated.

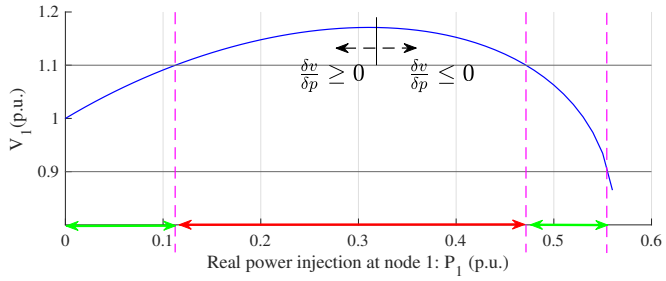

Figure 3.3: Voltage of node 1 for different real-power injections

The green / red arrows Figure 3.3 show the voltage feasible / infeasible points of the envelope. One can interpret the red region as an infeasible hole within the envelope. In other words, if the extreme is given as the envelope (0 to the third pink dotted line in Figure 3.3), there will be points within the envelope where the network constraints are violated while the extreme points themselves satisfy the voltage limits. This means checking the extreme points alone (as we suggest) will not be enough to ensure a voltage-safe envelope. However, notice that in such a case, the sensitivity of voltage to real power injection will be negative, i.e., $\frac{\delta v}{\delta p} \leq 0$, while we design our approach for regions where $\frac{\delta v}{\delta p} \geq 0$. In other words, our suggested envelope, in this case, will be from 0 to the first pink dotted line. Notice that losses in the next green region are significantly high, and power systems are not designed to work at these inefficient operating points. We plot the current and injected power at bus one, together with the power received at the top of the feeder (what reaches the market) in Figure 3.4.

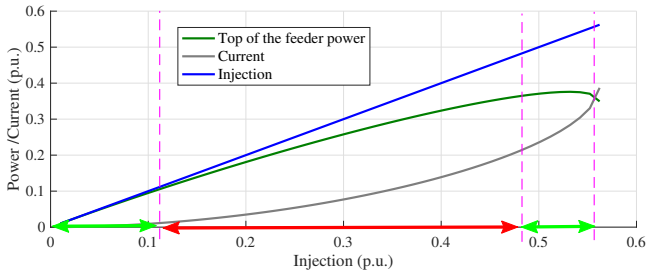

Figure 3.4: Top of the feeder power and current for different real power injection

The dark green diagram shows the power reaching the market, and the blue line is the power injected at bus 1 (the difference between the two shows the losses). As can be seen in Figure 3.4, the losses and current are significantly higher in the second green interval where the OPF solution (ignoring the thermal limits in this case) is feasible, yet $\frac{\delta v}{\delta p} \leq 0$. Notice that charts in Figure 3.4 finish at the voltage collapse point – a point from which onwards

the power flow equations do not have a solution.

3.3.2 Realistic Case

We have plotted a similar figure as in 3.3, but instead of arbitrary values for r and x, we have summed the impedance of all lines in the 69-bus and 141-bus distribution networks and used it to generate the equivalent two bus network. The total impedance for 69 and 141-bust test systems are respectively 14.75+j6.69 p.u. and 4.92+j3.32 p.u[2]. These values are calculated using the nominal voltage as the based voltage (V_{base}) and apparent base power, i.e., $S_{base} = 100$MVA. We show the voltage profile for the injection at bus 1 in Figure 3.5.

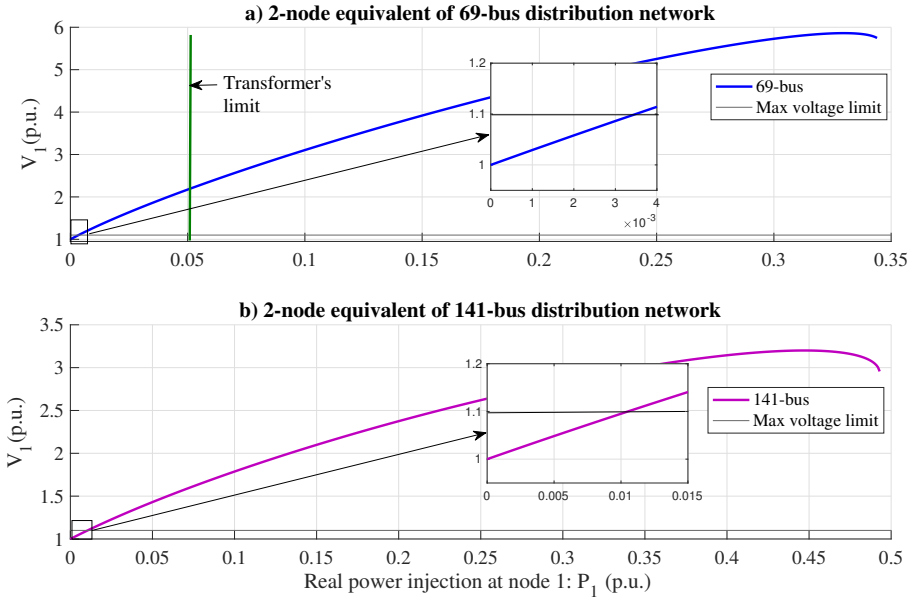

Figure 3.5: Voltage of bus 1 for different real-power injections

As plotted in Figure 3.5, using realistic impedance values, the system reaches the voltage collapse point (where OPF becomes infeasible) before the voltage can get back to the feasible region and create infeasible holes. Thus, even if $\frac{\delta v}{\delta p} \geq 0$ condition is neglected, in practice, only the first green arrow in Figure 3.3 is acceptable. Also, it is worth mentioning that these figures are plotted neglecting the thermal limits of the lines / transformers. However, if thermal constraints are included, the feasible region will shrink further. For example, as shown in Figure 3.5-a, the thermal limit of the transformer hits before the voltage sensitivity to real-power injection becomes negative. In

[2]Notice that, unlike the previous case, in these networks we have: $\frac{r}{x} > 1$.

this chapter, we have neglected reactive power; we further discuss the effect of reactive power on the feasible region in Chapter 4.

Remark The above example is for a balanced network. If the network is not balanced, using 2 OPFs for the extremes of the envelopes might not provide enough guarantee for the network feasibility. This is because the negative mutual impedance of lines may result in conditions in which the OPF is satisfied for the extreme condition, yet if one consumer injects less than the extreme, the network can be violated. In this thesis, we only focus on balanced networks and leave further study in this regard to future work.

3.4 The ADMM Algorithm

We treat each consumer $n \in C$ as a generating unit exchanging with the grid the real power $p_n^e \in \mathbb{R}^{|T|}$ at each time step in horizon T. Consumers can increase / decrease their output (with respect to p_n^e) to provide raise / lower reserve services p_n^r / $p_n^l \in \mathbb{R}^{|T|}$ leading to their maximum $\overline{p}_n$ / minimum $\underline{p}_n$ power exchange with the grid (i.e., $[\underline{p}_n \ \overline{p}_n]$ presents the operating envelope of the consumer). We put $\overline{p}_n$ and $\underline{p}_n$ in a vector $p_n \in \mathbb{R}^{2|T|}$ to increase readability. Consumers also have their own internal variables x_n as well as the objective and constraint functions f_n and g_n which take p_n and x_n as inputs. We drop the subscript to represent all consumer exchange powers, $p \in \mathbb{R}^{2\times|C|\times|T|}$, which together with the network internal variables y are inputs to the network's own constraint function h. The multi-period OPF can be written as:

$$\min \sum_{n\in C} f_n(p_n, x_n) \tag{3.1a}$$

$$\text{s.t.} \quad \forall n \in C : g_n(p_n, x_n) \leq 0 \tag{3.1b}$$

$$h(p', y) \leq 0 \tag{3.1c}$$

$$p - p' = 0 \tag{3.1d}$$

In the above, we have duplicated the real power exchange variables, so the consumers and the network have their copies (p and p'). The duplicated variables are enforced to have the same values through (3.1d), which is the equation we will now relax to decompose the consumers from the network.

The penalty term of the augmented Lagrangian applied to the equality connection constraint (3.1d) is:

$$\mathcal{L}^*(p, p', \lambda) = \lambda^\intercal(p - p') + \frac{\rho}{2}||(p - p')||_2^2 \tag{3.2}$$

$\lambda := [\lambda_r \ \lambda_l]^\intercal$ is the vector of dual variables for the relaxed constraints (3.1d)

and $\rho \geq 0$ is the penalty parameter of the augmented Lagrangian. We use the ADMM algorithm, explained in Section 2.3.3 to iteratively solve (3.1a)−(3.1d) to its optimum. The ADMM algorithm has three phases per iteration k:

$$p^{(k)} := \min_{p,x} \sum_{n \in C} \left[f_n(p_n, x_n) + \mathcal{L}_n^*(p_n, p_n'^{(k-1)}, \lambda_n^{(k-1)}) \right]$$
$$\text{s.t. } \forall n \in C : g_n(p_n, x_n) \leq 0 \tag{3.3a}$$

$$p'^{(k)} := \min_{p',y} \mathcal{L}^*(p^{(k)}, p', \lambda^{(k-1)})$$
$$\text{s.t. } h(p', y) \leq 0 \tag{3.3b}$$

$$\lambda^{(k)} := \lambda^{(k-1)} + \rho^{(k)} \cdot (p^{(k)} - p'^{(k)}) \tag{3.3c}$$

Notice that both the objective and constraints of each consumer $n \in N$ in (3.3a) are independent; thus, every consumer can solve their problem separately and in parallel. In the first phase (3.3a), consumers optimise for p, holding p', and λ constant at their $k-1$-th values. In the second phase (3.3b), the network optimises for p', holding p and λ constant at their k-th and $k-1$-th values, respectively. Finally, the dual variables λ are updated in (3.3c), completing the k-th iteration.

Through (3.3a)–(3.3c), consumers schedule their appliances to obtain their bids for each market. They then communicate with the network their preferred operating envelope that covers the potential maximum and minimum CPPs that can realise as a result of their raise and lower reserve bid activation. The DSO then checks whether consumer envelopes satisfy the network constraints and updates λ accordingly. When the algorithm converges, λ represents the price of having the network constraints satisfied at the extremes of the envelope. Compared to a central approach which requires *all* of the information of *all* of the consumers[3], our approach only requires consumers' preferred minimum and maximum connection point power, i.e., operating envelopes. Thus, not only does our approach provide a higher privacy level for consumers, but also (from the data communication perspective) the necessary data exchange is much simplified.

[3]This information includes consumers' battery SoC, PV power, their uncontrollable load and any other appliances a consumer might have.

3.4.1 Stopping Criteria and Convergence

In line with Boyd et al. [2011], we define the stopping criteria using primal and dual residuals as follows:

$$R_p^{(k)} := \big((p_1^{(k)} - p_1'^{(k)}), (p_2^{(k)} - p_2'^{(k)}), ...\big)^\intercal \tag{3.4a}$$

$$R_d^{(k)} := \big(\rho(p_1'^{(k)} - p_1'^{(k-1)}), \rho(p_2'^{(k)} - p_2'^{(k-1)})...\big)^\intercal \tag{3.4b}$$

The primal residuals (3.4a) represent the constraint violation at the current solution, and the dual residuals (3.4b) the violation of the KKT stationarity constraint Boyd et al. [2011].

To feed the proposed approach with the latest uncertainty information and obtain more accurate results, we implement (3.3a)–(3.3c) within a model predictive control framework. More explanation on our model predictive control implementation is given in Section 3.7.

3.5 Consumer Subproblem

We break the DER constraints into two groups: constraints for linking the absolute raise and lower quantities to biddable values for the FCAS markets, and those related to the physical and operating limits of the DER. Notice that consumers solve their bidding problems independently. Thus, we work with one consumer at a time, so here, we drop the subscript n to increase readability.

3.5.1 Market Linking Constraints

Let $p^e \in \mathbb{R}^{|T|}$ be the vector, including consumer bids into the energy market at different time steps. We also introduce a pair of variable vectors $\Delta p_m^r, \Delta p_m^l \in \mathbb{R}_{\geq 0}^{|T|}$ for each frequency market $m \in M$, to represent the amount of raise and lower capacity to bid into the market. Consumers increase / decrease their injection by Δp_m^r / Δp_m^l, with respect to their energy bid p^e, to provide raise or lower reserve services. Therefore, the corresponding power exchanged with the network in each case can be given by the related variables $p_m^r, p_m^l \in \mathbb{R}^{|T|}$, where:

$$p_m^r = p^e + \Delta p_m^r \tag{3.5a}$$

$$p_m^l = p^e - \Delta p_m^l \tag{3.5b}$$

A reserve response is only required from one market at a time. So, when

checking network feasibility, we only need to consider the most extreme raise / lower values. We write this as the max and min over the markets, which we relax as follows:

$$\overline{p} = \max_{m \in M}(p^r_m) \rightsquigarrow \overline{p} \geq p^r_m \quad \forall m \in M \tag{3.5c}$$

$$\underline{p} = \min_{m \in M}(p^l_m) \rightsquigarrow \underline{p} \leq p^l_m \quad \forall m \in M \tag{3.5d}$$

We expect this to be an exact relaxation since larger $\overline{p}$ or smaller $\underline{p}$ will lead to more active network constraints (relative to p^e) rather than any benefit to the network subproblem. Depending on the required frequency response, the consumer injection can be anywhere between the minimum $\underline{p}$ and maximum $\overline{p}$, which makes the consumer's operating envelope.

The cost associated with the market participation is given by the following component to the objective function:

$$\sum_{t \in T} \delta_t \left(\pi^e_t p^e_t + \sum_{m \in M} \left(\pi^r_{m,t} \Delta p^r_{m,t} + \pi^l_{m,t} \Delta p^l_{m,t} \right) \right) \tag{3.5e}$$

where δ_t is the time step duration in hours; π^e_t is the wholesale energy market price at t; and $\pi^r_{m,t}$ / $\pi^l_{m,t}$ are the prices of the raise / lower reserve market m at t. These amounts are payable whether or not a contingency actually occurs. However, a contingency can have a small impact on the SoC of the battery. To approximate any lost or gained energy due to reserve deployment, we model the probability of a contingency event occurring for each market $\mu^l_{m,t}$ and $\mu^r_{m,t}$[4], and assume that the value of the lost / gained energy is at the energy market price π^e_t:

$$\sum_{t \in T} \sum_{m \in M} \pi^e_t \cdot \delta'_m \left(\mu^r_{m,t} \cdot \Delta p^r_{m,t} - \mu^l_{m,t} \cdot \Delta p^l_{m,t} \right) \tag{3.5f}$$

where δ'_m is the worst-case number of seconds, we would need to be deployed for each market m for a single contingency. The significance of these deployment costs shrinks to zero as contingencies become rarer.

In our example, (3.5e), (3.5f) and the Lagrangian penalty term (3.2) are the only values in the objective; however, other forms of DER might have additional costs associated with the operation, and there may be other electricity charges such as network tariffs.

[4]These values can be updated every five minutes as our MPC moves forward.

3.5.2 DER Constraints

We need to ensure the DER constraints are satisfied under participation in each market, including a case where no frequency support is required. We presented the DER constraints in Section 2.5.1. We duplicate the same DER variables and constraints for each scenario of interest, i.e., p^e, p^r_m, or p^l_m. Regarding the battery SoC constraint (2.27), we use the previous SoC form the energy market, i.e., E_{t-1} for raise and lower FCAS scenarios. The reason is that raise, and lower bids are capacities, and thus, there is no guarantee whether they are deployed. Every 5 minutes, when we rerun our optimisation, we take the latest SoC into account. Therefore, if reserves happen to be deployed within a time step, our approach still takes it into account.

3.5.3 The Combined EMS Subproblem

We model the optimisation problem of consumers within a home energy management system (EMS). In summary, the EMS subproblem for a single customer is to minimise the sum of (3.5e), (3.5f) and the associated Lagrangian penalty term (3.2). The constraints consist of the market linking constraints (3.5a–3.5d), and 7 copies of the DER variables and constraints (2.27–2.30), one for each market: p^e, p^r_m and p^l_m, where $m \in \{1, 2, 3\}$.

3.6 Network Subproblem

Since there are no time coupling constraints in the network subproblem (unlike in the EMS subproblem due to the battery SoC constraint), the network subproblem for each time step t can be solved separately. The objective value for the network subproblem consists of just the corresponding Lagrangian penalty term (3.2).

Our network model includes two OPFs, one for each extreme case in the operating intervals $\underline{p}$ and $\overline{p}$. Therefore, we repeat constraints (2.31)–(2.36) twice for the duplicated envelope variables, i.e., $\underline{p}', \overline{p}'$. It is worth mentioning that the two sets of OPFs are solved within one ADMM approach. This is because the upper and lower bound of the operating envelopes are dependent in the original central problem. Thus, we cannot use two separate ADMM approaches (one for the upper and another for the lower bounds of the envelope). Fortunately, since ADMM breaks the central problem into smaller subproblems, it can deal with large-scale problems that might not be solvable centrally. We provide further discussion on the performance of ADMM on larger networks in Chapter 5 using a realistic network.

Remark Notice that we only check the network constraints at the edge cases. In other words, we assume that if the network is not violated at its edge operating points, it also will not be violated for operating points less extreme

than the edge cases. For this assumption to hold, we need the network to be radial and operate in the voltage-stable band. As explained in our 2-node example, since the distribution networks are either radial or operated radially, we expect that such an assumption does not limit the real-world application of our approach. For more information on this, please see our proof in Appendix A.4.

3.7 Model Predictive Control

To use the latest uncertainty information, including the most accurate PV power, residential demand, the energy and reserve market price forecasts, we apply our proposed network-aware optimisation approach within a model predictive control framework. In this method, we run our proposed approach in lock with the electricity market time frame (i.e., every 5 minutes as in the NEM). This also allows us to update the SoC value in every re-optimisation (as the SoC might change when consumers respond to the frequency deviations). Note that even though consumer decisions are enacted only for the first five minutes of every optimisation, we solve a multi-period problem at every horizon. This ensures that the decisions in the first five minutes are not shortsighted.

In summary, at each MPC iteration, our ADMM approach negotiates between two blocks of subproblems (i.e., consumers and network). In the consumer block, we have consumers solve a self-scheduling problem independently, and since the problem is for one consumer, it is easily solvable. The network block includes 576 OPFs[5] that can be solved independently and in parallel.

3.8 Results

To illustrate the effectiveness of the proposed approach, we use the 69-bus distribution network Savier and Das [2007], given in Appendix A, modified with 207 consumers. Each consumer is equipped with a 5kW PV system and a 5kW / 10kWh battery with round-trip efficiencies of $\eta^2 = 90\%$. We use anonymised solar and demand data for 27 consumers in Tasmania, Australia Scott et al. [2019], and randomly assign this data to the consumers in our networks. The 207 consumers on our study day consume a total of 3,613 kWh ($\approx$ 17.5 kWh per consumer per day). Minimum and maximum overall load at different hours are 63.5 kWh and 281.1 kWh, respectively, with average hourly consumption of 150.5 kWh. PV power generation of our 207 consumers for

[5]This includes 288 OPFs (24 hours discretised every 5 minutes) for the upper bound of the envelope and 288 OPFs for the lower bound of the envelopes for the next 24 hours.

the same day aggregates to a total of 4,166 kWh ($\approx$ 20 kWh per day per consumer). Total hourly PV generation (during our study day) varies between 0 kWh to 772.9 kWh, with the average hourly generation of 173.6 kWh. The PV/load proportion during peak PV generation in our study day is 4.49.

We participate in 7 markets (1 energy, three raise and three lower contingency FCAS markets). The 5-minute energy and reserve market prices are taken from the NEM, which are also provided in Appendix A. Finally, we use the Gurobi and IPOPT solvers in JuMP, Julia Dunning et al. [2017] to solve our consumer and network subproblems.

Notice that the approach presented in this section is independent of the markets and can work for any electricity market that allows aggregator bidding. In fact, we only need to set m to the number of available reserve markets and use the price forecasts from the desired market (either day-ahead or real-time forecasts depending on the market) in the objective function (3.5e).

3.8.1 No Market Participation

In this section, we assume that consumers do not directly participate in the electricity market. Consumers use one of the following strategies to schedule their DER:

1. *Self Consumption*: in which consumers cannot inject any power into the grid. Thus, they use their DER to meet their own demand and reduce their electricity bill when there are time-of-use (ToU) retail tariffs.

2. *ToU+FiT*: in which consumers are paid according to a feed-in tariff (FiT) for the power they inject into the grid. The consumer objective function minimises the combined cost of purchasing electricity at a ToU tariff and selling it at a FiT.

Table 3.1 reports the ToU and FiT prices used in our experiments.

Table 3.1: Time-of-use and feed-in tariffs

ToU			FiT
Peak 7-9am, 5-8pm	Shoulder 9am-5pm, 8-10pm	Off peak All other time	
21.868 ¢	17.160 ¢	12.793 ¢	7.5 ¢

We report the total benefit obtained using self-consumption and ToU+FiT approaches together with a case where consumers do not own any battery (*No Battery*) in Table 3.2. Notice that when consumers do not own any battery, they are not able to shift their load from peak price to off-peak price in the ToU tariff. Thus, as reported in Table 3.2, they have obtained the least

benefit. On the contrary, with batteries, consumers manage to significantly reduce their bills by 208% (self-consumption) and 790% (ToU+FiT). Since these approaches limit DER flexibility to either self-consumption or injection at FiT, they did not push the distribution network towards its limits.

Table 3.2: Total benefits: no market participation

Approach	No Battery	Self Consumption	ToU+FiT
Total Benefit ($)	-1295.9	-420.3	-145.4

3.8.2 Active Market Participation

In this section, we study the case where consumers actively participate in the wholesale market. To evaluate the benefit of our bidding approach, we compare the performance of the following three methods:

1. *Energy*: in which consumers only participate in the energy market. We use energy prices in the consumer objective subject to constraints (2.27)–(2.30) to ensure DER operational limits only for the energy market. We develop this approach to investigate the benefit that participating in the energy market brings compared to the no-market-participation strategy presented in the previous section. Plus, this approach provides insights into the effectiveness of participating in the reserve market on top of the energy market.

2. *Sequential*: in which consumers sequentially participate in the energy and reserve markets. To do so, consumers first use a similar approach as in Energy to obtain their bids for the energy market. They then calculate their raise and lower reserve capacities for their obtained energy bids.

3. *Co-optimised*: in which consumers co-optimise their decisions in energy and reserve markets, based on the approach we presented in this chapter.

To compare different aspects of our bidding approach, we will introduce other approaches (where needed) in the rest of this section. To study our approach in detail, we first report the one-day performance of our approach and then present the three-month benefit of consumers using different approaches at the end of this section.

3.8.2.1 Network-Free Economic Performance

Table 3.3 gives the total benefit broken down into each market when the network is neglected for the market price data on 22 January 2020.

Table 3.3: Total benefits ($) network-free

Market		Approach		
		Energy	Sequential	Co-optimised
Energy		679.5	679.5	252.2
Raise	6-sec	–	982.8	1700.0
	60-sec	–	477.4	920.2
	5-min	–	73.4	87.9
Lower	6-sec	–	13.8	113.4
	60-sec	–	19.0	22.7
	5-min	–	19.4	22.4
Total		679.5	2265.1	3118.7

Compared to Table 3.2, consumers obtain a significantly higher benefit when actively participating in the wholesale market. The reason is that consumer DER, such as batteries, obtain benefits by arbitraging energy (charging at low-priced periods and discharging at high-priced periods). However, using a ToU+FiT approach, consumers still use their batteries for self-consumption as FiT price is lower than prices within the ToU tariff.

Moreover, as expected, participating in reserve markets improves the total benefits significantly. Compared to the energy approach, sequential and co-optimised approaches could respectively obtain $\approx$ 230% and $\approx$ 360% higher benefits. The reason is that the co-optimised approach is able to make the best decisions as it can allocate the available flexibility optimally to each market. However, the sequential strategy focuses on the energy market. That is why the benefit of the sequential in the energy market is equal to the Energy case and higher than the energy benefit in the co-optimised approach.

Since the network constraints are neglected, the above approaches can violate the distribution network constraints. Table 3.4 reports the number of voltage violations in each approach. Notice that to report under / overvoltages for the FCAS market, we do not model a contingency. Instead, we have checked whether the consumer response violates any network constraints when, hypothetically, a contingency occurs. Notice that there are 69 nodes in our network, and thus, a voltage violation of 69 is possible at every operating interval. Given our 5-minute time discretisation, the total possible violation in each market is 19,872 (69×288). Since the energy case does not participate in any FCAS market, no network violation has been reported for it in the FCAS market.

We next include network constraints and complete our network-secure bidding approach. We find that the Co-optimised approach only takes a small loss once it is network-secure. So, it still significantly outperforms the other methods. For this reason, we focus on the co-optimised approach in the rest

Table 3.4: Voltage violations in the network-free scenario

Approach	Number of Violations				
	Undervoltage		Overvoltage		Total
	Energy	FCAS	Energy	FCAS	
Energy	166	–	151	–	317
Sequential	166	1591	151	584	2492
Co-optimised	238	3283	406	1164	5091

of our experiments.

3.8.2.2 Network-Secure Economic Performance

Figure 3.6 reports the network-secure benefits obtained by the proposed co-optimised approach compared to the network-free case. As can be seen, slightly lower benefits are obtained when the network is included ($ 3094.9 vs. $ 3118.7). This is because the DER integration level is higher than the network's capacity, and thus, DER need to be limited to avoid network violation.

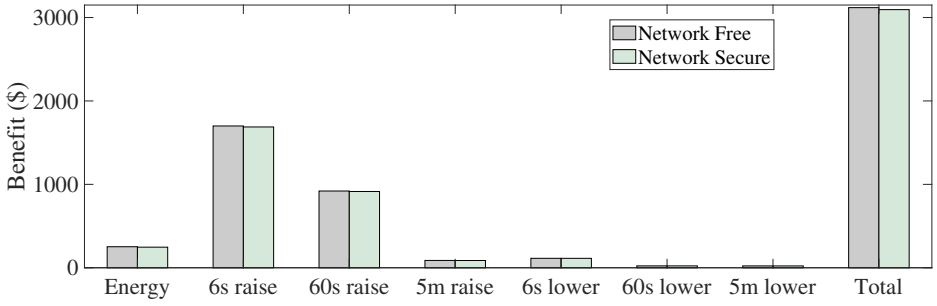

Figure 3.6: Total benefit: network-secure vs. network-free

Minimum and maximum voltages across all nodes and all markets for our co-optimised approach are given in Figure 3.7. The Grey colour shows the network-free voltages while the green colour shows the network-secure results.

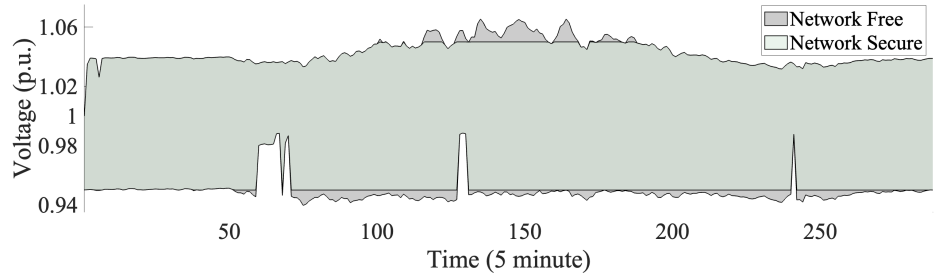

Figure 3.7: Min and max voltages: network-secure vs. network-free

As plotted in figure 3.7 the voltages of our network-secure approach falls into the safe voltage envelope (i.e., $0.95 \leq v \leq 1.05$) for any energy or raise / lower reserve activation scenario.

3.8.2.3 ADMM-based Envelopes vs. Literature

In this section, we investigate the effectiveness of our proposed envelopes based on the ADMM approach with some available envelopes as follows:

1. Fixed Export Limits: here, inspired by real-world practice, we impose a 5kW export limit on every consumer.
2. Fixed Envelopes: here, the DSO uses the maximum PV and minimum demand during a day to obtain envelopes of the same width for every consumer. Notice that in practice, this is done over a year or a season. Therefore, in reality, such envelopes are much more restrictive. Plus, here, we also assume that the DSO has a perfect forecast of every house demand and PV power generation for the entire day.
3. Dynamic Operating Envelope: here, the DSO runs an OPF every 5 minutes to obtain envelopes of different widths for every consumer. The goal here is to maximise the network throughput given consumer background loads, PV generations and batteries. Including consumer information allows the DSO to obtain representative envelopes, yet in reality, such information is not available to the DSOs, and thus, the envelopes could not be this representative.

Table 3.5 reports the total benefits obtained using the introduced operating envelopes as well as network-free and our proposed NAC-based envelopes. The reported run times are obtained using a laptop computer with a 2.50 GHz Intel$^{(R)}$ Core$^{(TM)}$ i7 and 8 GB of memory.

Table 3.5: Total benefit: network-aware vs. operating envelopes

Approaches	Benefit ($)	Time (s)	# Violations
Network-Free	3118.7	0.018	4524
Fixed Export	2796.8	0.031	1756
Fixed Envelope	2936.8	0.053	0
Dynamic Envelope	3015.9	0.053	0
Proposed	3094.9	27.21	0

As reported in Table 3.5 fixed export limits could not meet the constraints of the network. The reason is that when batteries come into the picture, limits for withdrawing power also become crucial. Moreover, as the 5kW limit is not obtained through optimisation, this approach reduces the aggregator benefit more than other approaches. Coming up next, both fixed and dynamic

operating envelopes assume that perfect information is available. So, they can obtain representative envelopes. However, our network-aware approach could attain higher benefits (+5% and +3% compared to fixed and dynamic envelopes, respectively), whilst the DSO in our approach does not require any consumer information other than their CPPs. The time reported for fixed and dynamic operating envelopes do not include network optimisation time. The reason is that we assume the DSO could do this in advance of the operating interval. However, the time reported for our network-aware approach does include both consumers and network solve time. Given the 5-minute operation clock of the electricity market, all the reported times are reasonable and not limiting in a real-time biding context.

3.8.3 Computation Performance

We decompose each consumer from the network. Thus, within a single ADMM iteration, all our consumer subproblems can be solved separately (either in parallel or sequentially). Also, notice that the energy coupling constraints are a part of the consumer subproblem (e.g., battery SoC constraint). Meaning that from the grid perspective, there is no time-coupling constraint in the network subproblem, and thus our network subproblem can be separated into an OPF for each time step and each power flow scenario under consideration, i.e., extremes of the envelopes. Therefore, the multiperiod network problem will translate into multiple single-period subproblems. This allows parallel computation, which reduces the computational time significantly.

We report the total computational time of our expected fully parallel time in Table 3.6. In the reported time, we consider the slowest separate subproblem at every iteration. In a practical setting, while the parallel computation time presented for the consumer and network subproblems is representative, we expect an additional overhead due to any communications latency. For instance, if there is a 500 ms delay in the communication infrastructure, given 95 iterations, this adds 47.5 seconds over the reported time. Table 3.6 reports the model size and solve time for the subproblems in a single horizon (the longest horizon) and their contribution to the overall solve time in our parallel implementation. Notice that the constraints and variables reported in Table 3.6 is for a single problem that can be solved in parallel. We report the total number of the same problem that we need to solve in every iteration in parentheses in Table 3.6.

As can be seen in Table 3.6, the total convergence time for a single horizon of our approach, in parallel computation, is 27.21s for our 69-bus distribution network. This computation time is reasonable, given the problem sizes as well as our strict convergence tolerance (i.e. 10^{-5}), which represents at most a 0.5 Watt error. Yet, in practice, we could run our approach with weaker tolerances

to reduce the number of iterations, and thus, overall time. In addition to this, when employed in an MPC context, warm-starting solutions can lead to further significant iteration reductions.

Table 3.6: Problem size and solve time

Sub problem	Problem size Single Opt. (#total)		# Iter	Time (s)
	# Constraints	# Variables		
Consumer	9497	12384 (207)		15.73
Network	275	482 (576)	95	11.48
Total	2,203 k	2,980 k		27.21

3.8.4 Optimality and Convergence

Notice that our ADMM algorithm converges when the primal (3.4a) and dual residuals (3.4b) are smaller than 0.5 watts. To check the optimally of our distributed approach at our 0.5 watts convergence tolerance, we solve the bidding problem centrally and compare the results with the ones obtained via our distributed approach in Table 3.7. Notice that the central approach leads to a large-scale optimisation problem that includes all the variables / constraints of both consumers and the network subproblems. The total number of variables / constraints is reported in the last column of Table 3.6.

Table 3.7: Central vs. distributed

Approch	Benefit ($)	Time (s)	Improvement % (benefit , time)
Central	3095.5	1404.4	(-,-)
Distributed	3094.9	27.21	(-0.02, 3845)

Remark Whether central or distributed, this thesis deals with a non-convex OPF problem. While in practice, the IPOPT solver can sufficiently solve the OPF problem, in theory, we can only be sure that the benefits reported in Table 3.7 are local optimum solutions.

3.8.5 Additional Improvement to Envelopes

In the real world, there might be some cases in which the DSO needs to obtain a set point for its own facilities, such as on-load tap changers (OLTC), voltage regulators and capacitor banks. In the context of envelopes, the DSO only has access to the extreme CPPs that may not occur due to the rare nature of contingency. So, it might be challenging for the DSO to find the optimum set-points for these technologies. To account for this, we suggest communicating

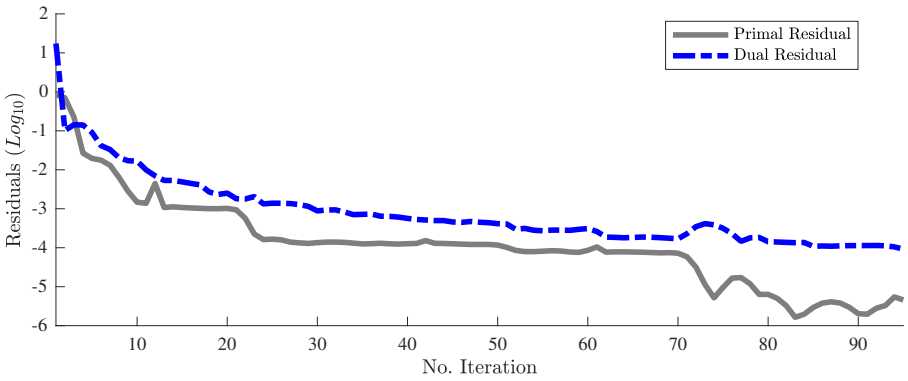

Figure 3.8: The primal and dual residual convergence

another point within the envelope reflecting consumers' CPP in the normal operating condition, i.e., p^e in which no reserve service is activated. Here, consumers communicate three points with the grid. These points are their envelopes $\overline{p}$, and $\underline{p}$ as well as their CPP in the energy market, i.e., p^e. The DSO also solves three OPFs, one for the energy case and two others for the extremes of the envelope. Since the energy case represents the normal operating condition, the DSO can operate its technology using the OPF associated with the energy case p^e.

Table 3.8 compares the performance of negotiating only the operating envelopes (2 points) versus negotiating 3 points (2 points for the envelope and 1 for the energy dispatch). In our experiments, the DSO does not own any particular technologies. Thus, as reported, both approaches obtain the same total benefits for the consumers. Notice that although the additional operating point adds 288 OPFs to every ADMM iteration, the convergence time of the parallel implementation only increased by 3 seconds.

Table 3.8: Total benefit, size and time: two vs. three points envelopes

Negotiation	Benefit ($)	No. OPFs per Iter.	Convergence Time
$\underline{p}$, $\overline{p}$	3094.9	576	27s
$\underline{p}$, p^e, $\overline{p}$	3094.9	864	30s
Increase	0%	+33%	+11%

3.8.6 Longer-Term Network-Secure Consumer Benefit

To show the longer-term consumer benefit, we report the average consumer benefit over 3 months for different use of DER. Table 3.9 reports the total benefit when consumers use ToU tariff + FiT prices and do not actively participate in the electricity markets (tariff prices are given in Table 3.1). Plus,

when they only participate in the energy market, and finally, when they participate in both energy and FCAS markets. The market prices used in this study are for the NSW region from 1 January until 31 March 2021.

Table 3.9: Three months electricity bills of a single consumer

Approach	Benefit ($)			
	Daily			3 Months
	Min	Max	Ave.	
ToU+FiT	-2.98	1.55	-0.21	-18.72
Energy	-0.59	6.14	0.58	51.97
Energy+FCAS	0.22	8.05	1.75	158.03

3.9 Summary

We developed an ADMM-based approach in distribution networks to enable residential consumers to participate in both energy and reserve markets. In our approach, the DSO and consumers negotiate frequently using the ADMM algorithm and converge on a consensus solution that does not violate consumers or the network constraints.

We illustrated the effectiveness of our approach using 207 consumers, served through AEMO, within a 69-bus network. Our results show significant improvements compared to cases in which the decisions in energy and FCAS markets are not co-optimised. Also, through a voltage analysis, we compared the voltages on the network when the co-optimisation neglects the network constraints with the proposed approach. The results revealed that neglecting the network can lead to infeasible solutions violating the safe voltage limits at different times of the day. We also compared the results of our NAC-based envelope with three operating envelope approaches. Although we used the perfect information to obtain dynamic envelopes, our NAC-based envelope could still obtain higher benefits whilst not requiring detailed consumer information.

In this chapter, we assumed that the forecast for the next five minutes is accurate, meaning that consumers can stick to their envelopes during the 5-minute operating interval. However, consumers might deviate from their envelope if the uncertainty realisations are different from the forecasts. Such envelope violations can push the network outside its borders, especially if the grid is operating at its edges. In the next chapter, we build an adjustable controller within the consumer subproblem that enables consumers to commit to their envelopes.

In addition, based on the results of Section 3.8.2.2, we identified that the voltages in our test system are the main network issue restricting consumers.

In the upcoming chapter, we enable consumers to provide reactive power for voltage support purposes and investigate whether this can increase consumers' network access, i.e., wider operating envelopes.

Chapter 4

Operating Envelopes for Reliable Consumer Bidding

4.1 Introduction

Similarly to Chapter 3, here, our approach to guaranteeing network technical limits in a consumer bidding problem builds on the notions of operating envelopes and distributed optimisation. Yet, here, we additionally model data uncertainty (using piecewise affine controllers); and extend the operating envelopes to include reactive power in addition to the real power. These improvements enable consumers to 1) deliver their market commitments while sticking to their operating envelopes and 2) provide reactive power support that can increase network throughput.

Over the life of this thesis, operating envelopes have also become increasingly popular amongst system operators. In 2019, the Australian Energy Market Operator (AEMO) and Energy Network Australia published a report identifying operating envelopes as a required capability to ease DER market participation AEMO and Energy Networks Australia [2019]. Placing limits on the real power injection to the grid (e.g., on excess solar PV) is a common practice worldwide, such as in Germany and Arizona, USA. When storage comes into the picture, these limits must be two-sided, forming an operating envelope.

In a bidding process, participants need to submit their bids in advance of an operating interval (5 minutes in Australia). Thus, when obtaining operating envelopes for the upcoming interval, only forecast information is available. The discrepancy between the forecast and reality might lead to envelopes that cannot cover consumers' uncertainty range, leading to network violations. Note that this issue is not specific to operating envelopes and other approaches, such as those using a centralised framework, face the same challenge, as they also need to count on forecast information. In addition to possible network violation, uncertainty realisations different from forecasts

might lead to bid deliveries different from what initially was submitted to the market. In most electricity markets, including the NEM, participants are penalised for not honouring their market commitments.

To overcome the challenges mentioned above, this chapter enables consumers to account for their local uncertainties within their envelopes. To do so, we model consumers' uncertain parameters within polyhedral uncertainty sets and empower every consumer with a controller based on the piecewise affinely adjustable robust constrained optimisation (PWA-ARCO). During the optimisation, we obtain bids, operating envelopes, and parameters of the PWA-ARCO controller such that consumers can compensate for any realisation of the uncertain parameters within their uncertainty sets. In live operation, our PWA-ARCO controllers take the uncertainty realisations as inputs and tune the outputs so that consumers are within their operating envelopes while honouring their market commitments.

Moreover, as we identified in the previous chapter (Section 3.8.2.2), the voltages in our test system are the main network issues restricting consumers. Therefore, if voltages are improved, the network can have greater throughput. As shown in Jabr [2019], reactive power support of the consumer-owned inverters (such as solar PV and battery inverters) can effectively improve voltages across the distribution network. Thus, here, we enable consumers to negotiate their reactive power support with the grid alongside their real-power envelopes.

Notice that since we only check the network limits at the extremes of the envelope, at the convergence of the ADMM algorithm, we obtain the allowed maximum and minimum real power exchange, as well as the required reactive power at those real power extremes. In other words, this does not provide any information on the required reactive power support at operating points away from the extremes. If consumers do not exchange the right amount of reactive power across the envelope, the network constraints might be violated, despite sticking to the real power envelopes. To resolve this issue, we propose an additional Q-P controller that enables consumers to exchange the required reactive power for any real power exchange within the envelope.

In what follows, we first provide an up-front description of our approach in Section 4.2. We then introduce our piecewise affine uncertainty characterisation approach in Section 4.3, which is next illustrated within the bidding context in high-level and details in sections 4.4 and 4.5, respectively. We introduce our comparative approaches and provide our results and discussions in Section 4.6. Finally, we summarise our approach and list our findings in Section 4.7.

4.2 Overall Approach

Our main goal for every 5-minute interval is to obtain bids for the energy, 3 raise, and 3 lower contingency reserve markets (7 markets in total) that are both robust against uncertainty and respect the grid operating limits.

To reflect the distributed nature of the problem and the possible privacy concerns of stakeholders, as in Chapter 3, we decompose the problem into consumer and DSO subproblems and use the alternating direction method of multipliers (ADMM) to obtain the operating envelopes. Figure 4.1 shows a high-level scheme of our proposed approach, which is repeated at every MPC iteration to generate and submit consumer bids to the wholesale market every 5 minutes. At the heart of our MPC framework lies an ADMM technique to enable consumers and the DSO to negotiate every five minutes for an operating envelope that covers all market actions of the consumer.

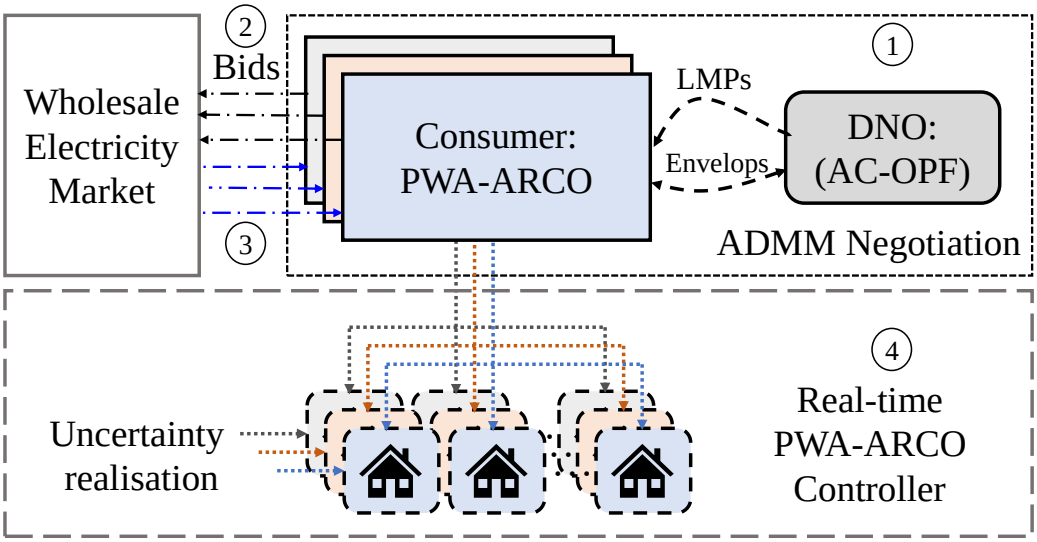

Figure 4.1: High-level structure of PWA-ARCO.

To ensure that uncertainty realisation neither leads to network violation (due to violating the envelope) nor penalises consumers (due to failing to honour bids), we build a piecewise affinely adjustable robust constraint optimisation (PWA-ARCO) into our consumer subproblem. PWA-ARCO extends the conventional affinely ARCO (AARCO) Ben-Tal et al. [2004] and increases flexibility by breaking the uncertainty set into more pieces, enabling the response to be better optimised when operating away from worst-case conditions. Furthermore, we include market bid deviation penalties in the consumer objective function to help consumers make informed decisions about the parameters of their piecewise functions. We also equip consumers with a Q-P controller that enables them to offer their reactive power support (gener-

ated / consumed by their inverters) to the DSO to increase network throughput.

As shown in box ① Figure 4.1, each consumer solves a PWA-ARCO problem to obtain their preferred market participation (bids), their required envelopes as well as the parameters of their piecewise functions. Each envelope includes the minimum and maximum real power at the connection point, together with the available reactive power support output of a Q-P controller at the two real-power extremes. These envelopes are then communicated to the network subproblem. Next, the DSO solves two OPFs (one for each extreme) to check whether the envelopes are network secure and updates the locational marginal prices (LMPs) accordingly. Although the DSO only checks the extreme scenarios, our Q-P controllers ensure that the network constraints remain feasible for less extreme scenarios as they keep generating / consuming reactive power proportionally to real-power changes at the connection point. At the convergence of the ADMM approach ①, the bids for each market, network-secure envelopes and the parameters of our PWA-ARCO controllers are obtained.

The network-secure bids are then submitted to the electricity markets ② and get dispatched according to the market-clearing price ③. In live operation, the controllers take local recourse actions to keep consumers CPPs within the operating envelope on which the network and consumers agreed at the convergence of the ADMM algorithm and avoid market penalties ④.

4.3 General Piecewise Affinely ARCO

As discussed in Section 2.3.4, an affinely adjustable robust constrained optimisation (AARCO) enables the decision variables to adjust themselves affinely in response to uncertainty realisation. However, making (2.23) robust to uncertainty variations via affine functions can lead to over conservative solutions, as it provides a similar response (A in $A\epsilon + b$) for any realisation within the uncertainty set. To improve the performance, adjustable optimisation can be improved to optimise for piecewise affine functions Jabr [2020]. This can enable consumers to tune their behaviour more efficiently for different uncertainty realisations within the uncertainty set. We next formulate a general model for PWA-ARCO, which we later use in Section 4.4 to model our bidding problem.

The idea here is to partition the uncertainty set (2.19) into contiguous subsets and then optimise $x(\cdot)$ as a piecewise affine function. We begin with encoding a piecewise affine function (see Figure 4.2 for a visualisation of a piecewise affine function with 4 breakpoints):

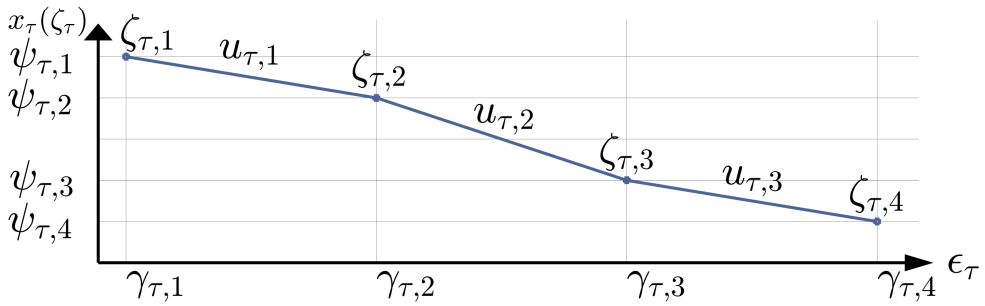

Figure 4.2: Visualisation of a piecewise affine function

$$x(\zeta) \triangleq \sum_{\tau=1}^{l} \psi_\tau \zeta_\tau \tag{4.1}$$

where $\psi_\tau \in \mathbb{R}^{n \times \alpha_\tau}$ are the "y-axis" breakpoints for each variable, for the τ-th random parameter (what we optimise), α_τ is the number of breakpoints and $\zeta_\tau \in [0,1]^{\alpha_\tau}$ are weights for the τ-th random parameter. These weights encode the position in the uncertainty set through:

$$\epsilon_\tau = \gamma_\tau^\intercal \zeta_\tau \qquad \sum_{a=1}^{\alpha_\tau} \zeta_{\tau,a} = 1 \tag{4.2}$$

where $\gamma_\tau \in \mathbb{R}^{\alpha_\tau}$ are the "x-axis" breakpoints (each entry is unique) for the τ-th random parameter. Notice that the weights for each random parameter must sum to 1.

To further restrict the weights, so they encode a piecewise linear function, we introduce binary variables $u_\tau \in \{0,1\}^{\alpha_\tau - 1}$ and the following set of constraints:

$$\sum_{a=1}^{\alpha_{\tau-1}} u_{\tau,a} = 1 \tag{4.3a}$$

$$\zeta_{\tau,a} \leq u_{\tau,a-1} + u_{\tau,a} \qquad \forall a \in \{2, ..., \alpha_\tau - 1\} \tag{4.3b}$$

$$\zeta_{\tau,1} \leq u_{\tau,1} \tag{4.3c}$$

$$\zeta_{\tau,\alpha_\tau} \leq u_{\tau,\alpha_\tau - 1} \tag{4.3d}$$

When ensuring that (2.20) holds for all values in the uncertainty set, on a per constraint basis, similarly to (2.23)–(2.24), we get:

$$\max_{\epsilon \in E} \left(\mathcal{B}x(\epsilon) + \mathcal{C}\epsilon\right) + d \leq 0 \tag{4.4}$$

When constraints (4.2) and (4.3a)–(4.3d) hold, there is a unique mapping from ϵ to ζ, allowing us to replace $x(\epsilon)$ with $x(\zeta)$. Expanding out the maximisation, we have:

$$z + d \leq 0 \tag{4.5a}$$

where

$$z = \max_{\zeta,\epsilon} \left(\mathcal{B} \sum_{\tau=1}^{l} \psi_\tau \zeta_\tau + \mathcal{C}\epsilon \right) \tag{4.5b}$$

$$W\epsilon \leq v \tag{4.5c}$$

$$\text{(4.2), (4.3a)–(4.3d)} \tag{4.5d}$$

Equations (4.5b)–(4.5d) represent a MILP problem and thus it is not possible to directly use duality theory and reformulate it, so, a similar approach as in (2.25a)–(2.25b) will not work here. Note that if we relax the binaries in (4.5b)–(4.5d), the feasible region of the resulting LP problem will capture the convex hull of the original problem, which is greater than or equal to the feasible region of the original MILP problem. Thus, in a maximisation sense, the result of the binary-relaxed LP problem on the left-hand side will be greater or equal to the original MILP problem. This means that if we utilise the binary-relaxed formulation in order to obtain a dual, our solution will still be robust but potentially more than it needs to be. In other words, we immunise the system against a value that is potentially higher than the maximum of the left-hand side in (4.5a). In the result section, we compare our results with a perfect case and discuss the conservativeness of different approaches. Relaxing the binary variables u_τ allows $(\epsilon, \psi_\tau \zeta_\tau)$ to take on a position anywhere in the convex hull of the breakpoints of the relaxed piecewise linear function (recall $\zeta_{\tau,a} \in [0, 1]$). Writing the relaxation out explicitly and indicating how the duals associate with the constraints (quantifiers over τ and a are implicit), we have:

$$z = \max_{\epsilon,\zeta} \left(\mathcal{B} \sum_{\tau=1}^{l} \psi_\tau \zeta_\tau + \mathcal{C}\epsilon \right) \tag{4.6a}$$

$$W\epsilon \leq v \qquad (\mu \geq 0) \tag{4.6b}$$

$$\epsilon_\tau - \lambda_\tau^\intercal \zeta_\tau = 0 \qquad (\mu'_\tau) \tag{4.6c}$$

$$\sum_{a=1}^{\alpha_\tau} \zeta_{\tau,a} = 1 \qquad (\mu''_\tau) \tag{4.6d}$$

$$\zeta_{\tau,a} \leq 1 \qquad (\mu'''_{\tau,a} \geq 0) \tag{4.6e}$$

Taking the dual leads to:

$$z = \min \left(v^\intercal \mu + \sum_{\tau=1}^{l} \mu''_\tau + \sum_{\tau=1}^{l} \sum_{a=1}^{\alpha_\tau} \mu'''_{\tau,a} \right) \tag{4.7a}$$

$$W^\intercal \mu + \mu' \geq \mathcal{C}_i \tag{4.7b}$$

$$\mu'' - \lambda_{\tau,a} \mu'_{\tau,a} + \mu'''_{\tau,a} \geq \mathcal{B}_i \psi_{\tau,a} \tag{4.7c}$$

Recall that these dual variables and constraints will have a copy for each constraint in the original problem (i.e. a further index of i that has been treated implicitly in the above). Finally constraints (4.5a)–(4.5d) can be written into the following linear form:

$$\left(v^\intercal \mu + \sum_{\tau=1}^{l} \mu''_\tau + \sum_{\tau=1}^{l} \sum_{a=1}^{\alpha_\tau} \mu'''_{\tau,a} \right) + d \leq 0 \tag{4.7d}$$

$$\text{s.t.} \quad (4.7b) - (4.7c) \tag{4.7e}$$

Notice that we have removed the min operator from (4.7d), the reason is that if (4.7d) holds for any value of $\left(v^\intercal \mu + \sum_{\tau=1}^{l} \mu''_\tau + \sum_{\tau=1}^{l} \sum_{a=1}^{\alpha_\tau} \mu'''_{\tau,a} \right)$, it will also hold for its minimum value.

4.4 High Level Consumer and Network Negotiation

This section aims to provide a high-level presentation of the ADMM approach and what is being negotiated between the consumer and the DSO subproblems. Thus, we do not go into details of consumers and DSO subproblems. In Section 4.4.1, we only model the uncertainty sets and our piecewise affine operating envelopes based on the theory we just covered. We then present our high-level network subproblem and the ADMM approach in Section 4.4.2. The details of the consumer objective and constraints that interact with the envelope, as well as DSO constraints, are left until Section 4.5.

4.4.1 Consumer Subproblem

In our bidding problem, the uncertain parameter ϵ includes FCAS activation $\epsilon^F \in [-1, 1]$, PV power $\epsilon^{PV} \in [\overline{P}^{PV}, \underline{P}^{PV}]$ and residential demand $\epsilon^D \in [\overline{P}^D, \underline{P}^D]$. Regarding the FCAS activation, notice that the raise and lower FCAS services will not be activated at the same time, plus, the activation of 6-sec, 60-sec and 5-min reserves (raise or lower) are sequential, e.g., if 5MW is bid into 6-sec, 60-sec and 5-min, then at most a 5MW response is required at any one moment (rather than 15MW). In line with this, we assume that consumers will participate equally in all raise markets and equally in all lower markets.

Thus, for a contingency, in the worst case, we have to respond fully for the entire 5 minutes. We therefore use a single uncertain parameter ϵ^F to account for the most extreme reserve activation across all markets. Similarly to $x(\zeta)$, we write the real power generated by a consumer $p(\zeta) \in \mathbb{R}^{|T|}$ as:

$$p(\zeta) \triangleq \sum_{a=1}^{\alpha_F} \psi_a^F \zeta_a^F + \sum_{a=1}^{\alpha_{PV}} \psi_a^{PV} \zeta_a^{PV} + \sum_{a=1}^{\alpha_D} \psi_a^D \zeta_a^D \tag{4.8a}$$

$$\epsilon^F = \gamma^{F\intercal} \zeta^F \qquad \sum_{a=1}^{\alpha_F} \zeta_a^F = 1 \tag{4.8b}$$

$$\epsilon^{PV} = \gamma^{PV\intercal} \zeta^{PV} \qquad \sum_{a=1}^{\alpha_{PV}} \zeta_a^{PV} = 1 \tag{4.8c}$$

$$\epsilon^D = \gamma^{D\intercal} \zeta^D \qquad \sum_{a=1}^{\alpha_D} \zeta_a^D = 1 \tag{4.8d}$$

(4.8a)–(4.8d) correspond to (4.1)–(4.2) yet with the uncertain parameters broken up into independent subsets. Notice that $p(\zeta)$ represents all possible CPPs of the consumer for any realisation of uncertain parameters ϵ. To increase readability, we interchangeably use $p(\zeta)$ and $p(\epsilon)$ throughout this chapter (both meaning that p is a function of uncertain parameters). To have an upper and lower bound on these CPPs, we define the vector variables $\underline{p}, \overline{p} \in \mathbb{R}^t$ indicating the operating envelope where:

$$p(\epsilon) \in [\underline{p},\ \overline{p}] \quad \forall \epsilon \in E \tag{4.8e}$$

The above equation indicates that the CPP resulting from participating in any or all 7 energy and reserve markets for any realisation of uncertainty within the polyhedron E will remain within the operating envelope $[\underline{p},\ \overline{p}]$. When network constraints are neglected, the operating envelope will not limit the market actions, i.e., $[-\infty,\ \infty]$. However, this envelope might significantly limit consumers when the network constraints are taken into account. To increase network throughput and to enable consumers to bid with less network restriction, we obtain the reactive power support associated with the operating envelope with the following Q-P controller:

$$q(\zeta) \triangleq \sum_{a=1}^{\alpha_F} \psi_a'^F \zeta_a^F + \sum_{a=1}^{\alpha_{PV}} \psi_a'^{PV} \zeta_a^{PV} + \sum_{a=1}^{\alpha_D} \psi_a'^D \zeta_a^D \tag{4.8f}$$

We use the above decision rule to obtain the reactive power that can be exchanged with the grid at the uncertainty realisation ζ. Let $q_{\underline{p}}$ be the reactive power associated with $\underline{p}$ and $q_{\overline{p}}$ denote the reactive power associated with $\overline{p}$. When reactive power is neglected both $q_{\underline{p}}$ and $q_{\overline{p}}$ are zero. More details about

this is provided in Section 4.5. In the next section, we negotiate the pairs $\underline{s} \triangleq (\underline{p}, q_{\underline{p}})$ and $\overline{s} \triangleq (\overline{p}, q_{\overline{p}})$ with the grid. We then solve two OPFs, one for each pair, to ensure network feasibility. To ease the presentation, we put $\underline{s}$ and $\overline{s}$ in a vector s, where $s \triangleq (\underline{s}, \overline{s})$.

4.4.2 Network Subproblem and ADMM Algorithm

So far, at a high level, we explained the operating envelope s obtained at the consumer subproblem. To ensure that consumer envelopes are network secure, here, we negotiate them with the DSO using the ADMM approach. This completes ① in Figure 4.1. Using s' for the same variable (i.e., duplication of s) but from the network perspective, in the final solution, to within a required tolerance, we have:

$$s - s' = 0 \qquad (\lambda) \tag{4.9a}$$

We write the augmented Lagrangian associated with (4.9a) as:

$$\mathcal{L}^*(s, s', \lambda) = \lambda^\intercal (s - s') + \frac{\rho}{2} ||s - s'||_2^2 \tag{4.9b}$$

where λ is a vector of dual variables of (4.9a) and ρ is the penalty parameter of the augmented Lagrangian. We use the ADMM algorithm Boyd et al. [2011] as a negotiation tool between consumers and the network to obtain network-secure results. Given the consumer objective f; the network internal variables z and the objective and constraint functions $\mathcal{G}$ and $\mathcal{H}$, our ADMM approach solves the following per iteration k:

$$s^{(k)} := \min_{x(\epsilon)} \left[f(.) + \mathcal{L}^*(s, s'^{(k-1)}, \lambda^{(k-1)}) \right]$$

$$\text{s.t.} \qquad \text{(4.7a)–(4.7c), (4.8a)–(4.8f)} \tag{4.10a}$$

$$s'^{(k)} := \min_{z} \left[\mathcal{G}(s', z) + \mathcal{L}^*(s^{(k)}, s', \lambda^{(k-1)}) \right]$$

$$\mathcal{H}(s', z) \leq 0 \tag{4.10b}$$

$$\lambda^{(k)} := \lambda^{(k-1)} + \rho^{(k)} (s^{(k)} - s'^{(k)}) \tag{4.10c}$$

In the first phase (4.10a), consumers are optimised for s, while holding s' and λ constant at their $k-1$-th value. In the second phase (4.10b), the network is optimised for s', while holding s and λ constant at their k and $k-1$-th values respectively. Finally, the dual variables λ are updated in (4.10c), completing the k-th iteration. we use the same convergence criteria as in Chapter 3. In other words, our approach converges if the infinity norms of the primal $||R_p^{(k)}||_\infty$ and dual residuals $||R_d^{(k)}||_\infty$ are both smaller than a threshold.

4.5 Detailed Consumer and Network Subproblem

Here, we first develop in detail a PWA-ARCO energy management system (EMS) for a consumer participating in energy, and 6-sec, 60-sec, and 5-min raise and lower reserve markets. We then model the detailed DSO subproblem.

4.5.1 Detailed EMS Subproblem

DER Constraints

We need to ensure the DER constraints are satisfied for any CPP realisation resulting from reserve market activation or PV and demand realisations. To do so, we represent DER variables as piecewise affine functions of uncertainty and then use these functions to write each constraint. The consumer subproblem also includes real-power (4.8a), the uncertainty set (4.8b)–(4.8d), the envelope (4.8e) and the reactive power (4.8f).

Solar PV: Solar PV forecast has been modelled in the uncertainty set. We also use a piecewise affine function $p_t^{cur}(\zeta_t) \in [0, \epsilon_t^{PV}]$ to model the curtailment as a function of uncertainty. Using the max protection function, this can be modelled as:

$$\max_{\zeta}\{p_t^{cur}(\zeta_t) - \gamma_t^{PV\intercal}\zeta_t^{PV}\} \leq 0 \tag{4.11a}$$

Battery Storage: We define the piecewise affine functions for battery charge $p_t^C(\zeta_\tau) \in [0, \mathcal{R}]$ and discharge $p_t^D(\zeta_\tau) \in [0, \mathcal{R}]$ variables. Given battery efficiency η, the protection functions for battery's bounding constraints can be written as:

$$0 \leq \max_{\zeta_\tau}\{p_t^C(\zeta_\tau)\} \leq \mathcal{R} \tag{4.11b}$$

$$0 \leq \max_{\zeta_\tau}\{p_t^D(\zeta_\tau)\} \leq \mathcal{R} \tag{4.11c}$$

$$\max_{\zeta_\tau}\{e_0 + \sum_{\delta=1}^{t}(\eta p_\delta^C(\zeta_\tau) - p_\delta^D(\zeta_\tau)/\eta)\} \leq \bar{e} \tag{4.11d}$$

$$\min_{\zeta_\tau}\{e_0 + \sum_{\delta=1}^{t}(\eta p_\delta^C(\zeta_\tau) - p_\delta^D(\zeta_\tau)/\eta)\} \geq \underline{e} \tag{4.11e}$$

where $\mathcal{R}$ is the charging / discharging rate and $\underline{e}$ and $\bar{e}$ are the minimum and maximum values for battery SoC.

To ensure that simultaneous charge and discharge does not occur, we use

a binary variable u_t and the following constraints:

$$0 \leq p_t^C(\overline{\zeta}) \leq \mathcal{R} \cdot u_t \tag{4.11f}$$

$$0 \leq p_t^C(\overline{\zeta}) \leq \mathcal{R} \cdot (1 - u_t) \tag{4.11g}$$

We only apply these binaries to the energy market, i.e., $\zeta = \overline{\zeta}$. Because in reserve markets, the battery can transit from charge to discharge (or visa versa) to provide a greater response. For instance, imaging a half-full battery neither charging nor discharging in the energy market. This battery is able to bid its rated capacity to either raise (discharge) or lower (charge) reserve markets. However, using a binary variable limits battery's flexibility to only one market (rise or lower). This is why we do not use an additional binary variable in the reserve market.

Combined Power: The combined household power can be written as follows:

$$p(\zeta_\tau) = p_t^D(\zeta_\tau) - p_t^C(\zeta_\tau) - p_t^{cur}(\zeta_\tau) + \gamma_t^{PV\intercal}\zeta_t^{PV} - \gamma_t^{D\intercal}\zeta_t^D \tag{4.11h}$$

The equality constraint (4.11h) gives the relation between the combination of the piecewise affine parameters on the left hand side with the piecewise affine parameters of the CPP on the right hand side of (4.11h). Having obtained all the protection functions, we use duality theory to convert each protection function into some linear constraints as in (4.7d)–(4.7e).

Objective Function

The market payments to the customer consist of what energy they exchange with the network and the reserve market commitments (whether deployed or not). They are also penalised if the energy they exchange deviates from their energy market amount unless this deviation is accounted for by reserve market activation. What we propose to do is evaluate the revenue from the energy market at the most likely realisation of uncertainty (i.e., forecast, shown by $\bar{\epsilon} = \{\epsilon^F = 0, \epsilon^{PV} = \bar{\epsilon}^{PV}, \epsilon^D = \bar{\epsilon}^D\}$, given by $p(\bar{\epsilon})$. This will also be the amount we bid into the energy market.

For the reserve markets, we assume that we have to meet and bid capacity under all circumstances. Also, the reserve activation ϵ^F can vary between -1 (max lower activation) to 1 (max raise activation) where $\epsilon^F = 0$ represents a case where no reserve is required (energy case). Using r' for raise and l' for lower, we can write:

$$r' = p(\epsilon^F = 1, \epsilon^{PV}, \epsilon^D) - p(\epsilon^F = 0, \epsilon^{PV}, \epsilon^D) \tag{4.12a}$$

$$l' = p(\epsilon^F = 0, \epsilon^{PV}, \epsilon^D) - p(\epsilon^F = -1, \epsilon^{PV}, \epsilon^D) \tag{4.12b}$$

Notice that the contribution of ϵ^F in $p(\epsilon)$ is separable from the other sources of uncertainty because it is an independent piecewise affine function and ϵ^F can be considered not part of the E polyhedron. This means the rest (uncertain PV and demand) cancel out, and we do not have to resort to doing a forall ϵ. In other words, our reserve bids are robust to PV and demand uncertainty and are deliverable for any realisations within the PV and demand uncertainty sets. This is an important feature of our approach since it makes consumers reliable participants for reserve purposes. In the NEM, if a participant cannot honour its reserve bids (e.g., a frequent scenario for consumers due to uncertainty), they will be excluded from future FCAS participation. However, by obtaining FCAS bids, which are independent of uncertainty realisation, our approach secures a spot for consumers in these highly-priced yet rarely activated markets.

Since the contingency reserve market in the NEM is activated sequentially, the NEM allows the same capacity to be submitted to any or all contingency reserve markets. Let r^6 / l^6, r^{60} / l^{60}, and r^5 / l^5 respectively denote raise / lower reserve offers to 6-sec, 60-sec, and 5-min reserve markets, using (4.12a) and (4.12b), we have:

$$r^6 \leq r'; \qquad r^{60} \leq r'; \qquad r^5 \leq r' \tag{4.12c}$$

$$l^6 \leq l'; \qquad l^{60} \leq l'; \qquad l^5 \leq l' \tag{4.12d}$$

Let π^e denote the energy market price; $\pi^r = \{\pi^{r6}, \pi^{r60}, \pi^{r5}\}$ and $\pi^l = \{\pi^{l6}, \pi^{l60}, \pi^{l5}\}$ be the raise and lower 6-sec, 60-sec and 5-min market prices, $r = \{r^6, r^{60}, r^5\}$ and $l = \{l^6, l^{60}, l^5\}$ be the offers to the raise and lower reserve market. The obtained benefit can be modelled as follows:

$$C^{Ben} = \pi^e p(\bar{\epsilon}) + \pi^r r + \pi^l l \tag{4.12e}$$

The above equation calculates the benefits obtained in the energy and FCAS market. However, as we mentioned earlier, there is a penalty associated with bid violations in the energy market. To model this penalty, we interpret the causer pays policy in the NEM as to penalis energy-bid deviation at the regulation market price[1]. This adds the penalty C^{Pen} to the objective function. Given the penalty price π^-, this can be written as:

$$C^{Pen}(\epsilon^{PV}, \epsilon^D) = \pi^- |p(\bar{\epsilon}^F, \bar{\epsilon}^{PV}, \bar{\epsilon}^D) - p(\bar{\epsilon}^F, \epsilon^{PV}, \epsilon^D)| \tag{4.12f}$$

We use auxiliary variables to model the absolute value function $|\cdot|$ in a linear manner, which is then treated robustly to account for the worst-case market

[1]The reason for this is that the regulation market is activated to compensate for violations in the energy market.

penalty.

Reactive Power Network Support

The reactive power generated / consumed by the inverters is limited by the following quadratic constraint:

$$q^2 \leq s^2 - {p^{inv}}^2 \tag{4.13a}$$

The above equation is a circle in (q, p^{inv}) coordinates, which can be linearised using a set of linear constraints as follows:

$$q(cos(\phi) + sin(\phi)) \leq \sqrt{2}s - p^{inv}(cos(\phi) - sin(\phi)) \tag{4.13b}$$

where $\phi \in \{0, \pi/b, 2\pi/b, ..., (2b-1)\pi/b\}$, and b is an arbitrary integer number. Here, we use 24 lines[2] (i.e., an icositetragon), which overestimates the circle with at most 0.001% error. Note that p^{inv} in our case can be battery charge / discharge and PV power which are modelled via piecewise affine functions $x(\zeta)$. As explained in (4.8f) q is also a function of the uncertain parameter. Using the piecewise linear $x(\zeta)$ and $q(\zeta)$ (4.13b) can be written as:

$$q(\zeta)(cos(\phi)+sin(\phi)) \leq \sqrt{2}s-x(\zeta)(cos(\phi)-sin(\phi)) \tag{4.13c}$$

Providing reactive power support aims to improve voltages so consumers can have wider operating envelopes. However, the grid and consumers only negotiate on the required reactive power at the extremes. Thus, this does not provide any information about the required reactive power away from the extremes. Notice that if we only calculate reactive power for the extremes, there might be points within the envelopes for which the network is violated. This is shown in Figure 4.3.

As shown in Figure 4.3, consumers can have operating envelope $[0, P^{up}]$ if they provide the right amount of reactive power. The red line shows a path within the region that is infeasible, while the blue line is the feasible path. Similarly to Nazir and Almassalkhi Nazir and Almassalkhi [2021], which find a feasible path to avoid holes in the region, we find a path (using a piecewise affine function) to ensure consumers are within the feasible region.

To obtain the required reactive power within the envelope, we take advantage of the results presented in Jabr [2019], where the authors provide a closed-form solution to the problem of how much reactive power injection / absorption is needed at a node to fully compensate voltage changes due to real power deviations at that node. As discussed in Jabr [2019], a $q(\zeta)$ affine

[2]Due to the distributed nature of our approach, each consumer subproblem can be solved separately. Thus, adding even more lines does not significantly add to the computational complexity.

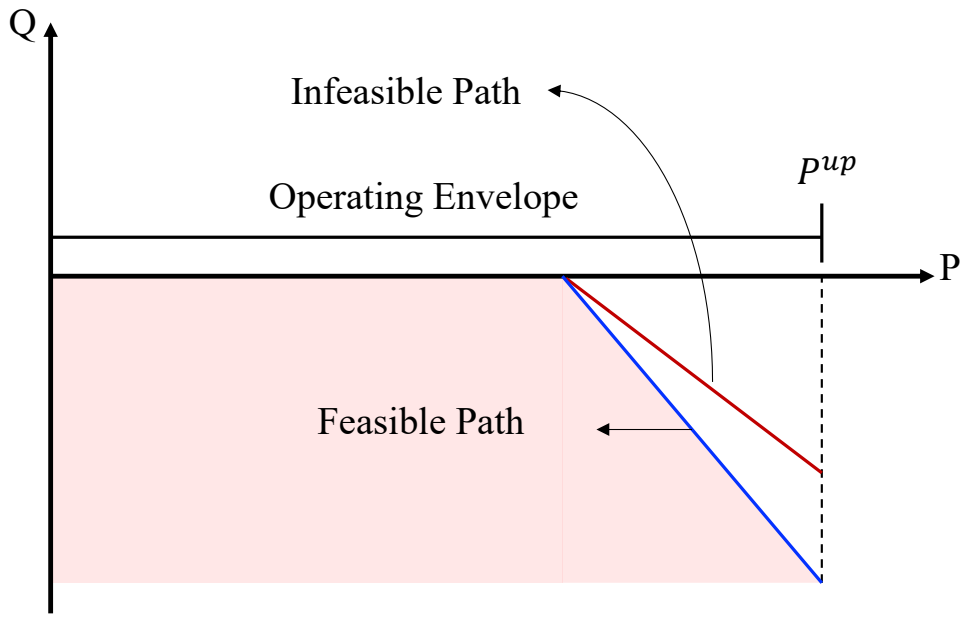

Figure 4.3: Hole in the region

function with a slope equal to the closed-form solution $R^j \in \mathcal{R}$ (where j is a network node) would completely compensate the voltage deviation due to the active power deviations. This, for τ-th uncertain parameter, can be written as:

$$\frac{\partial q(\zeta)}{\partial \zeta_\tau} \leq R^j \frac{\partial p(\zeta)}{\partial \zeta_\tau} \tag{4.13d}$$

Finally, given the piecewise function (5) the partial differential equations can be written as:

$$\psi'_{\tau,i+1} - \psi'_{\tau,i} \leq R^j \psi_{\tau,i+1} - R^j \psi_{\tau,i} \quad \forall \tau, i \in \{1, ..., \alpha_\tau\} \tag{4.13e}$$

where R^j is the closed form solution from Jabr [2019]:

$$R^j = -\frac{\sum_{j=2}^{n} K_{jk}^{|v|q} K_{jk}^{|v|p}}{\sum_{j=2}^{n} K_{jk}^{|v|q^2}} \tag{4.13f}$$

where, $K_{jk}^{|v|q} = \frac{\partial v_j}{\partial q_k}$ and $K_{jk}^{|v|p} = \frac{\partial v_j}{\partial p_k}$. In summary, the constraints of our piecewise affinely ARCO EMS subproblem for a single customer consist of the objective function (4.12a)–(4.12f), the affine functions (4.8a)–(4.8f), DER oper-

ating constraints (4.11a)–(4.11h), and the Q-P controller (4.13c)–(4.13e).

4.5.2 Detailed Network Subproblem

The network subproblem needs to solve two multi-period OPFs associated with the extremes of s' at every MPC iteration. Notice that there are no time coupling constraints in the network subproblem because all such constraints are part of the consumer sub-problems, such as the SoC coupling constraint (4.11d)–(4.11e). Therefore, these OPFs can be decomposed over time and solved in parallel. To encode this, we repeat (2.31)–(2.36) for two sets of scenarios one for $\overline{s'}$ and another for $\underline{s'}$.

4.5.3 Model Predictive Control Implementation

We presented our PWA-ARCO treatment for all t in Section IV-B. However, when integrated within our MPC framework, we apply the robust treatment for PV power and demand only to the first time-step. The reason is that our MPC framework enables us to use the latest (most accurate) forecast information every 5 minutes when a new optimisation problem is solved. Since the uncertainty variation within the next 5 minutes is often insignificant, the uncertainty set can cover the deviations from the forecast. On the contrary, constructing the uncertainty set for future time steps might lead to over-conservative results, as the forecast values (around which we construct the uncertainty set) can change significantly. In our simulations, this could bring 3% higher benefits compared to the case where the entire horizon was treated robustly.

4.6 Numerical Results

To illustrate the effectiveness of the proposed approach, we use the same 69-bus distribution network Savier and Das [2007] as in Chapter 3. We also participate in 7 markets (1 energy, three raise and three lower contingency FCAS markets). The 5-minute energy and reserve market prices are taken from the NEM, provided in Appendix A. We use the same load and PV power data explained in Chapter 3 as forecast values to run the experiments of this chapter. In addition, we assume that both PV and load can vary within $\pm 20\%$ around their forecast values. For each uncertain parameter, we pick three points from its uncertainty sets to write our piecewise functions. These points are associated with the lower bound, forecast and upper bound of each uncertainty set. We use the regulation market price for the market deviation penalty π^-. The ADMM penalty parameter ρ for real and reactive power are 1 and 0.01, respectively. Finally, we use the Gurobi and IPOPT solvers in JuMP, Julia Dunning et al. [2017] to solve our consumer and network subproblems.

As explained in the introduction Section 4.1, this chapter contributes to the literature and our previous chapter in two main ways: accounting for uncertainties and enabling reactive power support. In the following, we separately study the effectiveness of each contribution. We first investigate how providing reactive power support can improve the bidding performance in a deterministic setting in Section 4.6.1. Next, we take the uncertainty into account and study the effectiveness of our approach in a non-deterministic setting. In Section 4.6.2, we introduce some comparative approaches against which we compare the effectiveness of PWA-ARCO. In Section 4.6.3, we analyse our P-Q controller under uncertainty. Section 4.6.4 illustrates the effectiveness of our PWA-ARCO bidding approach when using other dynamic operating envelopes, reviewed in Chapter 2. Finally, Section 4.6.5 discusses the convergence and the problem size.

4.6.1 Reactive Power Support

To study the effectiveness of providing reactive power network support, here, we assume that consumers solve a deterministic optimisation problem. Table 4.1 reports the total benefit and computational performance of our approach with and without providing reactive power support. As reported in Table 4.1, reactive power support has improved both the consumer benefit and the convergence time of our ADMM algorithm. From the benefit perspective, reactive power support enables the network to provide consumers with wider envelopes. So, consumers can participate in the market with fewer network limitations, resulting in higher benefits. Regarding convergence, reactive power support enables the network subproblem to agree with consumers' preferred envelopes in more operating scenarios. Thus, the ADMM algorithm can converge within a fewer number of iterations. As reported in Table 4.1, this could reduce the number of iterations from 87 to 10 in our case.

Table 4.1: Performance comparison with regards to reactive power support

Reactive Power Support	Total Benefits ($)	No. of Iter.	Convergence Time
No	3094.9	87	28s
Yes	3118.7	10	2s

In the results reported in Table 4.1, consumers will end up with an operating envelope for their real power as well as reactive power support required at the extremes of their envelopes. Notice that depending on reserve activation, consumer CPPs can vary within these envelopes. Yet, consumers have no information on how much reactive power support they need to inject / absorb when operating away from the extremes. Our Q-P controller aims to solve this problem as it outputs the required reactive power for any given real

power exchange with the grid. We further discuss this in Section 4.6.3.

4.6.2 Effectiveness of PWA-ARCO

To assess the performance of our proposed PWA-ARCO approach, we study the following four approaches:

- *Deterministic*: This is our previous work presented in Chapter 3. In this approach consumers and the grid negotiate every five minutes through the standard multi-period ADMM algorithm (4.10a)−(4.10c). The consumer subproblem is only satisfied for the forecast scenario.
- *Perfect*: This approach intends to provide a perfect but unachievable baseline in which (assuming that computation and communication time are not limiting) two multi-period OPFs (associated with the operating envelope) are solved every minute to ensure the grid feasibility for all scenarios. Since all the future information is assumed to be available, the FCAS bid offers of this case are all made to be deliverable. This is the same case we considered in the previous section to study the effectiveness of reactive power.
- *AARCO*: This is the conventional affinely ARCO where we use the affine decision rule $x(\epsilon) \triangleq A\epsilon + b$ and (2.25a)–(2.25b) to obtain our robust bids.
- *PWA-ARCO*: This is the proposed approach in which the grid envelopes and the parameters of our piecewise affine controllers are obtained using a grid-wide ADMM coordination. In real-time, our controllers continually take recourse actions to keep the CPP within the negotiated envelope.

We implement the above approaches within an MPC framework that moves forward every 5 minutes. We use the 5-minute data to run each method prior to the realisation of uncertainty. We then use 1-minute data as realisations to evaluate the effectiveness and actual cost of each approach. Having the whole horizon covered minutely, we track the SoC of batteries and move to the next horizon, in which the same process is repeated until we cover the entire horizon, i.e., 288 time-step with 1440 realisation scenarios.

Total Benefit in Energy and Reserve Markets

Table 4.2 reports the total benefits obtained by the introduced approaches, network violations, as well as the number of times that the available FCAS capacity was less than the bid submitted to the market. As reported, PWA-ARCO obtains 2.6% less benefit compared to the perfect yet unachievable

case. However, our approach requires 5 times less computation and communication than Perfect. Plus, unlike Perfect, we do not have all the future information. Also, remember that we relaxed binary variables (4.3a)–(4.3b), which can potentially make PWA-ARCO more conservative. However, notice that the perfect case does not count on PWA-ARCO local control and solve optimisation every minute to find the optimum solution. Therefore, it serves as the best upper bound to the benefit we could obtain. In our case, our PWA-ARCO could get as close as 2.6% to this perfect yet unachievable solution. Notice that Deterministic obtained 2.5% less benefit compared to the perfect case, which is higher than PWA-ARCO. However, here, we have not applied any penalty for reserve bid violations. As reported in Table 4.2, in 2001 scenarios out of our total 1440 $\times$ 6 reserve markets scenarios, Deterministic was not able to honour the accepted FCAS bids[3]. If aggregators bid deterministically, they would likely be excluded from future FCAS participation. We further discuss the economic aspect of this in Figure 4.4. Additionally, the Deterministic approach violates the network-safe limits in 693 scenarios.

Table 4.2: Total Benefit, Network / Reserve Bid Violations

Approach	Total Benefit ($)	Rel. to Perfect (%)	Violations	
			Network	FCAS bids
Deterministic	3,033.5	-2.5	693	2001
Perfect	3,111.0	-	-	-
AARCO	2,345.3	-24.6	-	-
PWA-ARCO	3,030.5	-2.6	-	-

While AARCO could keep the voltages within safe limits and honour its FCAS bids, it adds a significant cost to the bidding problem. The reason is that, compared to a piecewise function, compensating uncertainty with affine functions will lead to over-conservative results.

Figure 4.4 breaks down the total benefit obtained by each approach to the energy and reserve market components. As shown in Figure 4.4, majority of the total benefit for all cases is made through the FCAS market. If consumers were suspended from the FCAS market, due to not fulfilling their reserve bids, a likely scenario for Deterministic, their total benefit would shrink significantly. Also, AARCO has obtained the lowest benefit in the FCAS market, highlighting the limitation of optimising for affine functions rather than piecewise affine ones. We further discuss the difference between PWA-ARCO and AARCO in the next section.

[3]Notice that we are not replaying a particular event, but checking if a consumer would hypothetically be able to meet the requirement in every moment.

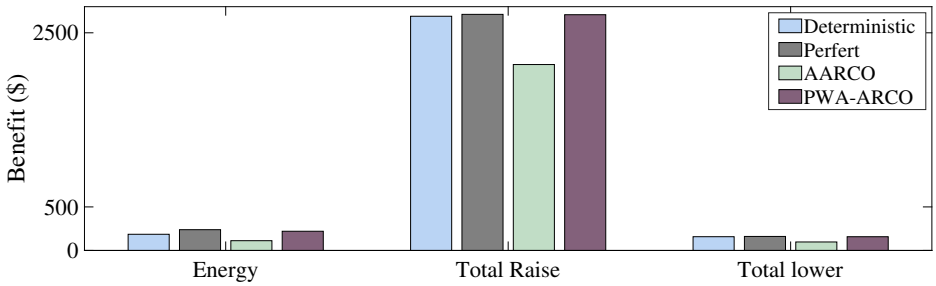

Figure 4.4: Energy and FCAS benefits breakdown

PWA-ARCO vs. AARCO

To compare the piecewise affine policy with just affine, we plot the obtained CPP function by the AARCO and PWA-ARCO approaches for a random consumer at 2:30 PM in Figure 4.5. Subfigures **a**, **b**, **c** are respectively associated with the first (reserve activation), second (PV) and third (demand) terms in (4.8a). As can be seen, while the connection point power with respect to demand uncertainty follows a similar pattern, it differs significantly with respect to PV and FCAS activation uncertainty. In fact, the flexibility introduced into the consumer subproblem by PWA-ARCO (at this time step) could significantly increase the raise FCAS bid of the consumer (Figure 4.5, **a**: $p(\zeta_3^F) - p(\zeta_2^F)$).

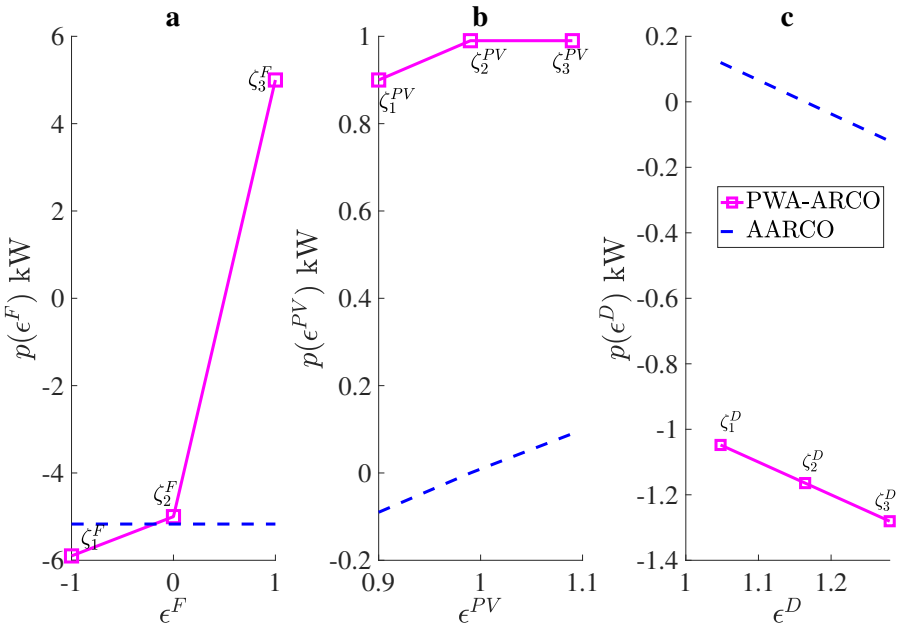

Figure 4.5: An example of CPP function: PWA-ARCO vs. AARCO

Analysing Network Voltages

We plot the maximum and minimum voltages in the network for our 1440 realisation scenarios in Figure 4.6 and Figure 4.7, respectively. While the perfect case solves a problem with a 1-minute resolution, the rest of the approaches optimise every 5 minutes (288 rather than 1440 time steps) and act locally during a 5-minute interval between two optimisations. We check power flow (PF) every minute to find the voltages reported in Figures 4.6 and 4.7. As can be seen in figures 4.6 and 4.7, Perfect, AARCO, and the proposed PWA-ARCO approaches could keep the voltage within its safe limits. However, Deterministic could not do so in several operating scenarios.

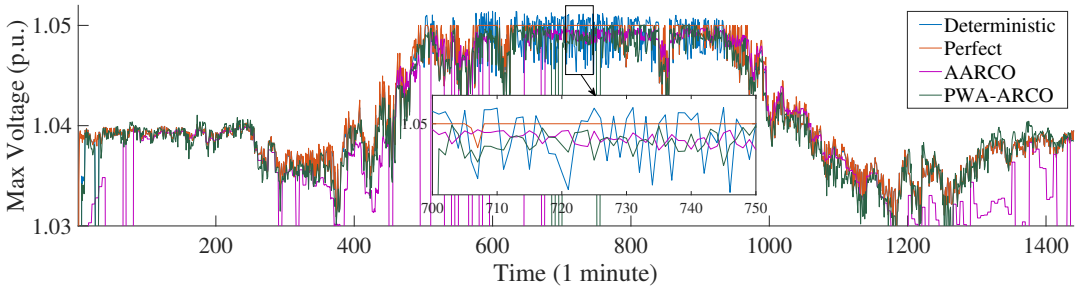

Figure 4.6: Max voltages across all nodes

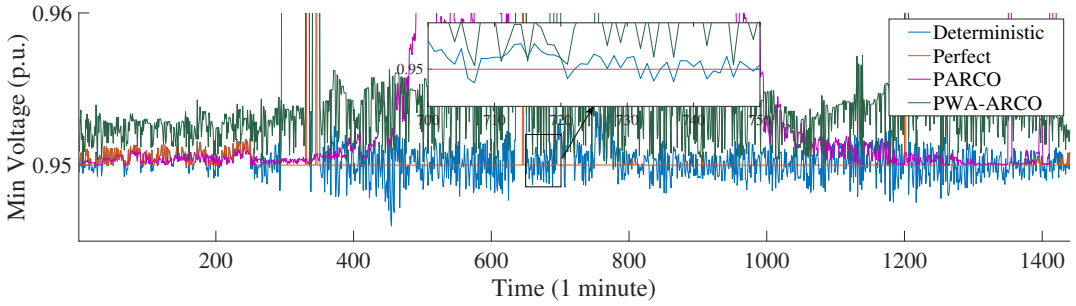

Figure 4.7: Min voltages across all nodes

4.6.3 Reactive Power Support in PWA-ARCO

In this section, we study the effectiveness of providing reactive power support in our PWA-ARCO framework. To do so, we develop another case similar to PWA-ARCO but without the reactive power support, i.e., removing constraints (4.8f) and (4.13c)–(4.13e). Figure 4.8 plots the difference between the bids submitted to each market with and without reactive power support. As reported in Figure 4.8, on average, greater bids will reach each market when considering reactive power support (in total, 0.18 MW, 0.87MW, and 1.8MW

greater bids reach the energy, raise and lower reserve markets, respectively). In our experiments, this could also bring about a 0.8% higher benefit in total ($3,030.5 vs. $3,008.6). We also report the reactive power function output of a random consumer in Figure 4.9. Sub figure a, b and c respectively show the first, second and third terms in (4.8f).

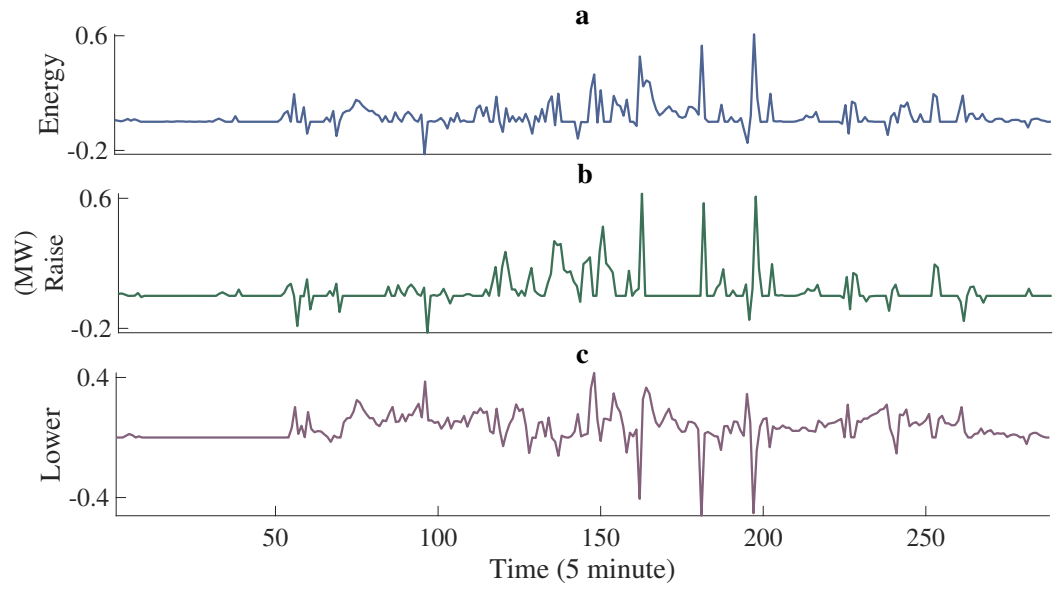

Figure 4.8: Bids differences: reactive support vs. no reactive support. Fig a) The difference in bids submitted to the energy market. Figure b) The difference in bids submitted to the raise reserve market. Figure c) The difference in bids submitted to the lower reserve market (a positive / negative value shows an increase / decrease in the amount of submitted bids)

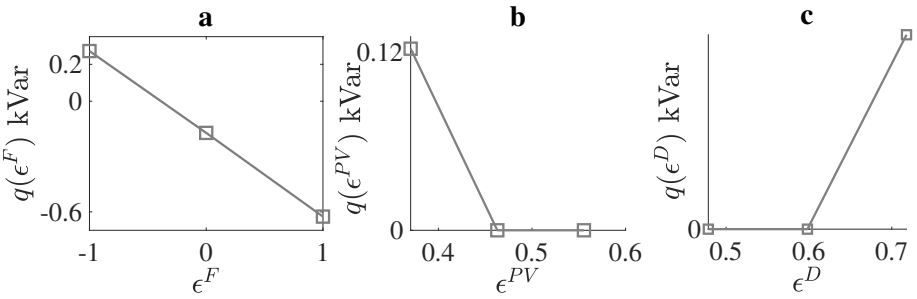

Figure 4.9: An example of a Q-P function

4.6.4 PWA-ARCO within Available Envelopes

To study the effectiveness of our proposed PWA-ARCO approach, implemented within different envelopes, we develop 3 other case studies in which

the DSO obtains dynamic envelopes and allocates them to each consumer. Afterwards, consumers used these envelopes as hard constraints to optimise their bids. We study the following envelopes:

1. *Equal-Width Envelopes*: In which the DSO allocates equal-width envelopes to all consumers owning DER.
2. *Max Export Envelopes* Petrou et al. [2020]: In which the DSO allocates envelopes of different widths to consumers at different nodes such that the absolute network throughput is maximised.
3. *Fair Envelopes*: We use the objective function (1) in Petrou et al. [2020] to obtain fair operating envelopes for each consumer. In summary, fairness is defined in Petrou et al. [2020] based on internet traffic control and is implemented by maximising the sum of $w_b \log x_b$, where x_b corresponds to the variable that is to be fairly maximised, and w_b is a proportional weighting factor associated with each party. As with Petrou et al. [2020], we use the inverter capacity of each prosumer as the weighting factor and the household active power exports p as the variable to be maximised.

Table 4.3 reports the benefit obtained via the equal-width, max export and fair envelopes versus our proposed ADMM-based envelope. Since our approach obtains the operating envelopes by negotiating between consumers and the DSO, it attains the best results amongst the comparative approaches. Notice that in line with Petrou et al. [2021], the equal-width, max-export and fair envelopes are obtained, assuming that the DSO has full observability of consumers' DER. However, in reality, such observability often does not exist. Therefore, such operating envelopes might not account for the true need of consumers. This can significantly limit consumers, leading to solutions far from the optimum.

Table 4.3: Dynamic Operating Envelopes vs. Proposed

Approach	Total Benefit ($)	Rel. to Proposed (%)
Fixed Envelope	2858.06	-5.7
Dynamic Envelope	2937.6	-3.2
Max Export	2969.3	-2.0
Fair Envelope	2979.9	-1.7
Proposed	3030.5	–

4.6.5 Convergence and Problem Size

As explained in Chapter 3, the ADMM decomposition enables us to use parallel computing in both consumer and network subproblems. In our consumer

subproblem, each consumer can solve their problem independently. Likewise, the OPF for each time step in our network subproblem can be solved independently. These will help reduce the computation time, as the time for every ADMM iteration would be equal to the longest time taken by a single optimisation problem in consumer and network subproblems. For example, in our simulation using PWA-ARCO, in the consumer and DSO subproblems, the longest optimisation takes 0.16s and 0.058s (on a laptop computer with a 2.50 GHz Intel$^{(R)}$ Core$^{(TM)}$ i7 and 8 GB of memory), respectively. Hence, each ADMM iteration takes at most 0.218s (0.16s + 0.058s) to compute the values. We report the number of optimisation problems needed to be solved in each subproblem, the number of variables[4] of a single optimisation problem, as well as the total number of ADMM iterations in Table 4.4. The parallel implementation makes the total convergence time of a single horizon to be 8.1s, 36.4s, 9.4s and 2.18s for the Deterministic, Perfect, AARCO and PWA-ARCO approaches, respectively.

Table 4.4: Problem Size and Convergence

Approach	No. Iter	No. of Problems × Var. of a Problem	
		Consumer	DSO
Deterministic	87	207 × 4.5k	564 × 482
Perfect	95	207 × 27.4k	2880 × 482
AARCO	33	207 × 5.2k	564 × 482
PWA-ARCO	10	207 × 12.9k	564 × 482

4.7 Conclusion and Summary

In this chapter, we enabled consumers to account for their local uncertainties while improving the operating envelopes to include consumer reactive power support. Consumers and the DSO negotiate for operating envelopes that allow network-secure DER bidding. Unlike Chapter 3, the envelopes here consist of both active and reactive power. This enables consumers to support the grid with their reactive power and increase their network access. Moreover, the consumer subproblem here solves a PWA-ARCO problem. PWA-ARCO is a more flexible extension to AARCO that enables consumers to commit to their envelopes, account for bid violation penalties, and generate reliable reserve bids. Both the envelopes and parameters of the piecewise affine controllers are obtained during ADMM negotiation. This tunes our local controllers based on global measurements and helps improve the results. In live operation, PV power and demand are continually measured and fed into PWA-ARCO controllers together with any FCAS activation signal. The

[4]The number of constraints in our optimisations is approximately equal to the number of variables.

controllers then take the proper recourse actions. This is a valuable feature of our approach as it can reduce the need for frequent negotiations making PWA-ARCO more functional in practice. Our results demonstrate that our PWA-ARCO approach serves its purpose whilst providing an excellent compromise between computational cost and solution quality.

It is worth mentioning that providing a concrete guarantee in robust optimisation can be very expensive if there is no clear bound on the uncertain parameters. In this chapter, we repeatedly solve the problem on a model predictive control (MPC) framework, and thus we expect the uncertainty deviations to be less extreme (the deviation bounds be more predicable) during a 5-minute MPC iteration. However, if the optimisation frequency decreases or significant deviations are more probable, choosing a wide enough uncertainty set can be challenging / over-conservative. In such cases, our approach can be modified to a distributionally robust optimisation (DRO) method. DRO can avoid expensive solutions by taking the probability of events into account.

In addition, it is worth mentioning that uncertainty at the level of consumers is more severe than when aggregated. However, the network constraints are sensitive to nodal injection / absorption. In other words, even if the aggregate forecast error is zero, still network constraints might be violated depending on how individual errors are distributed across the grid. This is why, in this chapter, we treated the uncertainty locally. This being said, the market penalty associated with misdelivery is applied to aggregate bids (what reaches the market). However, applying such penalties to aggregate bids connects consumer subproblems. Therefore, it will no longer be straightforward to solve consumer subproblems independently. In this chapter, to fully decompose the problem and solve consumer subproblems separately, we applied the misdelivery penalty to the individual consumer. Future work is needed to study the effect of uncertainty aggregation on market penalties.

So far, we have assumed that consumers have an accurate forecast of market prices. This simplifies consumer bidding to a self-scheduling problem in which consumers use a price forecast to schedule their DER. The obtained schedules are then submitted to the market at either market cap or floor prices. However, such a strategy is optimum as long as the realised market prices are close to the forecasts used in the optimisations. If the market prices are notably different, such a bidding approach might even lead to economic loss. In the next chapter, we propose a more flexible bidding approach that enables consumers to hedge the price uncertainty by obtaining a bid stack that includes multiple capacity bands and prices.

Chapter 5

Price-Sensitive DER Bidding

5.1 Introduction

This chapter provides a price-sensitive aggregator bidding solution for participating in the energy and reserve markets. As with chapters 3 and 4, we ensure that any energy, raise, and lower reserve capacity that reaches the market is network-secure. However, here, we generate a bid stack that is submitted to the market at different price bands. Not only does this hedge the price uncertainty, but also it provides the market operator with a wider range of consumer flexibility which can be used to dispatch the market more efficiently.

In chapters 3 and 4, we optimised consumer resources according to a price forecast and bid the obtained schedule at either market floor or cap prices. Assuming that the market does not reach its floor or cap prices, these bids get fully dispatched; hence, we called them *price-insensitive* bids. Such a bidding policy simplifies the problem as it narrows the DER flexibility down to a single band that obtains the highest benefits if the price forecast occurs in reality. However, the price-insensitive bidding approaches, e.g., Vayá and Andersson [2014]; Wang et al. [2018]; Iria et al. [2018]; Lee et al. [2016]; Ottesen et al. [2018]; Yao et al. [2018]; Zhu and Zhang [2019]; Neyestani et al. [2016]; Vatandoust et al. [2018]; Good and Mancarella [2017]; Attarha et al. [2020], can negatively affect both the market and aggregators. From the market perspective, such bids always need to be settled. Therefore, the market is constrained to dispatch these DER bids at a predetermined operating point, despite the underlying flexibility of DER.

Moreover, for aggregators, restricting DER to operate at one operating point according to forecasts as with price-insensitive approaches Iria et al. [2018]; Lee et al. [2016]; Ottesen et al. [2018]; Wang et al. [2018]; Vayá and Andersson [2014]; Yao et al. [2018]; Zhu and Zhang [2019]; Neyestani et al. [2016]; Vatandoust et al. [2018]; Good and Mancarella [2017]; Attarha et al. [2020], not only misses opportunities for providing higher value market ser-

vices but also can lead to economic loss in cases where cleared electricity prices deviate from forecasts.

To get the best out of DER flexibility and avoid the abovementioned issues, we argue the need for a more flexible DER bidding framework that enables consumers to offer a wider range of their DER flexibility to the market. In other words, rather than one bid band, consumers submit multiple bid bands, each at a different price. Thus, the dispatches can vary, depending on the price realisation, bringing the name *price-sensitive* to our bidding approach. In the following, we provide a simple example that compares the performance of price-insensitive and price-sensitive approaches.

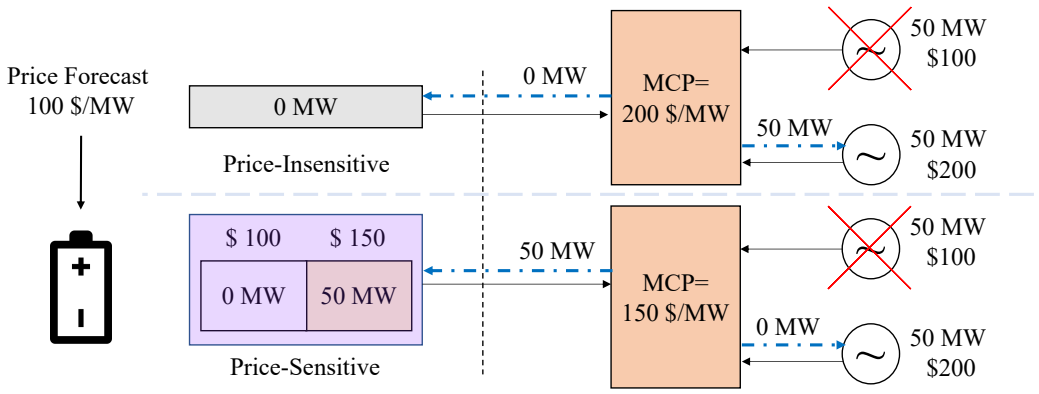

Figure 5.1: An example illustrating price-insensitive and price-sensitive bidding approaches.

Figure 5.1 shows a 100MWh / 50MW battery storage system (you can assume this is the aggregate of many residential DER) that participates in the energy market using a) a price-insensitive approach and b) a price-sensitive approach. In both bidding approaches, the battery owner forecasts that the market clears at 100 $/MW. Using the first policy, the participant decides to bid 0 MW into the energy market. However, using the price-sensitive policy, the participant bids 0 MW at 100 $/MW and 50 MW at 150$/MW. As shown in the figure, assume that an economic generating unit, offering 50 MW at $ 100, trips on the market side. Thus, the market operator needs to replace the lost generation with other resources. In the price-insensitive policy, the operator must include the next available generator (50 MW at $ 200, the dotted blue lines show market dispatches); thus, the price will be 200 $/MW. However, in the price-sensitive policy, the market operator will dispatch the battery in discharge mode, and thus, the price will be 150 $/MW. In this example, the price-sensitive approach benefited both the aggregator and the wholesale market.

Notice that large grid-scale batteries are already providing price-sensitive bids in practice. The research community, however, often neglects this, particularly for residential DER. Notice that bidding the available operating range

of DER, rather than just a single band, generates new challenges not encountered by the price-insensitive approaches. One of these new challenges is the inter-dependency between the energy and the reserve markets, where participation in one market can limit the bids in another. In fact, when bidding a wider operating range of DER, consumers need to obtain a feasible region accounting for any energy and reserve dispatch combinations. Another challenge is to calculate prices associated with different segments along the DER feasible region. Yet, DER have mainly zero marginal cost, and thus, it is not straightforward to find representative prices. In addition, as with chapters 3 and 4, we must ensure that the aggregation of bids do not violate the distribution network technical limits.

The intrinsically distributed nature of the problem, the sensitivity of private participant data and computational complexity all contribute to increasing the difficulty of the problem. We address these by decomposing the problem into smaller subproblems, namely consumer and network subproblems, that are solved separately. Instead of using the ADMM approach as a negotiation tool between the consumer and network subproblems, here, we opt for a simplified calculation which is equivalent to the communication and computational effort of a single iteration of the ADMM-based approaches. The downside is that our solutions might be sub-optimal compared to ADMM. As we show in our result section, our approach was able to reduce the computational effort by the number of ADMM iterations (166 times in our approach) at the cost of a 2.5% benefit reduction.

In our approach, consumers first send their offers and prices to the network subproblem. The network then solves OPFs and comes up with bid curtailments at each node to guarantee network constraints. We then apply this curtailment to the bids from the most to the least expensive offer. This reduces the total operation cost, which aligns with the objective of both the market and the DSO.

Similarly to chapters 3 and 4, our setting allows sharing the computational burden amongst all the parties, which can significantly decrease the runtime through parallel computing. We also implement the approach in this chapter on an MPC framework that moves forward in lock with the real-time market. This enables consumers to use the latest (most accurate) forecast information and their realised SoC in every optimisation. In this chapter, we ignore consumer uncertainty between two optimisations (i.e., assume the forecast is accurate for the next 5 minutes) and instead focus on the impact of market price uncertainty. We also enable consumers to provide reactive power support for the grid. Similarly to Chapter 4, the DSO can use this reactive power support to increase network throughput.

This chapter extends the previous chapters with two main contributions:

1. A novel price-sensitive consumer bidding approach for the energy and

reserve markets, which more accurately captures the flexibility and value of DER and enables DER dispatch to adjust to the uncertain realisation of market prices.

2. A new network optimisation layer that shapes the energy and reserve bids jointly to make them conform with distribution network boundaries while encouraging competition between aggregators. This is done prior to bids reaching the market to avoid disruption to existing market structures, enabling the approach to be more readily taken up.

Notice that in this chapter, without loss of generality, we assume that an aggregator computes the price-sensitive consumer bids. Thus, hereinafter, where relevant, we use the term aggregator for the third party who manages consumers to obtain the bids and the prices.

In what follows, we first provide an upfront description of our approach in Section 5.2. we next introduce the aggregator and network subproblems of our approach respectively in sections 5.3 and 5.4. We introduce our comparative approaches and numerically illustrate the effectiveness of our approach in Section 5.5. Finally, we provide a summary of our approach and list our findings in Section 5.6.

5.2 The Overall Approach

Figure 5.2 illustrates how our network-secure price-sensitive bidding approach interacts with the NEM wholesale market. Every 5 minutes, participating aggregators receive (or calculate) a new wholesale market price forecast over a forward horizon (shown by ① in Figure 5.2). The aggregators use this price forecast as a basis for calculating multi-band bids (represented in the NEM as bid trapeziums) for the next 5-minute dispatch interval and for each node of the distribution network where they have customers ②. The network takes these bids, merges them to obtain a polygon at each node ③, and solves a set of OPFs and curtails the bids to obtain an overall bid region that will always remain within the network limits for any combination of ways in which the wholesale market could dispatch energy and reserve ④. The curtailments are then applied to the original aggregator bids in the order of the least to the most competitive (in terms of price) bids ⑤, before being sent to the wholesale market for consideration ⑥.

In this overall approach, aggregators are free to calculate their multi-band bids as they please, as long as it conforms to the bidding structure. Here, we propose a particular method based on the fact that in a competitive and efficiently operating market, the bids of participants will tend toward reflecting their true underlying costs and constraints. The bidding requirements of existing markets are not expressive enough to capture these underlying

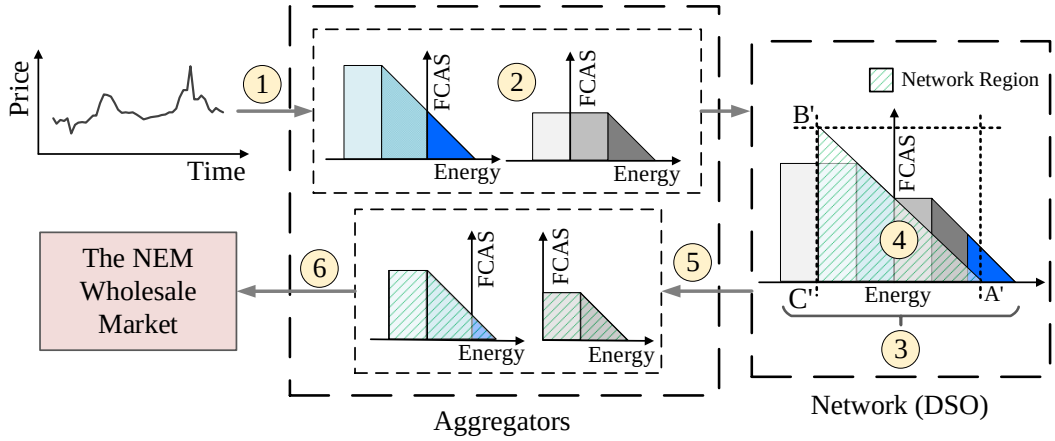

Figure 5.2: Schematic overview of our price-sensitive bidding approach.

requirements of participants to high accuracy, so we will have to allow for some assumptions and approximations in this process.

For the network subproblem, when the DSO has to make a decision between two bids (i.e. if the combination of them would lead to a network violation), all else being equal, it will opt for the bid with the more competitive price offering. The idea is that the wholesale market would favour this bid over the less competitive one in order to achieve an efficient dispatch, so we should similarly be offering the most competitive subset of bids that will remain within the network's limits.

We implement our approach within a model predictive control framework that moves forward every 5 minutes. This allows aggregators to account for the gradual revelation of uncertainty and include the latest (most accurate) uncertainty information in their optimisation problem. While we expect a reasonably accurate PV forecast for the next 5-minute interval, we are not prescribing that aggregators solve a deterministic optimisation problem to obtain their bids. In fact, our overall approach does not stop aggregators from considering a stochastic / robust optimisation for generating their feasible regions (trapeziums), e.g., like what we did in Chapter 4. Such uncertainty characterisation does not affect the network subproblem as the uncertainty of load / PV / electricity prices is only reflected in the consumer subproblem. This means the network subproblem will not face any extra computational challenge when the uncertainties are taken into account. However, consumer subproblems will differ (both optimally and computationally) as consumers need to solve more sophisticated problems. We leave a detailed study of such a case to future work. In the following, we present our aggregator and network subproblems.

5.3 Aggregator Sub-Problem

Here, we assume that consumers are equipped with EMSs that are controlled via aggregators to make price-sensitive energy and reserve bids. These bids are then submitted to the DSO to be shaped before aggregators submit their bids to the market.

5.3.1 Consumer EMS Problem

Similarly to chapters 3 and 5, our consumers own a battery, PV and a background load. Notice that it is relatively straightforward, depending on the convexity of the model, to include any load type into the consumer subproblem.

Our consumer subproblem will include the market linking constraints (3.5a) and (3.5b); solar PV (2.26) and battery constraints (2.27); the linearised reactive power constraint (4.13b); and finally the combined power (2.30). Similarly, to chapters 3 and 4, our consumer subproblem will include 3 copies of consumer's variables and constraints one for each output case: p_t^e, p_t^r and p_t^l. Notice that these constraints provide all the required bounds on our variables, including up and down reserve limits. To simplify, we use $x_{n,t}$ and $p_{n,t} = (p_t^e, p_t^r, p_t^l)$ respectively for the internal variables and the connection point powers of consumer $n \in C$. We use $g_n(p_{n,t}, x_{n,t})$ for the constraints associated with consumer n.

Notice that there is no objective function in the EMS model as the consumers are scheduled according to the aggregator's objective. However, if a consumer has a specific objective, our approach can easily include that. Here, the objective of aggregators is to maximise the benefit of co-participating in energy and reserve markets. Therefore, aggregators receive consumers' constraints (g_n) and co-optimise them for the energy and reserve market, as explained in the following section.

Next, we formulate the basic aggregator problem in Section 5.3.2, which is used to build our price-sensitive bids in Section 5.3.3.

5.3.2 Aggregator Energy-Reserve Co-optimisation Problem

We start with modelling the optimisation problem of a price-insensitive bidding approach. Let us use the variables $P_{i,t}^{a,e}$, $P_{i,t}^{a,r}$, and $P_{i,t}^{a,l}$, respectively for the energy, raise, and lower bids of aggregator a at network node i. For the sake of presentation, we use the vector $P_{i,t}^{a}$ to show the combined aggregator bids, where $P_{i,t}^{a} = (P_{i,t}^{a,e}, P_{i,t}^{a,r}, P_{i,t}^{a,l})$. Given the energy, FCAS raise and lower price

forecasts, $\bar{\pi}_t = (\bar{\pi}_t^e, \bar{\pi}_t^r, \bar{\pi}_t^l)$, aggregator a solves the following problem:

$$\max_P \sum_{i \in N} \sum_{t \in T} \delta \cdot \bar{\pi}_t \cdot P_{i,t}^a + \sum_{n \in C_i^a} \sum_{t \in T} D_{n,t} \tag{5.1a}$$

$$P_{i,t}^a = \sum_{n \in C_i^a} p_{n,t} \qquad \forall i \in N, t \in T \tag{5.1b}$$

$$g_n(p_{n,t}, x_{n,t}) \leq 0 \qquad \forall n \in C^a \tag{5.1c}$$

The first term in the objective function maximises the benefit of aggregators in energy and FCAS markets. The second term adds the reserve deployment cost $D_{n,t}$ obtained via:

$$D_{n,t} = \bar{\pi}_t^e \cdot \delta' \left(\mu_t^r \cdot p_{n,t}^r - \mu_t^l \cdot p_{n,t}^l \right) \tag{5.1d}$$

where δ' is the worst number of seconds, we would need to respond for a single contingency. Assuming that the value of the lost/gained energy is at the energy market price $\bar{\pi}_t^e$, (5.1d) calculates the reserve deployment cost given the probability of a contingency event occurring for lower and raise reserves μ_t^l and μ_t^r. The significance of these deployment costs shrinks to zero as contingencies become rarer.

In the following, we use the above co-optimisation problem to obtain the three important parts of our aggregator subproblem, i.e., the feasible energy-reserve region (Section 5.3.3), up to 10 price bands (in the NEM) across the feasible region (Section 5.3.4) and finally the reactive power aggregators can exchange with the grid for network support purposes (Section 5.3.5).

5.3.3 Aggregator Feasible Region

Aggregators need to obtain their feasible region together with their price bands for each market. Prior to submitting to the market, aggregators communicate to the grid their available operating region at each node, together with their prices. The DSO then shapes the bids to ensure network feasibility and sends the shaped regions back to the aggregators. Since aggregators mainly own inverter-based DER technologies, their overall energy-FCAS region has a triangle shape. This is because, unlike a general trapezium (e.g., Figure 2.3), their feasible region will not be limited by ramp rates Operator [2015]. An example of a feasible region with three price bands for the energy market is given in Figure 5.3. Notice that irrespective of ramp rates, aggregators might want to bid a trapezium as some consumers might either not participate or only partially participate in the FCAS market. Such partial market participation brings consumer preferences into our model. Therefore, aggregators can bid a trapezium shown by (A, B, C, D) for lower and (A, E, F, D) for raise FCAS market. In the following, we use (5.1a)–(5.1c) to obtain the

coordinates of points A–F, making the aggregator's feasible region at node i.

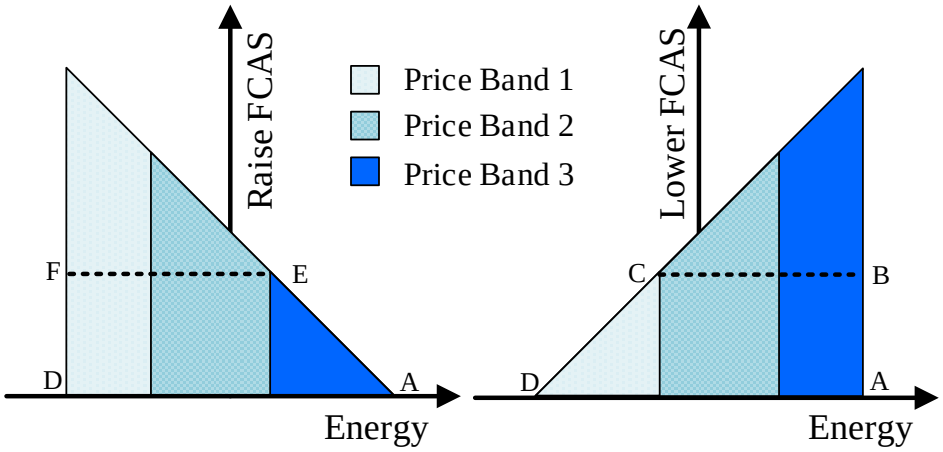

Figure 5.3: Feasible region of an aggregator with 3 price-bands.

Point A

To get the coordinates of point A, we maximise the energy market participation at the first time step as follows:

$$P_{i,1}^{a,e(max)} := \max \sum_{i \in N} P_{i,1}^{a,e} \tag{5.2a}$$

$$\text{s.t.} \qquad g_n(p_{n,t}, x_{n,t}) \leq 0 \qquad \forall n \in C_i^a \tag{5.2b}$$

Thus, $(P_{i,1}^{a,e(max)}, 0)$ is the coordinates associated with point A in Figure 5.3.

Point B

To get point B, we maximise the lower FCAS market participation at the first time step as follows:

$$P_{i,1}^{a,l(max)} := \max \sum_{i \in N} P_{i,1}^{a,l} \tag{5.3a}$$

$$\text{s.t.} \qquad P_{i,1}^{a,e} = P_{i,1}^{a,e(max)} \tag{5.3b}$$

$$g_n(p_{n,t}, x_{n,t}) \leq 0 \qquad \forall n \in C_i^a \tag{5.3c}$$

The above optimisation generates the coordinates of point B= ($P_{i,1}^{a,e(max)}$, $P_{i,1}^{a,l(max)}$).

Point C

To get point C, we minimise the energy market participation at the first time step when the lower FCAS bid is fixed at the obtained value for point B. This can be written as follows:

$$P_{i,1}^{a,eC} := \min \sum_{i \in N} P_{i,1}^{a,e} \tag{5.4a}$$

$$\text{s.t.} \quad P_{i,1}^{a,l} = P_{i,1}^{a,l(max)} \tag{5.4b}$$

$$g_n(p_{n,t}, x_{n,t}) \leq 0 \qquad \forall n \in C_i^a \tag{5.4c}$$

Thus, C= ($P_{i,1}^{a,e(C)}$, $P_{i,1}^{a,l(max)}$). Notice that if an aggregator decides to bid a triangle, then according to (5.3a)–(5.3c) and (5.4a)–(5.4c), the coordinates of points C and B will be identical.

Point D

To get point D, we minimise the market participation in the energy market at the first time step as follows:

$$P_{i,1}^{a,e(min)} := \min \sum_{i \in N} P_{i,1}^{a,e} \tag{5.5a}$$

$$\text{s.t.} \quad g_n(p_{n,t}, x_{n,t}) \leq 0 \qquad \forall n \in C_i^a \tag{5.5b}$$

Thus, ($P_{i,1}^{a,e(min)}$, 0) is the coordinates associated with point D in Figure 5.3.

Point E

To get point E, we maximise the raise FCAS market participation at the first time step as follows:

$$P_{i,1}^{a,r(max)} := \max \sum_{i \in N} P_{i,1}^{a,r} \tag{5.6a}$$

$$\text{s.t.} \quad P_{i,1}^{a,e} = P_{i,1}^{a,e(min)} \tag{5.6b}$$

$$g_n(p_{n,t}, x_{n,t}) \leq 0 \qquad \forall n \in C_i^a \tag{5.6c}$$

Thus, E= ($P_{i,1}^{a,e(min)}$, $P_{i,1}^{a,r(max)}$).

Point F

Finally, to get point F, we maximise the energy market participation at the first time step when the raise FCAS bid is fixed at the obtained value for point F. This can be written as follows:

$$P_{i,1}^{a,eE} := \max \sum_{i \in N} P_{i,1}^{a,e} \tag{5.7a}$$

$$\text{s.t.} \qquad P_{i,1}^{a,r} = P_{i,1}^{a,r(max)} \tag{5.7b}$$

$$g_n(p_{n,t}, x_{n,t}) \leq 0 \qquad \forall n \in C_i^a \tag{5.7c}$$

Thus, F= ($P_{i,1}^{a,e(E)}$, $P_{i,1}^{a,r(max)}$). Similarly to point C, if the aggregator decides to bid a triangle, then according to (5.6a)–(5.6c) and (5.7a)–(5.7c), the coordinates of points E and F will be identical.

5.3.4 Price Bands

Consumer-owned technologies, such as batteries, make a profit by arbitraging energy (i.e., charge when the price is low and discharge when the price is high). Thus, finding representative price bands for aggregators relies on the price and dispatch over time. This means that to make sound decisions in the first operating interval, we need to account for the market prices in the future. To do so, we select b capacity bands (up to 10 in the NEM) across the energy-reserve region in the first time-step ($t = 1$). In fact, these bid bands are possible dispatch scenarios, each of which can lead to a different future schedule. We then obtain the schedule and the future benefit associated with getting dispatched at each bid band based on the forecasts of the future prices. Comparing the benefit obtained at each bid band with a base case (in which aggregators only have their consumers' background load), we calculate the minimum price for delivering that capacity.

Let $P_{i,t=1}^{b}$ denote the dispatch at price-band b, i.e., energy, maximum raise and maximum lower at the b-th segment of the energy-reserve region. The expected future benefit $\mathcal{B}_{exp}^{b}$ associated with $P_{i,t=1}^{b}$ is obtained as follows:

$$\mathcal{B}_{exp}^{b} := \max \sum_{t \in \{2,\ldots,T\}} \Big(\sum_{i \in N} \delta \cdot \pi_t \cdot P_{i,t}^{a} + \sum_{c \in C_i^a} (D_{c,t} - \Omega_{c,t}) \Big) \tag{5.8a}$$

$$P_{i,t=1}^{a} = P_{i,t=1}^{b} \tag{5.8b}$$

$$g_n(p_{n,t}, x_{n,t}) \leq 0 \qquad \forall n \in C_i^a \tag{5.8c}$$

Having obtained the expected future benefit associated with every band b, we need to transfer them into prices. To do so, we compare the total benefits (first time step + future benefit) of getting dispatched at each capacity

band with a base case ($b = 1$) where consumers are just withdrawing their background load from the grid at the first time step. The price of getting dispatched at each capacity band should be such that aggregators obtain higher benefits than in the base case (since otherwise, they would prefer the base case outcome). Let $\pi_b = (\pi_b^e, \pi_b^r, \pi_b^l)$ denote the energy, raise and lower price for capacity band b. Given $P_{i,t=1}^b$, $P_{i,t=1}^{b=1}$ and their future benefits $\mathcal{B}_{exp}^b$, $\mathcal{B}_{exp}^{b=1}$, this can be written as:

$$\delta \cdot \pi_b (P_{i,t=1}^b - P_{i,t=1}^{b=1}) + \mathcal{B}_{exp}^b \geq \mathcal{B}_{exp}^{b=1}. \tag{5.9}$$

Note that (5.9), in the marginal case, can be simplified to: $a\pi_b^e + b\pi_b^r + c\pi_b^l = d$ where a, b, c, and d are constants. Such an equation can be satisfied for an infinite combination of energy and FCAS prices. To limit this and obtain a unique solution, without loss of generality, we fix the FCAS prices to zero and obtain the energy price for which the aggregator can operate at band b in the energy market and provide the associated FCAS capacities. Note that even though the bids for each market are separate, in practice, the market cost function will be inseparable in NEMDE. Therefore, while it produces a unique solution for (5.9), it will not change the way NEMDE dispatches.

5.3.5 Aggregator Reactive Power Support

Here we obtain the reactive power the aggregator can exchange with the grid to provide greater network throughput. Based on Figure 5.3, we calculate the maximum reactive power that we can deliver at the extremes of aggregator triangles, i.e., points A and D. To ensure that the reactive power is being provided constantly for any other points within the aggregator flexibility region, we connect a line between the reactive power that we will be asked to provide at points A and D. For any operation point between A and B, we inject / absorb reactive power according to the obtained line. This is shown in Figure 5.4.

Here, we assume that the aggregators are not paid for their reactive power support, and their only benefit in providing such support is to open up network capacity to allow greater network access to consumers. This is also in line with the Australia / New Zealand standard, where the inverters are required to be able to provide reactive power support for the distribution network. However, such services can be contracted and paid for. This does not change our approach and will only increase aggregator benefits.

Having obtained the feasible regions, prices and reactive power support, aggregators communicate them with the DSO to have their bids shaped. Note that aggregators participating in other co-optimised markets that do not require a trapezium can use a similar process to generate multiple bands and

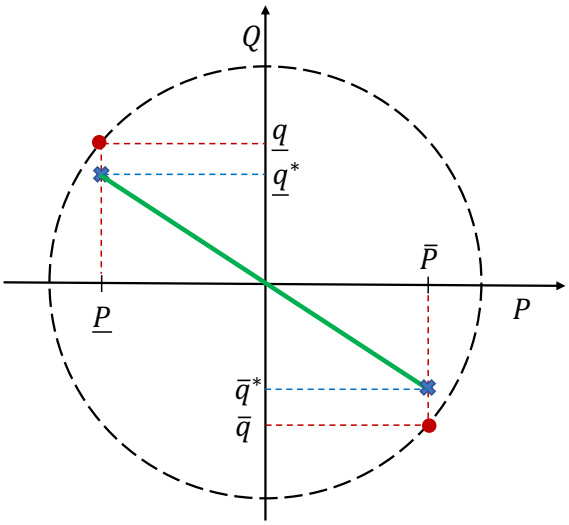

Figure 5.4: Reactive power support

submit them to the DSO / market in the spirit of multiple simple bids.

5.4 Network Sub-Problem

The goal of our network subproblem is to open up as much network capacity as possible for aggregators while ensuring grid security. To achieve this, we first merge aggregators' feasible regions to have a polygon at each network node i.e., $\mathcal{P}_i = \sum_{a \in A_i} P_i^a / S_{base}$ and $\mathcal{Q}_i = \sum_{a \in A_i} q_i^a / S_{base}$. For the two extremes (max and min power)[1] of the overall polygon (i.e., $\mathcal{P}_i^{Ex}$ and $\mathcal{Q}_i^{Ex}$), our network subproblem takes the total desired capacity, solves an OPF and then returns a curtailment Λ_i for each node. To reduce the total operation cost, we apply this curtailment to the bids from the least to the most competitive (in terms of price) and curtail in this order until we have curtailed the total of Λ_i at each node.

Similar to chapters 3 and 4, here we use the branch flow equations (2.31)–(2.36) to model the distribution network constraints. Let us use P_i' for the accepted bids and Q_i' for the required reactive power support at node i; we write our network subproblem as follows:

[1]The obtained polygon includes several bid scenarios. However, we only need to explore the worst scenarios, which are located at the extremes of the network polygon. This way, while keeping our network subproblem tractable, we ensure that the network constraints are satisfied even for the worst combination of scenarios.

$$\min \sum_{i \in N} ||\Lambda_i||_2^2 \tag{5.10a}$$

$$F_i^P - r_i I_i + P_i' = \sum_{j \in \phi_i} F_j^P \qquad \forall i \in N \tag{5.10b}$$

$$F_i^Q - x_i I_i + Q_i' = \sum_{j \in \phi_i} F_j^Q \qquad \forall i \in N \tag{5.10c}$$

$$P_i' + \Lambda_i = \mathcal{P}_i^{Ex} \qquad \forall i \in N \tag{5.10d}$$

$$Q_i' \leq \mathcal{Q}_i^{Ex} \qquad \forall i \in N \tag{5.10e}$$

$$(2.33), (2.34), (2.35), (2.36) \tag{5.10f}$$

The objective (5.10a) minimises the square l_2-norm of the bid curtailments. Since we apply the bid curtailment from the least to the most competitive price order, the more curtailment occurs at any particular node, the more likely we will start to curtail competitive bids. When the curtailment is spread across many nodes more evenly, as with the l_2-norm, we will tend to just curtail the least-competitive bids at each node. In other words, our $l2$ norm curtailment approach splits the curtailment more evenly across more consumers rather than only limiting those with a problematic connection. One can interpret this feature of our approach as treating consumers fairly. An l_1-norm curtailment policy has been used in the literature to limit PV systems, e.g., Liu et al. [2020]. However, such an l_1-norm policy curtails the bids at weaker nodes (mainly end nodes) until the network problem is fixed. Thus, both the least and the most competitive bids will be curtailed at these nodes. In the results section, we will illustrate the difference between the two norms and show that the l_2-norm is more appropriate.

Active and reactive power flow equations are given by (2.31)–(2.32), where, ϕ_i is the child nodes and at node i. The overall bid accepted by the network plus the bid curtailment is enforced to be equal to the overall aggregator bid in (5.10d). Finally, the reactive power used by the network is limited to aggregators' reactive power offers through (5.10e).

Note that (5.10a)–(5.10f) need to be solved for the extreme points of the overall polygon. As shown in Figure 5.2, the feasible regions accepted by the network might be smaller than the one aggregators have provided. Finally, the shaped bids are submitted to the market. When the market is cleared, each aggregator finds out where in their bid trapezium they will be dispatched for the upcoming interval. From here on, our approach is repeated with updated inputs.

5.5 Numerical Results

To illustrate the effectiveness of the proposed approach, we use the same 69-bus distribution network Savier and Das [2007] as in chapters 3 and 4. To evaluate the performance of our price-sensitive bidding approach and our network modelling in the presence of more DER, we study two different DER levels in this chapter: once where, similarly to chapters 3 and 4, there are 3 consumers per node (207 consumers in total), and another where there are 5 consumers per node (345 consumers in total). Similarly to previous chapters, we participate in 7 markets (1 energy, three raise and three lower contingency FCAS markets), but differently from them, we participate as a price-sensitive participant. The 5-minute energy and reserve price forecast, taken from the NEM pre-dispatch, are used to run our optimisation problems. We then use the real MCPs as the realisation to evaluate the effectiveness of our approach. Both the pre-dispatch and MCPs are provided in Appendix A. Finally, we use Gurobi and IPOPT solvers in JuMP, Julia Dunning et al. [2017] to solve our consumer and network subproblems.

In the following, we first introduce our comparative approaches in Section 5.5.1. We then discuss how we obtain the final benefit for each comparative approach in Section 5.5.2. We illustrate the effectiveness of our price elastic bidding approach in Section 5.5.3. In Section 5.5.4 we study the effectiveness of our network modellings when the objective function (5.10a) uses the l_1- and l_2 norm policies to minimise the bid curtailment and provide some comparisons with the network modelling in our previous chapters as well as some operating envelopes. Section 5.5.5 compares the performance of the one-shot network policy of Chapter 5 against the ADMM approach, used in chapters 3 and 4. Section 5.5.6 studies the effectiveness of providing reactive power support in the price-sensitive approach. Section 5.5.7 compares the voltages across the grid. Section 5.5.8 provides more discussions on the accepted price-sensitive vs. price-insensitive bids in the market. Section 5.5.9 compares the problem size and run time of different approaches. Finally, Section 5.5.10 provides results on the scalability of our proposed approaches to a real-world power system.

5.5.1 Comparative Approaches

To illustrate the performance of our more flexible bidding approach, we compare the results of three different approaches:

Price-Insensitive: in which aggregators optimise their portfolio using the optimisation model (5.1a)–(5.1c). The optimisation uses price forecasts provided by the AEMO's pre-dispatch. Both the pre-dispatch and market clearing prices are provided in Appendix A. The mean absolute error of the forecasts and the realised prices for energy, raise and lower FCAS market is \$9.6,

$7.4 and $3.0, respectively, for 22 Feb 2020. Demand bids are submitted at the cap price, and supply and FCAS bids are submitted at the floor price for the respective market.

Perfect: in which aggregators optimise their portfolio using the optimisation model (5.1a)–(5.1c). The optimisation uses market clearing prices instead of forecasts for the whole horizon (288 future time steps). Similarly to Price-insensitive, the demand bids are submitted at the cap price, and supply and FCAS bids are submitted at floor prices. This case is similar to what we had in Chapter 3.

Price-Sensitive: in which aggregators run the proposed approach to generate their energy-FCAS regions (both raise and lower FCAS markets) as well as their price bands. Note that we use the same forecasts as in price-insensitive to obtain the prices. Here, we only obtain three price bands, each reflecting the price of a highly likely transition that aggregators can experience: 1) moving from the base case in which the batteries are neither charging nor discharging to charge mode; 2) moving from the base case to discharge mode; 3) moving from the base case in which all PV is curtailed to a no-PV-curtailed point. The reason is that aggregators' problem is linear, and these transitions, especially over a 5-minute settlement, are representative.

Note all the above approaches are implemented within a model predictive framework that moves forward one time-step (5 minutes) at a time.

5.5.2 Market Clearing Process

More than 500 agents participate in the NEM energy and FCAS markets every day. NEMDE co-optimises all these participants every five minutes to obtain the market prices and the dispatch of every participant. Here, we implement a simplified version of NEMDE to dispatch our aggregators. To simplify, we assume that all the participants in the same market region (Australian states) are located at one transmission node. This leads to a transmission network with 5 nodes, each representing one of the Australian eastern states / territories. We assume our 69-bus distribution network is connected to the bus representing New South Wales (NSW). For each region, we extract the energy and FCAS bids of all participants as well as their demand and FCAS requirements from AEMO's website[2]. Similarly to NEMDE, we use a linear OPF to obtain the dispatch of all our participants (including aggregators) and the price of each market.

5.5.3 Price-Sensitive vs. Price-Insensitive

To highlight the effectiveness of bidding a wider range of DER operating points, we first report the total benefits of the above approaches when the

[2]http://nemweb.com.au/

network constraints are neglected. Let us use *Medium* and *High* to indicate different DER-integration levels associated with our 207 and 345 consumers, respectively. Table 5.1 reports the total benefit for Medium and High DER integration scenarios when neglecting the distribution network.

Table 5.1: Overall Benefit of Aggregators Neglecting Network

Approach	Benefit ($)		Average Rel. to Perfect
	Medium	High	
Price-Insensitive	2742.3	4575.2	-12.1
Price-Sensitive	2842.2	4741.6	-8.9
Perfect	3118.7	5202.5	–

As reported in Table 5.1, the proposed price-sensitive approach could obtain 3.2 % higher benefits compared to the price-insensitive approach[3]. The reason is that the price-insensitive bidding approaches submit their bids at either floor or market cap prices; therefore, no matter how much the realised price deviates from the forecasts, their bids are accepted by the market. On the contrary, the price-sensitive approach generates different capacities for different prices. Therefore, if the market price realises differently from the forecast, the participants will get dispatched in a band that maximises their benefit rather than a single predetermined capacity band according to the forecast. Moreover, as can be seen in Table 5.1, the perfect approach brings the highest benefit since it uses the market clearing prices (i.e., perfect information). Notice that since the network constraints are neglected, the results in Table 5.1 might be infeasible. We next include network constraints to avoid infeasible results.

5.5.4 Network Inclusion

Here, we illustrate the effect of including the network constraints on our bidding problem. To provide a fair comparison, we incorporate the network subproblems for both price-insensitive and perfect approaches. To do so, we use a similar approach as in Section 5.4, yet instead of multiple bid bands as in the price-sensitive approach, consumers obtain a single bid band (either according to the price forecast or MCP) and report their maximum and minimum CPP to the network subproblem. The DSO then solves two OPFs (one for each extreme) to obtain the curtailments.

Table 5.2 reports the total one-day benefits of our aggregator for the l_1- and l_2-norm network curtailment policies.

The relative benefit improvement of the two network cases (l_1- and l_2-norms) with respect to no network case (i.e., Table 5.1) is also reported in

[3]Depending on how market prices change, the extra benefit can be different.

Table 5.2: Network-Secure Consumer Benefit

Approach	DER Level	Total Benefit ($)		Rel to No Net. (%)	
		l_1-Norm	l_2-Norm	l_1-Norm	l_2-Norm
Price-Insensitive	M	2719.7	2732.5	-0.4	-0.8
	H	4117.0	4120.5	-10.0	-9.9
Price-Sensitive	M	2839.2	2837.6	0.11	0.16
	H	4281.5	4258.3	-9.7	-10.2
Perfect	M	3090.3	3083.7	-0.9	-1.1
	H	4677.0	4635.8	-10.1	-10.9

Table 5.2. Notice that since the network constraints are included, both cases obtain network-feasible results; however, a higher benefit is obtained for the l_1-norm curtailment policy. The reason is that here, we have not included any internal objective for consumers, and thus the benefit is only defined by market transfers. Since the l_1-norm curtailment policy maximises the throughput, it obtains the highest benefit. Compared to l_1-norm, l_2-norm spreads the curtailment on multiple nodes (rather than prioritising the end feeders as in l_1-norm). In other words, when using l_2-norm, the curtailment at each node is less than l_1-norm, yet the curtailment happens at more nodes. In our price-insensitive approach, we apply the curtailment from the most expensive to the least expensive offer. Thus, the more we curtail at any single node, the more likely we curtail the competitive bids. Thus, the maximum export might curtail efficient bids and let the more expensive bids reach the market. However, as our l_2-norm policy tends to curtail more expensive bids, to ensure network security, we need to curtail more capacity in total, but those bids reaching the market are the most efficient ones.

To show the impact of different curtailment policies when computing our network secure bids, we compare the bid curtailment under the l_1- and l_2-norms in the objective function (5.10a). Figure 5.5 compares the amount of curtailed bids for the three highest prices[4] at time step 164, where the highest voltage violation occurs. As shown in the figure, unlike the l_1-norm, the l_2-norm mainly limits the most expensive bid.

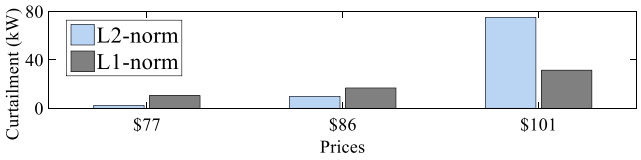

Figure 5.5: Bid curtailment at different prices.

[4]There was no curtailment for prices lower than $77.

5.5.5 ADMM-based vs. One-Shot Network Models

As mentioned before, Perfect is the same case we used in Chapter 3. Therefore, here we can directly compare the benefit of our network modelling, i.e., sequential implementation, as in this chapter and when we use ADMM to negotiate and converge on a consensus solution. Table 5.3 reports the results of our ADMM-based and one-shot policy approaches for both our medium (M) and high (H) DER penetration scenarios. As reported for the medium DER penetration scenario, our one-shot curtailment policy obtains results 0.1% lower than those of the ADMM approach. This difference for our high DER-penetrated scenario is -2%. However, please note that while the network and consumer subproblem size is the same in both cases, our one-shot approach only needs to solve the problem once. On the contrary, our ADMM approach converged respectively within 95 and 166 iterations for our medium and high DER scenarios. This means that our one-shot approach requires 95 and 166 times less computation than ADMM-based approaches.

Table 5.3: Sequential vs. consensus

Approach	Scenario	Benefit ($)			Rel. to ADMM
		Energy	FCAS	Total	
ADMM-Based	M	250.1	2844.8	3094.9	–
ADMM-Based	H	394.4	4401.6	4796.0	–
One-Shot	M	249.3	2841.0	3090.3	-0.1
One-Shot	H	304.1	4372.9	4677.0	-2.5

5.5.6 Reactive power support

In this section, we report the trapezium of a consumer with and without reactive power support and how the grid shapes the trapezium in each case.

Figure 5.6 shows the energy-raise feasible region at bus 27 for our medium DER integrated case and how it is shaped by the network with and without reactive power support. The reported trapezium is for 1:30 pm when there is high PV power available, and thus there is an over-voltage issue at the consumer network connection node. The trapezium on the left is when there is no reactive power support, while on the right, there is reactive power support available. Starting with the trapezium on the left, to resolve the over-voltage issue, the DSO curtails the injection energy from 6.8 kW to 4.2 kW. Therefore the network-secure trapezium is reduced to the green area. On the other hand, on the right, the DSO can use the reactive power support of consumers to reduce (or avoid) active power curtailment. As shown in Figure 5.6, consumers can bid their original trapezium if they consume 3.1 kVAR reactive power. Notice that to ensure the grid feasibility, if the consumers get dis-

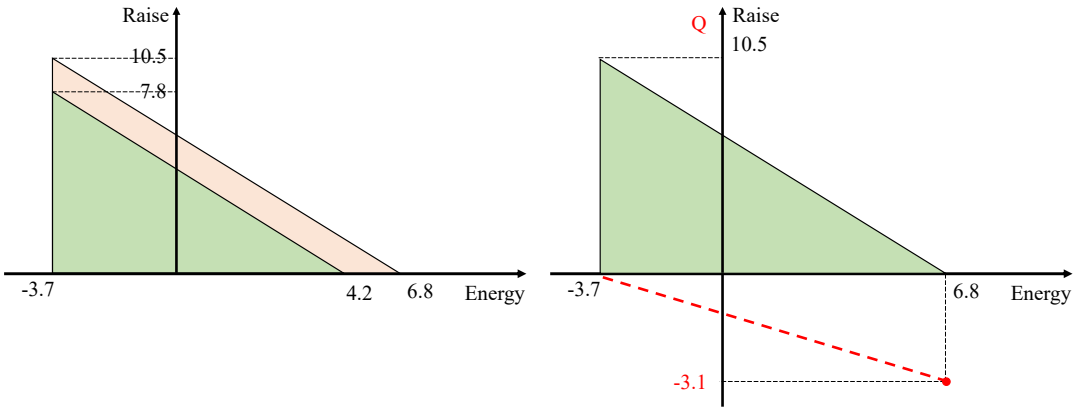

Figure 5.6: Reactive power support

patched less than 6.8 kW in the energy market (or combination of energy and reserves), they need to follow the dotted line and consume reactive power accordingly.

The reactive power support improved the consumer benefit both in medium and high DER scenarios. While the reactive power could mitigate all network violations in the Medium case, in the high DER scenarios, we could improve 5% on consumer benefit.

5.5.7 Distribution Network Voltage Analysis

After the market-clearing process, when the real dispatch of each aggregator is revealed, we solve three PFs (one where no FCAS action is required (energy alone), one for max raise FCAS activation, and another where max lower FCAS is activated) to obtain the actual voltages at each node. We plot the minimum and maximum voltages occurring in the system with and without network inclusion in Figure 5.7.

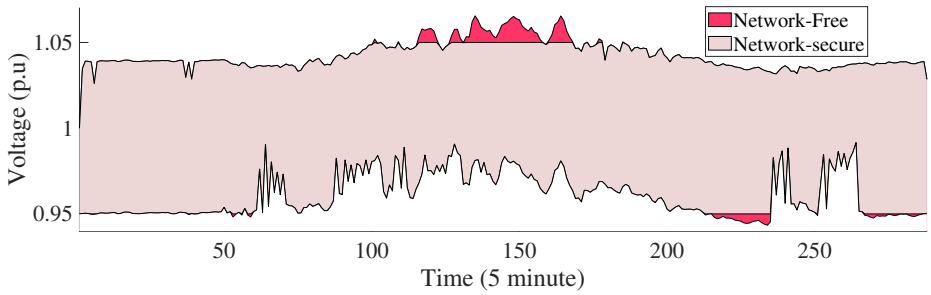

Figure 5.7: Maximum and minimum voltage across the grid: network-free vs. network-secure

As can be seen in Fig 5.7, the voltage of the system is always within the safe

limits for the proposed network-secure approach. Also, while the proposed approach could keep the voltage of all 69 nodes within the safe limits, 19 out of 69 nodes experienced at least one voltage violation in the Network Free case.

5.5.8 Accepted Bids: Price Insensitive vs. Sensitive

Figure 5.8 compares the accepted bids in the energy, raise and lower reserve markets generated by our price-insensitive and insensitive approaches.

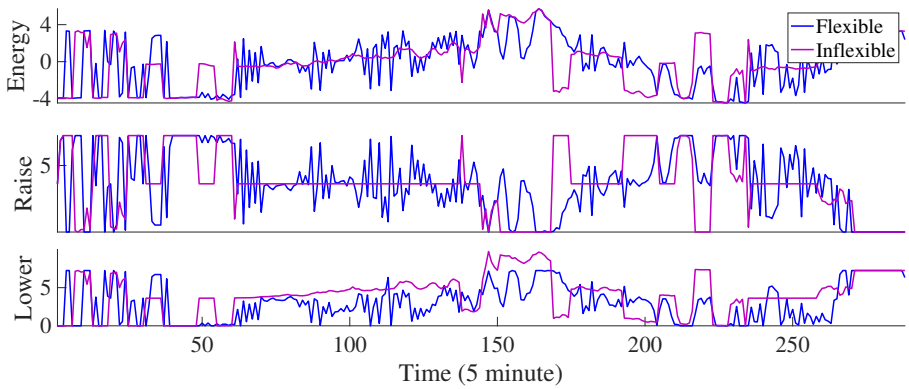

Figure 5.8: Market-accepted energy, raise, and lower reserve bids: Price-Insensitive vs. Sensitive

5.5.9 Computational Performance

Table 5.4 reports the total problem size and the computational time of price-insensitive, perfect and price-sensitive approaches for our sequential implementation together with the expected parallel time (using the time of the slowest subproblems at each iteration). Note that in the aggregator subproblem, the number of variables is linear in the number of consumers. The reason is that no two aggregators nor any two consumers of the same aggregators have common variables and constraints. Thus, the aggregator subproblem can be decomposed at the connection point of every consumer within a single model predictive iteration, and each of the consumer subproblems can be solved in parallel. A consumer subproblem (for the price-sensitive approach) includes 21k variables and 16k constraints. Similarly, our network subproblem can be separated into one OPF for each time step[5] and each power flow case under consideration: energy, FCAS raise, FCAS lower. This reduces the number of variables and constraints relevant to the parallel implementation of the network subproblem to 2k and 1.7k, respectively.

[5]Since there are no time coupling constraints in the network subproblem.

Table 5.4: Problem Size and Computation Time

Approach	Problem-part	Problem Size		Time(s)
		#Var.	#Cons.	Seq(Parallel)
Price-Insensitive / Perfect	Aggregator	18,680k	14,772k	272 (0.43)
	Network	2,701k	2,243k	281 (0.41)
	Total	23,347k	17,015k	553 (0.84)
Price-Sensitive	Aggregator	30,919k	22,774k	378 (0.91)
	Network	3,247k	2,514k	387 (0.39)
	Total	34,166k	25,288k	765 (1.30)

As can be seen in Table 5.4, the estimated parallel time to solve the price-insensitive and the proposed price-sensitive approaches, for a single horizon, are respectively 0.84s and 1.30s. Note that these are potential solve times for a fully parallel implementation. However, if the computational resources are not available to perform a fully parallel solve, and the solve time becomes a limiting factor, it is possible to approximate the problem by using a variable time discretisation of the horizon to reduce the number of time steps Scott et al. [2019]. By using 30-minute steps after the first time step in the horizon, experiments show that we are able to reduce the sequential solve time 16 fold, at the cost of a 6% decrease in overall benefits.

5.5.10 Experiments on a real-world MV-LV network

Here we compare the performance of the ADMM and the one-shot policies on an MV-LV distribution network provided by an Australian DSO. The distribution network includes 1 MV feeder of 11 kV and 5 LV feeders of 0.43 kV. In more detail, the MV feeder has 14 buses, 13 lines, 5 MV/LV transformers, and 1 MV load. The LV feeders have a total of 724 buses, 719 lines, and 522 LV customers. We study 3 different PV and battery penetration levels: PV20B10, PV40B20, and PV60B30. For instance, PV20B10 represents a scenario where 20% of customers own a solar PV system and 10% of them own battery storage. Similarly PV40B20 / PV60B30 are scenarios with 40% / 60% PV and 20% / 30% battery storage. Consumers can own 5 kW/13.5 kWh battery storage with a round trip efficiency of 0.9 and PV, ranging from 3 to 6 kW. The inflexible load and PV generation were modelled using 5-minute data of real houses Iria et al. [2022].

Table 5.5 shows the benefit obtained by ADMM approach used in chapters 3 and 4 and the one-shot curtailment approach in Chapter 5. In line with our results on a 69-bus network, as DER penetration increases and the network becomes more binding, the ADMM approach is able to obtain better results. However, unlike ADMM, the one-shot policy provides network feasibility in one iteration, which reduces the computation cost significantly. Table 5.6

reports the computational time of both approaches.

Table 5.5: Benefit obtained for different DER penetration level: ADMM vs. one-shot

DER penetration	Benefit $		
	ADMM	One-shot	Improvement %
PV20B10	-902	-902	0
PV40B20	792	792	0
PV60B30	1974	1862	6

Table 5.6: computation time for different DER penetration level: ADMM vs. one-shot

DER penetration	ADMM		Oneshot	Improvement (times)
	Iteration	time	time	
PV20B10	4	0.46s	0.12s	3.8
PV40B20	32	3.01s	0.12s	25.1
PV60B30	44	4.52s	0.12s	37.7

5.6 Conclusion

In this chapter, we answered the important question of how aggregators, who share the same distribution network, can efficiently participate in the energy and reserve markets while respecting the grid constraints. Unlike the common price-insensitive approaches, our approach generates bids and the prices for aggregators' available flexibility. By obtaining the grid operating region, we also ensure that aggregator bids will not go beyond the network capabilities.

We illustrated the effectiveness of our approach using 207 / 345 consumers in a 69-bus network. Our results show a 3.2% benefit improvement compared to a price-insensitive method. We also show the importance of network inclusion by using two curtailment policies in the network subproblem: 1) the inclusion of the network using an l_1-norm curtailment policy, 2) the inclusion of the network using an l_2-norm curtailment policy. We also compared the effectiveness of the one-shot curtailment policy presented in this chapter with the ADMM-based iterative approach presented in chapters 3 and 5. We showed that while both approaches can obtain feasible results, the ADMM-based method obtains better results at the expense of more communication and computation. We also show that if aggregators provide the network with their reactive power support, they can obtain higher benefits. The reason is that consumers' reactive power support can expand the network's feasible region.

In this chapter, we primarily focus on the security of the network while opening up network capacity. In other words, we introduce a new role for

the DSO and thus have not included losses into our calculations to avoid extra complications. However, our network subproblem can be extended to additionally consider reducing losses. Including different DER types and uncertainty (other than what our MPC implementation can capture) are two other possible extensions that we leave to future work.

In addition, this chapter ignored consumer uncertainty and solely focused on market price uncertainty. However, our approach can be extended to include consumer uncertainty, similarly to Chapter 4. Since our approach decomposes consumers and network subproblems, similarly to Chapter 4, the consumer uncertainty can be dealt with in the aggregator subproblem, adding negligible complexity to the DSO subproblem.

Notice that in this thesis, there are no incentives to encourage truthful DSO behaviour, and we have assumed that the DSO truthfully tries to get the best out of the existing networks. Additional considerations can be introduced to promote truthfulness in the DSO subproblem. For example, tariffs can be allocated to every kW within operating envelopes allowing the DSO to earn more if they provide greater network access for consumers. We leave this additional consideration to future work.

Chapter 6

Conclusion

The objective of this thesis was to enable consumers to provide energy and reserve services within the electricity market while respecting the technical limits of the distribution network. We studied different aspects of the problem, identified the challenges, and provided solutions to the key challenges in chapters 3, 4, and 5.

We suggested two bidding approaches that generate either a single bid band, called price-insensitive, or multiple bid bands at different prices, called the price-sensitive solution to the problem. We showed that if an accurate price forecast is available, it is best to put DER flexibility in one (price-insensitive) band. Yet, when there is uncertainty around prices, chunking DER flexibility and offering it at multiple (price-sensitive) bid bands can improve consumer benefit. Since consumer bids reach the market via the distribution network, our price-insensitive / sensitive offers accounted for the grid's technical limits before submitting bids to the market. This can be viewed as a pre-assessing phase that ensures the feasibility of bids prior to the market-clearing procedure without changing how current electricity markets work.

As discussed throughout this thesis, irrespective of the bidding type, there are challenges stemming from the size of the optimisation problem, consumer / grid privacy, and data uncertainty that a solution needs to overcome. We deal with these challenges by:

- breaking the large-scale optimisation problem down at the level of every consumer and solving the problem in a distributed fashion. This could be done as part of ADMM, as with our price-insensitive solution, or a simpler one-shot approach, as with our price-sensitive solution. While both methods can provide some level of privacy for consumers and the grid, the ADMM approach is able to obtain better (near) optimum results at the expense of more computation.

- implementing our approaches on a model predictive control framework

to solve the optimisation problem every 5 minutes. This enables consumers to include the latest uncertainty information into their optimisation problems and obtain more accurate results. In addition, we propose a piecewise affinely adjustable robust optimisation approach that empowers consumers with controllers to compensate for uncertainties during the 5-minute operating interval between the two successive MPC optimisations. We studied the effectiveness of our uncertainty modelling only within our price-insensitive bidding solution. However, our price-sensitive approach can also use a similar method to account for uncertainty more accurately.

6.1 Key Learnings

The solutions presented through chapters 3-5 each had their own key learnings that we summarise in the following:

In Chapter 3, we developed a network-secure bidding approach using the distributed optimisation ADMM. Our solution enables consumers and the network to negotiate for operating envelopes that indicate the network-secure operating domain for consumers. Comparing to the available literature, we found that our ADMM-based solution approach can obtain (near) optimum results, can scale to realistically sized networks, can provide some level of privacy for consumers and the DSO, and finally can converge within a reasonable time, when relying on consumer computational resources.

Chapter 4 builds on operating envelopes of Chapter 3 by modelling consumer uncertainties using a piecewise affinely adjustable robust approach and enabling reactive power exchange to increase network throughput. We found that our uncertainty characterisation improves the bidding solution in two main ways. It firstly provides the means for consumers to stick to their envelopes which in turn ensures network security. In addition, it enables consumers to account for market penalties that might apply to them in case they fail to deliver the offered capacity. Regarding the reactive power, we showed that such reactive power support opens up network capacity, and thus, consumers can participate in the market with fewer network limitations.

Chapter 5 builds on the bidding approach of chapters 3 and 4 by accounting for market price uncertainty while exploring a technique to improve scaling. Here, rather than a single price-insensitive bid band, we obtain multiple price-sensitive bid bands. We show that our price-sensitive solution can hedge the price uncertainty effect and improve consumer benefit when the prices cannot be forecast accurately. In addition, rather than ADMM, we explored the effectiveness of a simpler one-shot policy within our bidding approach. The computation / communication required by our one-shot policy is equivalent to one iteration of ADMM, which increases its application in

a real-world setting. However, this comes at a price of less optimum results (in our experiments, the one-shot policy reduced the benefit at a maximum of 2.5% while requiring 166 times less computation).

6.2 Future Research

In this thesis, we only assumed that consumers participate in energy and contingency reserve markets. Future work is needed to investigate the benefit of participating in the regulation market alongside the energy and contingency reserve markets. Since contingency is a rarely activated service, we simplified the probability of reserve activation with a constant value. However, regulation is continually activated. Thus, a more sophisticated probabilistic model is needed to take the regulation activation into account.

In chapters 3 and 4, we used the ADMM approach to coordinate consumers with the grid. Further research to improve ADMM convergence or the effectiveness of different distributed approaches, such as ALADIN Engelmann et al. [2017], needs to be investigated in future work.

Other uncertainty characterisation techniques, such as stochastic programming or distributionally robust approaches that can use the available uncertainly information, might achieve a better outcome than our piecewise affine approach in Chapter 4, especially if bounds on uncertainty deviations are not easily predictable. Exploring these approaches in the context of operating envelopes is worth investigating in future work. In addition, we applied the market penalty associated with not honouring the energy bids to individual consumers. This enabled us to fully decompose the problem at the level of every consumer. However, in reality, such penalties are applied to the aggregate of offers reaching the market. Notice that, on aggregate, some part of consumers' uncertainty might cancel out. Therefore, modelling this can increase consumer benefit at the expense of another constraint that couples consumers. The pros and cons of such modelling can be investigated in future work.

The bid shaping approach in Chapter 5 does not directly include aggregator prices when coming up with the required curtailment at each node. In other words, we first calculated the curtailment at each node and then applied the curtailment to the least competitive bids outside the optimisation. However, aggregator prices as well as network losses can be directly included within the network optimisation problem. Future work can study the pros and cons of such a modification. In addition, currently, our price-sensitive approach in Chapter 5 solely counts on an MPC implementation for uncertainties. However, a stochastic or robust approach (for example, a similar approach as in Chapter 4) can be incorporated to capture the uncertainty effects more accurately.

6.3 Summary

To summarise, this thesis addressed the important question of how residential DER can participate in the energy and reserve markets while respecting the constraints of the distribution network that is sitting between DER and the market. It has expanded the knowledge in the area of consumer bidding solutions, adjustable robust optimisation, and distributed optimisation. It has also discovered a range of interesting future research topics.

Moving away from fossil fuels and towards renewable makes it challenging to meet the reliability requirements of power systems, but one that is becoming ever more achievable due to advances such as those presented in this thesis. These challenges, along with the rapid pace of technological developments, make it an exciting time to work in power systems.

List of Publications

1. A. Attarha, S. M. Noori R. A., P. Scott, S. Thiébaux, "Network-Secure Envelopes Enabling Reliable DER Bidding in Energy and Reserve Markets," IEEE Transactions on Smart Grid. Jan. 2022.
2. A. Attarha, P. Scott, J. Iria, S. Thiébaux, "Network-Secure and Price-Elastic Aggregator Bidding in Energy and Reserve Markets," IEEE Transactions on Smart Grid. 2021.
3. A. Attarha, P. Scott, S. Thiébaux, "Network-aware co-optimisation of residential DER in energy and FCAS markets," Electric Power Systems Research, Dec. 2020
4. A. Attarha, P. Scott, S. Thiébaux, "Network-aware Participation of Aggregators in NEM Energy and FCAS Markets," Proceedings of the Eleventh ACM International Conference on Future Energy Systems June 2020.
5. A. Attarha, P. Scott, S. Thiébaux, "Affinely Adjustable Robust ADMM for Residential DER Coordination in Distribution Networks," IEEE Transactions on Smart Grid Sept. 2019

Other Publications

1. J. Iria, P. Scott, A. Attarha, D. Gordon, E. Franklin, "MV-LV network-secure bidding optimisation of an aggregator of prosumers in real-time energy and reserve markets," Energy, 2022.
2. S. M. Noori R. A., A. Attarha, P. Scott, S. Thiébaux, "Affinely Adjustable Robust Volt/Var Control for Distribution Systems with High PV penetration," IEEE Transactions on Power Systems, 2021.
3. J. Iria, P. Scott, A. Attarha, "Network-constrained bidding optimization strategy for aggregators of prosumers," Energy, Sept. 2020.

Appendix A

Test Systems and Data

This Appendix presents the test systems and the data used in this thesis for our experiments. This includes our network test systems in Section A.1; our consumer data in Section A.2; our market prices, both forecasts and realisations, in Section A.3; and finally our proof, showing the effectiveness of envelopes for balance radial networks in Section A.4.

A.1 Network Test Systems

We use a 69 bus distribution network test system Savier and Das [2007] to evaluate the performance of our approaches throughout this thesis. Figure A.1 shows the configuration of the 69-bus distribution network test system Savier and Das [2007]. We modify the 69-bus distribution network with three consumers at each node, i.e., a total of 207 consumers for chapters 3–5, and with five consumers at each node, i.e., a total of 345 consumers for comparisons in Chapter 5.

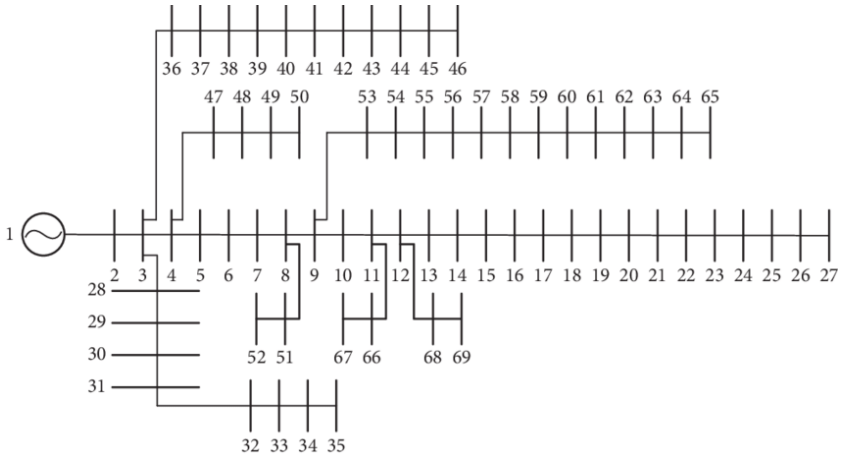

Figure A.1: 69-bus distribution system

A.2 Consumer Data

We utilise 5 kW rooftop PV, and 5 kW / 10 kWh batteries with round-trip efficiencies of $\eta^2 = 90\%$, at a subset of the consumers. We use anonymised solar and demand data for 27 consumers, each consuming 20 kWh per day on average, in Tasmania, Australia, provided by Reposit Power CONSORT [2019], and randomly assign this data to the consumers in our networks.

A.3 Market Prices

We take the 5-minute wholesale energy, and FCAS market prices from AEMO AEMO [2020]. These data are for the NSW region on 22 Feb 2020. Forecast and market clearing prices (MCP) for energy and FCAS markets are shown in figures A.2, and A.3, respectively.

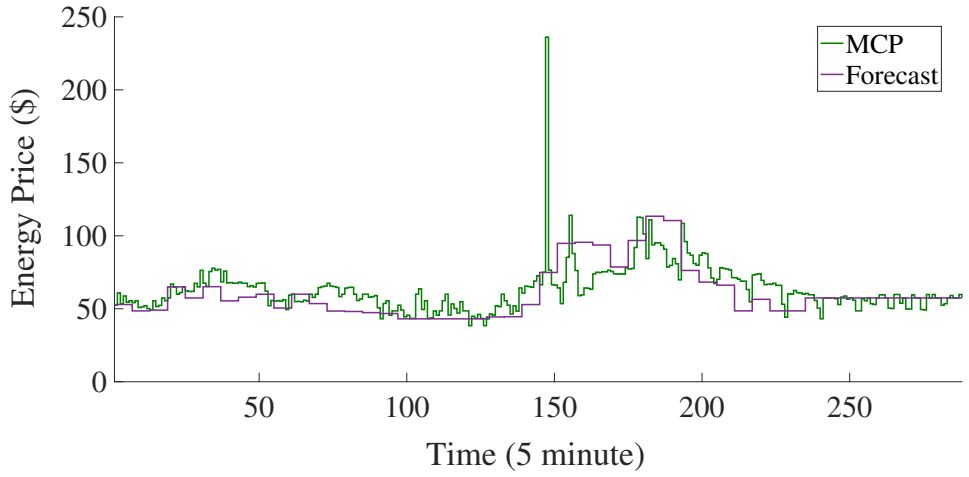

Figure A.2: Energy market prices, forecast vs. market clearing

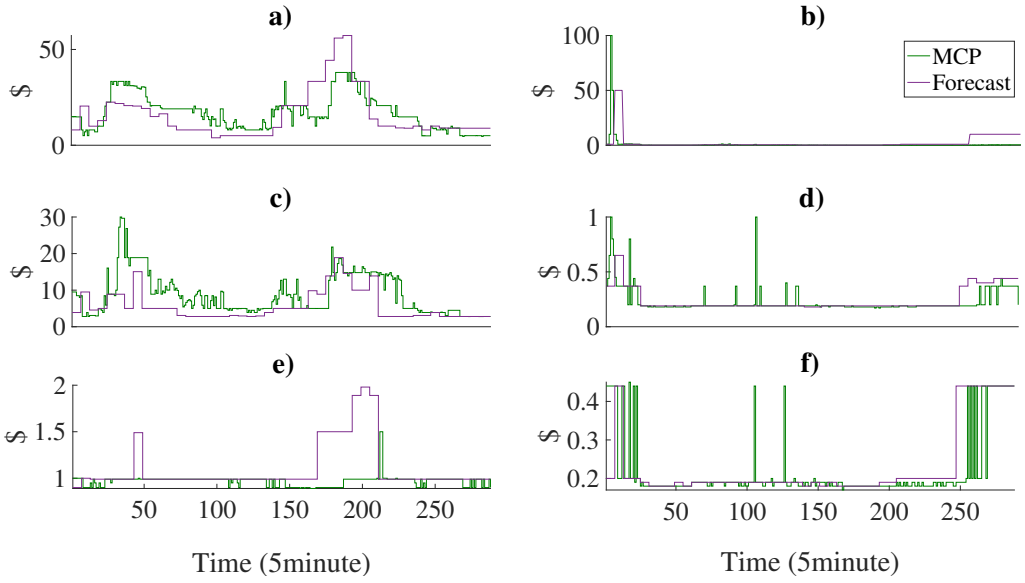

Figure A.3: FCAS market prices, forecast vs. market clearing: y axis in figure a) shows 6 second raise FCAS; in b) shows 6 second lower FCAS; in c) shows 60 second raise FCAS; in d) shows 60 second lower FCAS; in e) shows 5 minute raise FCAS; in f) shows 5 minute lower FCAS

A.4 Proofs

The goal of this proof is to show that in a radial balanced network that is operated in the voltage-stable region, solving two OPFs (for extremes) is sufficient to obtain feasible envelopes.

We first begin by linearising the power flow equations about an operating

point, which in our case can be considered the forecast values. Let $\tilde{V}_i$ denote the voltage magnitude at node i at an initial operating point, and let Δp_i denote the deviation of real power injection at node i from its value at that operating point. Also, let matrices K^p_{ij} denote the voltage magnitude sensitivity of node i to real power injection at node j. Assuming zero reactive power changes[1], we write the following relation:

$$V_i = \tilde{V}_i + \sum_{j=1}^{n} K^p_{ij} \Delta p_j, \tag{A.1}$$

where V_i denotes the voltage magnitude at node i, and n is the number of nodes in the network. We wish to obtain the conditions under which the voltage magnitude at all the nodes stays within a desired bound for all realisations of the nodal real power deviations within a box uncertainty set. More formally:

$$\underline{V_i} \leq \tilde{V}_i + \sum_{j=1}^{n} K^p_{ij} \Delta p_j \leq \overline{V_i} \qquad \forall \Delta p_j \in \mathcal{U}_j,\ \forall i \in \{1, ..., n\}. \tag{A.2}$$

where $\mathcal{U}_j = [\underline{\Delta p_j}\ ,\ \overline{\Delta p_j}]$, and $\underline{V_i}$ and $\overline{V_i}$ denote the acceptable lower and upper voltage limits at note i, respectively. Using *max* and *min* protect functions, we rewrite (A.2) as the followings:

$$\tilde{V}_i + \max_{\Delta p_j \in \mathcal{U}_j} \{\sum_{j=1}^{n} K^p_{ij} \Delta p_j\} \leq \overline{V_i} \tag{A.3a}$$

$$\tilde{V}_i + \min_{\Delta p_j \in \mathcal{U}_j} \{\sum_{j=1}^{n} K^p_{ij} \Delta p_j\} \geq \underline{V_i} \tag{A.3b}$$

We now assume that K^p_{ij} is a non-negative matrix, i.e., we assume that all its elements are equal to or greater than zero (we will get back to the requirements for this assumption to hold). Thus, we rewrite (A.3) as the following:

$$\tilde{V}_i + \sum_{j=1}^{n} K^p_{ij} \overline{\Delta p_j} \leq \overline{V_i} \tag{A.4a}$$

$$\tilde{V}_i + \sum_{j=1}^{n} K^p_{ij} \underline{\Delta p_j} \geq \underline{V_i}. \tag{A.4b}$$

Hence under the assumption that K^p_{ij} is a non-negative matrix, to make sure

[1]Notice that the same proof holds when the reactive power is included. The reason is that the reactive power is controllable in our work and only is meant to improve the voltage profile.

that all the combinations of real power deviations will not lead to voltage violations, we only need to check for the two scenarios where all the injections are simultaneously on either the maximum or minimum side of uncertainty set $\mathcal{U}_j$.

We now check the requirements for our assumption. Based on voltage stability definition Kundur et al. [1994], if the sensitivity of voltage magnitude to real power injection becomes negative, the system is voltage unstable. Hence our first requirement is that we work in a voltage-stable operating region, which is a fair assumption in a power system operation setting.

Notice that in the stability argument, we are only looking at the diagonal elements in the sensitivity matrix. For the rest of the elements in the sensitivity matrix, we look at the physical structure of nodal connections. For a radial network, neglecting the higher order real and reactive power loss terms, we can write the power flow equations as in (13). As shown in Farivar et al. [2013], this approximation introduces a small relative error of at most 0.25% if there is a 5% deviation in voltage magnitude.

$$V_i = V_0 + \sum_j R_{ij} p_j, \tag{A.5}$$

where V_0 denotes the voltage magnitude at the slack node, and R_{ij} denotes the resistance of the direct path between nodes i and j. Comparing (A.5) and (A.1), we can see that R_{ij} is an approximation of K^p_{ij}, and indeed, is equal to it when we are linearising the power flow equation at the no-load condition Jabr [2019]. Notice that since the elements in R are the summation of positive resistance of the lines on the path between the nodes, they all have positive values. Hence, in radial systems, the assumption of non-negative sensitivity is valid.

In the (weakly-) mesh networks, however, while the diagonal elements are positive in a voltage stable operating point Kundur et al. [1994], we could not find a general approximation of the non-diagonal elements in the sensitivity matrix. In all of our experiments in the mesh networks, we got non-negative sensitivity matrices when we were operating in voltage-stable conditions. Nevertheless, we leave this analysis to future work and here only argue that our approach will work in the radial systems.

Bibliography

Abadi, S. M. N. R.; Attarha, A.; Scott, P. M.; and Thiebaux, S., 2020. Affinely adjustable robust Volt/Var control for distribution systems with high PV penetration. *IEEE Transactions on Power Systems*, (2020).

AEMC, 2017. The Frequency operating standard. `https://www.aemc.gov.au`.

AEMO, 2020. Australian Energy Market Operator. `http://www.aemo.com.au`.

AEMO and ENA, 2018. Open energy networks consultation paper. *Energy Networks Australia*, (2018).

AEMO and Energy Networks Australia, 2019. Open energy networks–interim report: Required capabilities and recommended actions. Technical report, ARENA. Https://www.energynetworks.com.au/projects/open-energy-networks/.

Agarwal, A. and Duchi, J. C., 2011. Distributed delayed stochastic optimization. *Advances in neural information processing systems*, 24 (2011).

Aghamohammadi, M. R. and Abdolahinia, H., 2014. A new approach for optimal sizing of battery energy storage system for primary frequency control of islanded microgrid. *International Journal of Electrical Power & Energy Systems*, 54 (2014), 325–333.

Amin, M. R.; Negnevitsky, M.; Franklin, E.; and Naderi, S. B., 2019. Frequency response of synchronous generators and battery energy storage systems: a comparative study. In *2019 29th Australasian Universities Power Engineering Conference (AUPEC)*, 1–6. IEEE.

Arteaga, J. and Zareipour, H., 2019. A price-maker/price-taker model for the operation of battery storage systems in electricity markets. *IEEE Transactions on Smart Grid*, (2019).

Attarha, A.; Amjady, N.; and Conejo, A. J., 2018a. Adaptive robust ac optimal power flow considering load and wind power uncertainties. *International Journal of Electrical Power & Energy Systems*, 96 (2018), 132–142.

Attarha, A.; Amjady, N.; and Dehghan, S., 2018b. Affinely adjustable robust bidding strategy for a solar plant paired with a battery storage. *IEEE Transactions on Smart Grid*, 10, 3 (2018), 2629–2640.

Attarha, A.; Amjady, N.; Dehghan, S.; and Vatani, B., 2018c. Adaptive robust self-scheduling for a wind producer with compressed air energy storage. *IEEE Transactions on Sustainable Energy*, 9, 4 (2018), 1659–1671.

Attarha, A.; Scott, P.; and Thiébaux, S., 2019. Affinely adjustable robust ADMM for residential der coordination in distribution networks. *IEEE Transactions on Smart Grid*, (2019).

Attarha, A.; Scott, P.; and Thiébaux, S., 2020. Network-aware co-optimisation of residential der in energy and fcas markets. *PSCC 2020*, (2020).

Babaei, S.; Zhao, C.; and Fan, L., 2019. A data-driven model of virtual power plants in day-ahead unit commitment. *IEEE Transactions on Power Systems*, 34, 6 (2019), 5125–5135.

Bahramara, S.; Yazdani-Damavandi, M.; Contreras, J.; Shafie-Khah, M.; and Catalão, J. P., 2017. Modeling the strategic behavior of a distribution company in wholesale energy and reserve markets. *IEEE Transactions on Smart Grid*, 9, 4 (2017), 3857–3870.

Bai, L.; Wang, J.; Wang, C.; Chen, C.; and Li, F., 2017. Distribution locational marginal pricing (dlmp) for congestion management and voltage support. *IEEE Transactions on Power Systems*, 33, 4 (2017), 4061–4073.

Ben-Tal, A.; Goryashko, A.; Guslitzer, E.; and Nemirovski, A., 2004. Adjustable robust solutions of uncertain linear programs. *Mathematical Programming*, 99, 2 (2004), 351–376.

Berger, A. W. and Schweppe, F. C., 1989. Real time pricing to assist in load frequency control. *IEEE Power Engineering Review*, 9, 8 (1989), 38–38. doi:10.1109/MPER.1989.4310876.

Bertsimas, D. and Tsitsiklis, J. N., 1997. *Introduction to linear optimization*, vol. 6. Athena Scientific Belmont, MA.

Blackhall, L., 2020. On the calculation and use of dynamic operating envelopes. *https://arena.gov.au/projects/evolve-der-project*, (2020).

Borsche, T.; Ulbig, A.; Koller, M.; and Andersson, G., 2013. Power and energy capacity requirements of storages providing frequency control reserves. In *Power and Energy Society General Meeting (PES), 2013 IEEE*, 1–5. IEEE.

Boyd, S.; Parikh, N.; Chu, E.; Peleato, B.; Eckstein, J.; et al., 2011. Distributed optimization and statistical learning via the alternating direction method of multipliers. *Foundations and Trends® in Machine learning*, 3, 1 (2011), 1–122.

Burger, S.; Chaves-Avila, J. P.; Batlle, C.; and Pérez-Arriaga, I. J., 2016. The value of aggregators in electricity systems. *MIT Center for Energy and Environmental Policy Research*, (2016).

Callaway, D. S., 2011. Can smaller loads be profitably engaged in power system services? In *2011 IEEE Power and Energy Society General Meeting*, 1–3. IEEE.

Callaway, D. S. and Hiskens, I. A., 2010. Achieving controllability of electric loads. *Proceedings of the IEEE*, 99, 1 (2010), 184–199.

Capitanescu, F., 2018. Tso–dso interaction: Active distribution network power chart for tso ancillary services provision. *Electric Power Systems Research*, 163 (2018), 226–230.

Caramanis, M. C. and Foster, J. M., 2011. Uniform and complex bids for demand response and wind generation scheduling in multi-period linked transmission and distribution markets. In *2011 50th IEEE Conference on Decision and Control and European Control Conference*, 4340–4347. IEEE.

Chachuat, B., 2019. Mixed-integer linear programming (milp): Model formulation. *McMaster University Department of Chemical Engineering*, 17 (2019).

Chen, L.; Zhao, X.; Li, D.; Li, J.; and Ai, Q., 2020. Optimal bidding strategy for virtual power plant using information gap decision theory. In *2020 5th Asia Conference on Power and Electrical Engineering (ACPEE)*, 122–128. IEEE.

CONSORT, 2019. Reposit Power. `http://www.repositpower.com`.

Cplex, I. I., 2009. V12. 1: User's manual for cplex. *International Business Machines Corporation*, 46, 53 (2009), 157.

Dall'Anese, E.; Guggilam, S. S.; Simonetto, A.; Chen, Y. C.; and Dhople, S. V., 2017. Optimal regulation of virtual power plants. *IEEE Transactions on Power Systems*, 33, 2 (2017), 1868–1881.

De Carvalho, W.; Ratnam, E. L.; Blackhall, L.; and Von Meier, A., 2022. Optimization-based operation of distribution grids with residential battery storage: Assessing utility and customer benefits. *IEEE Transactions on Power Systems*, (2022).

de Klerk, E.; Kuhn, D.; and Postek, K., 2020. Distributionally robust optimization with polynomial densities: theory, models and algorithms. *Mathematical Programming*, 181, 2 (2020), 265–296.

Delfino, B.; Massucco, S.; Morini, A.; Scalera, P.; and Silvestro, F., 2001. Implementation and comparison of different under frequency load-shedding schemes. In *2001 Power Engineering Society Summer Meeting. Conference Proceedings (Cat. No.01CH37262)*, vol. 1, 307–312 vol.1. doi:10.1109/PESS.2001.970031.

Dozein, M. G. and Mancarella, P., 2019. Frequency response capabilities of utility-scale battery energy storage systems, with application to the august 2018 separation event in australia. In *2019 9th International Conference on Power and Energy Systems (ICPES)*, 1–6. IEEE.

Dunning, I.; Huchette, J.; and Lubin, M., 2017. Jump: A modeling language for mathematical optimization. *SIAM Review*, 59, 2 (2017), 295–320. doi:10.1137/15M1020575.

Ela, E.; Milligan, M.; and Kirby, B., 2011. Operating reserves and variable generation. Technical report, National Renewable Energy Lab.(NREL), Golden, CO (United States).

Engelmann, A.; Mühlpfordt, T.; Jiang, Y.; Houska, B.; and Faulwasser, T., 2017. Distributed ac optimal power flow using aladin. *IFAC-PapersOnLine*, 50, 1 (2017), 5536–5541.

Esfahani, P. M. and Kuhn, D., 2018. Data-driven distributionally robust optimization using the wasserstein metric: Performance guarantees and tractable reformulations. *Mathematical Programming*, 171, 1 (2018), 115–166.

Farivar, M.; Chen, L.; and Low, S., 2013. Equilibrium and dynamics of local voltage control in distribution systems. In *52nd IEEE Conference on Decision and Control*, 4329–4334. IEEE.

Farivar, M. and Low, S. H., 2013. Branch flow model: Relaxations and convexification—part i. *IEEE Transactions on Power Systems*, 28, 3 (2013), 2554–2564.

Feltes, J. W.; Fernandes, B. S.; and Senthil, J., 2014. Development of a controller to provide primary frequency response capability for a wind farm. In *2014 IEEE PES General Meeting— Conference & Exposition*, 1–5. IEEE.

Gao, G.; Lo, K.; and Lu, J., 2017a. Risk assessment due to electricity price forecast uncertainty in uk electricity market. In *2017 52nd International Universities Power Engineering Conference (UPEC)*, 1–6. IEEE.

Gao, H.; Liu, J.; Wang, L.; and Wei, Z., 2017b. Decentralized energy management for networked microgrids in future distribution systems. *IEEE Transactions on Power Systems*, 33, 4 (2017), 3599–3610.

Giraldo, J. S.; Castrillon, J. A.; López, J. C.; Rider, M. J.; and Castro, C. A., 2018. Microgrids energy management using robust convex programming. *IEEE Transactions on Smart Grid*, (2018).

González, P.; Villar, J.; Díaz, C. A.; and Campos, F. A., 2014. Joint energy and reserve markets: Current implementations and modeling trends. *Electric Power Systems Research*, 109 (2014), 101–111.

Good, N. and Mancarella, P., 2017. Flexibility in multi-energy communities with electrical and thermal storage: A stochastic, robust approach for multi-service demand response. *IEEE Transactions on Smart Grid*, 10, 1 (2017), 503–513.

Gurobi Optimization, LLC, 2022. Gurobi Optimizer Reference Manual. `https://www.gurobi.com`.

Haghifam, S.; Laaksonen, H.; and Shafie-khah, M., 2021. Integration of ders in the aggregator platform for the optimal participation in wholesale and local electricity markets. (2021).

Harrison, P., 1980. Considerations when planning a load-shedding program. *BROWN BOVERI REVIEW*, 67, 10 (1980), 593–598.

He, C.; Wu, L.; Liu, T.; and Shahidehpour, M., 2017. Robust co-optimization scheduling of electricity and natural gas systems via admm. *IEEE Transactions on Sustainable Energy*, 8, 2 (2017), 658–670.

Herrero, I.; Rodilla, P.; and Batlle, C., 2020. Evolving bidding formats and pricing schemes in usa and europe day-ahead electricity markets. *Energies*, 13, 19 (2020), 5020.

Hong, M.; Luo, Z.-Q.; and Razaviyayn, M., 2016. Convergence analysis of alternating direction method of multipliers for a family of nonconvex problems. *SIAM Journal on Optimization*, 26, 1 (2016), 337–364.

Huang, S.; Wu, Q.; Oren, S. S.; Li, R.; and Liu, Z., 2014. Distribution locational marginal pricing through quadratic programming for congestion management in distribution networks. *IEEE Transactions on Power Systems*, 30, 4 (2014), 2170–2178.

Iria, J.; Scott, P.; and Attarha, A., 2020. Network-constrained bidding optimization strategy for aggregators of prosumers. *Energy*, 207 (2020), 118266.

Iria, J.; Scott, P.; Attarha, A.; Gordon, D.; and Franklin, E., 2022. Mv-lv network-secure bidding optimisation of an aggregator of prosumers in real-time energy and reserve markets. *Energy*, 242 (2022), 122962.

Iria, J.; Soares, F.; and Matos, M., 2019. Optimal bidding strategy for an aggregator of prosumers in energy and secondary reserve markets. *Applied Energy*, 238 (2019), 1361–1372.

Iria, J. P.; Soares, F. J.; and Matos, M. A., 2018. Trading small prosumers flexibility in the energy and tertiary reserve markets. *IEEE Transactions on Smart Grid*, 10, 3 (2018), 2371–2382.

Iweh, C. D.; Gyamfi, S.; Tanyi, E.; and Effah-Donyina, E., 2021. Distributed generation and renewable energy integration into the grid: Prerequisites, push factors, practical options, issues and merits. *Energies*, 14, 17 (2021), 5375.

Jabr, R. A., 2019. Robust volt/var control with photovoltaics. *IEEE Transactions on Power Systems*, 34, 3 (2019), 2401–2408.

Jabr, R. A., 2020. Segregated linear decision rules for inverter watt-var control. *IEEE Transactions on Power Systems*, (2020), 1–1. doi:10.1109/TPWRS.2020.3032467.

Karlof, J. K., 2005. *Integer programming: theory and practice*. CRC Press.

Kasari, P. R. and Bhattacharjee, S., 2020. A modified control approach for voltage source converter to regulate voltage and power flow in distribution network. In *2020 IEEE Region 10 Symposium (TENSYMP)*, 872–875. IEEE.

Kazemi, M.; Zareipour, H.; Amjady, N.; Rosehart, W. D.; and Ehsan, M., 2017. Operation scheduling of battery storage systems in joint energy and ancillary services markets. *IEEE Transactions on Sustainable Energy*, 8, 4 (2017), 1726–1735.

Kundur, P.; Prabha; Balu, N. J.; and Lauby, M. J., 1994. *Power system stability and control*, vol. 7. McGraw-hill New York.

Lee, D.; Nguyen, H. D.; Dvijotham, K.; and Turitsyn, K., 2019. Convex restriction of power flow feasibility sets. *IEEE Transactions on Control of Network Systems*, 6, 3 (2019), 1235–1245.

Lee, S.-J.; Kim, J.-H.; Kim, C.-H.; Kim, S.-K.; Kim, E.-S.; Kim, D.-U.; Mehmood, K. K.; and Khan, S. U., 2016. Coordinated control algorithm for distributed battery energy storage systems for mitigating voltage and frequency deviations. *IEEE Trans. Smart Grid*, 7, 3 (2016), 1713–1722.

Li, B.; Jiang, R.; and Mathieu, J. L., 2019. Distributionally robust chance-constrained optimal power flow assuming unimodal distributions with misspecified modes. *IEEE Transactions on Control of Network Systems*, 6, 3 (2019), 1223–1234.

Liu, M. Z.; Procopiou, A. T.; Petrou, K.; Ochoa, L. F.; Langstaff, T.; Harding, J.; and Theunissen, J., 2020. On the fairness of pv curtailment schemes in residential distribution networks. *IEEE Transactions on Smart Grid*, (2020).

Liu, R.-S. and Hsu, Y.-F., 2018. A scalable and robust approach to demand side management for smart grids with uncertain renewable power generation and bi-directional energy trading. *International Journal of Electrical Power & Energy Systems*, 97 (2018), 396–407.

Ma, Z.; Callaway, D. S.; and Hiskens, I. A., 2011. Decentralized charging control of large populations of plug-in electric vehicles. *IEEE Transactions on control systems technology*, 21, 1 (2011), 67–78.

Mahmoodi, M.; Attarha, A.; RA, S. M. N.; Scott, P.; and Blackhall, L., 2022. Adjustable robust approach to increase dg hosting capacity in active distribution systems. *Electric Power Systems Research*, 211 (2022), 108347.

Markovic, U.; Kaffe, E.; Mountouri, D.; Kienzle, F.; Karagiannopoulos, S.; and Ulbig, A., 2016. The future role of a DSO in distribution networks with high penetration of flexible prosumers. (2016).

Mashhour, E. and Moghaddas-Tafreshi, S. M., 2010. Bidding strategy of virtual power plant for participating in energy and spinning reserve markets—part i: Problem formulation. *IEEE Transactions on Power Systems*, 26, 2 (2010), 949–956.

Mercier, P.; Cherkaoui, R.; and Oudalov, A., 2009. Optimizing a battery energy storage system for frequency control application in an isolated power system. *IEEE Transactions on Power Systems*, 24, 3 (2009), 1469–1477.

Meyn, S. and Busic, A., 2020. Using loads with discrete finite states of power to provide ancillary services for a power grid. US Patent 10,692,158.

Mhanna, S.; Verbič, G.; and Chapman, A. C., 2019. Adaptive ADMM for distributed AC optimal power flow. *IEEE Transactions on Power Systems*, 34, 3 (2019), 2025–2035.

Mieth, R. and Dvorkin, Y., 2018. Data-driven distributionally robust optimal power flow for distribution systems. *IEEE Control Systems Letters*, 2, 3 (2018), 363–368.

Milford, T. and Krause, O., 2021. Managing der in distribution networks using state estimation & dynamic operating envelopes. In *2021 IEEE PES Innovative Smart Grid Technologies-Asia (ISGT Asia)*, 1–5. IEEE.

Mohiti, M.; Monsef, H.; Anvari-Moghaddam, A.; Guerrero, J.; and Lesani, H., 2019. A decentralized robust model for optimal operation of distribution companies with private microgrids. *International Journal of Electrical Power & Energy Systems*, 106 (2019), 105–123.

Molina-Garcia, A.; Bouffard, F.; and Kirschen, D. S., 2010. Decentralized demand-side contribution to primary frequency control. *IEEE Transactions on Power Systems*, 26, 1 (2010), 411–419.

Morgan, M. G. and Talukdar, S. N., 1979. Electric power load management: Some technical, economic, regulatory and social issues. *Proceedings of the IEEE*, 67, 2 (1979), 241–312.

Mousavi, M. and Wu, M., 2021a. A dso framework for market participation of der aggregators in unbalanced distribution networks. *IEEE Transactions on Power Systems*, (2021).

Mousavi, M. and Wu, M., 2021b. A two-stage stochastic programming dso framework for comprehensive market participation of der aggregators under uncertainty. In *2020 52nd North American Power Symposium (NAPS)*, 1–6. IEEE.

Nazir, M., 2020. *Coordination and Control of Distributed Energy Resources: Modeling and Analysis Techniques*. Ph.D. thesis.

Nazir, N. and Almassalkhi, M., 2019. Convex inner approximation of the feeder hosting capacity limits on dispatchable demand. In *2019 IEEE 58th Conference on Decision and Control (CDC)*, 4858–4864. IEEE.

Nazir, N. and Almassalkhi, M., 2020. Voltage positioning using co-optimization of controllable grid assets in radial networks. *IEEE Transactions on Power Systems*, 36, 4 (2020), 2761–2770.

Nazir, N. and Almassalkhi, M., 2021. Grid-aware aggregation and realtime disaggregation of distributed energy resources in radial networks. *IEEE Transactions on Power Systems*, (2021).

Neidhöfer, G., 2011. 50-hz frequency [history]. *IEEE Power and Energy Magazine*, 9, 4 (2011), 66–81.

Neyestani, N.; Damavandi, M. Y.; Shafie-Khah, M.; Bakirtzis, A. G.; and Catalão, J. P., 2016. Plug-in electric vehicles parking lot equilibria with energy and reserve markets. *IEEE Transactions on Power Systems*, 32, 3 (2016), 2001–2016.

Nezamabadi, H. and Nazar, M. S., 2016. Arbitrage strategy of virtual power plants in energy, spinning reserve and reactive power markets. *IET Generation, Transmission & Distribution*, 10, 3 (2016), 750–763.

Nirenberg, S. A.; McInnis, D.; and Sparks, K., 1992. Fast acting load shedding. *IEEE Transactions on Power Systems*, 7, 2 (1992), 873–877.

Olivella-Rosell, P.; Bullich-Massagué, E.; Aragüés-Peñalba, M.; Sumper, A.; Ottesen, S. Ø.; Vidal-Clos, J.-A.; and Villafáfila-Robles, R., 2018. Optimization problem for meeting distribution system operator requests in local flexibility markets with distributed energy resources. *Applied energy*, 210 (2018), 881–895.

Operator, A. E. M., 2015. Guide to ancillary services in the national electricity market. *Australian Energy Market Operator: Melbourne, Australia*, (2015).

Ottesen, S. Ø.; Tomasgard, A.; and Fleten, S.-E., 2018. Multi market bidding strategies for demand side flexibility aggregators in electricity markets. *Energy*, 149 (2018), 120–134.

Oudalov, A.; Chartouni, D.; and Ohler, C., 2007. Optimizing a battery energy storage system for primary frequency control. *IEEE Transactions on Power Systems*, 22, 3 (2007), 1259–1266.

Oudalov, A.; Chartouni, D.; Ohler, C.; and Linhofer, G., 2006. Value analysis of battery energy storage applications in power systems. In *Power Systems Conference and Exposition, 2006. PSCE'06. 2006 IEEE PES*, 2206–2211. IEEE.

Papadimitriou, C. H. and Steiglitz, K., 1998. *Combinatorial optimization: algorithms and complexity*. Courier Corporation.

Petrou, K.; Liu, M. Z.; Procopiou, A. T.; Ochoa, L. F.; Theunissen, J.; and Harding, J., 2020. Operating envelopes for prosumers in LV networks: A weighted proportional fairness approach. In *2020 IEEE PES Innovative Smart Grid Technologies Europe (ISGT-Europe)*, 579–583. IEEE.

Petrou, K.; Procopiou, A. T.; Gutierrez-Lagos, L.; Liu, M. Z.; Ochoa, L. F.; Langstaff, T.; and Theunissen, J., 2021. Ensuring distribution network integrity using dynamic operating limits for prosumers. *IEEE Transactions on Smart Grid*, (2021).

Phan, D. and Ghosh, S., 2014. Two-stage stochastic optimization for optimal power flow under renewable generation uncertainty. *ACM Transactions on Modeling and Computer Simulation (TOMACS)*, 24 (2014).

Poolla, B. K.; Hota, A. R.; Bolognani, S.; Callaway, D. S.; and Cherukuri, A., 2020. Wasserstein distributionally robust look-ahead economic dispatch. *IEEE Transactions on Power Systems*, 36, 3 (2020), 2010–2022.

RA, S. M. N.; Scott, P.; Mahmoodi, M.; and Attarha, A., 2022. Data-driven adjustable robust solution to voltage-regulation problem in pv-rich distribution systems. *International Journal of Electrical Power & Energy Systems*, 141 (2022), 108118.

Rahimi, F. and Ipakchi, A., 2010. Demand response as a market resource under the smart grid paradigm. *IEEE Transactions on Smart Grid*, 1, 1 (2010), 82–88. doi:10.1109/TSG.2010.2045906.

Ricciardi, T. R.; Petrou, K.; Franco, J. F.; and Ochoa, L. F., 2018. Defining customer export limits in pv-rich low voltage networks. *IEEE Transactions on Power Systems*, 34, 1 (2018), 87–97.

Riesz, J.; Gilmore, J.; and MacGill, I., 2015. Frequency control ancillary service market design: Insights from the australian national electricity market. *The Electricity Journal*, 28, 3 (2015), 86–99.

Ross, S. and Mathieu, J., 2021. Strategies for network-safe load control with a third-party aggregator and a distribution operator. *IEEE Transactions on Power Systems*, 36, 4 (2021), 3329–3339.

Ross, S. C. and Mathieu, J. L., 2020. A method for ensuring a load aggregator's power deviations are safe for distribution networks. *Electric Power Systems Research*, 189 (2020), 106781.

Ross, S. C.; Ozay, N.; and Mathieu, J. L., 2019. Coordination between an aggregator and distribution operator to achieve network-aware load control. In *2019 IEEE Milan PowerTech*, 1–6. IEEE.

Ruibal, C. M. and Mazumdar, M., 2008. Forecasting the mean and the variance of electricity prices in deregulated markets. *IEEE Transactions on Power Systems*, 23, 1 (2008), 25–32.

Saint-Pierre, A. and Mancarella, P., 2016. Active distribution system management: A dual-horizon scheduling framework for dso/tso interface under uncertainty. *IEEE Transactions on Smart Grid*, 8, 5 (2016), 2186–2197.

Savier, J. and Das, D., 2007. Impact of network reconfiguration on loss allocation of radial distribution systems. *IEEE Transactions on Power Delivery*, 22, 4 (2007), 2473–2480.

Schweppe, F. C.; Tabors, R. D.; Kirtley, J. L.; Outhred, H. R.; Pickel, F. H.; and Cox, A. J., 1980. Homeostatic utility control. *IEEE Transactions on Power Apparatus and Systems*, 9, 3 (1980), 1151–1163.

Scott, P.; Gordon, D.; Franklin, E.; Jones, L.; and Thiébaux, S., 2019. Network-aware coordination of residential distributed energy resources. *IEEE Transactions on Smart Grid*, (2019).

Scott, P. and Thiébaux, S., 2015. Distributed multi-period optimal power flow for demand response in microgrids. In *Proceedings of the 2015 ACM Sixth International Conference on Future Energy Systems*, 17–26. ACM.

Scott, P. M. et al., 2016. Distributed coordination and optimisation of network-aware electricity prosumers. *The Australian National University*, (2016).

Shafiee, S.; Zamani-Dehkordi, P.; Zareipour, H.; and Knight, A. M., 2016. Economic assessment of a price-maker energy storage facility in the alberta electricity market. *Energy*, 111 (2016), 537–547.

Shafiee, S.; Zareipour, H.; and Knight, A. M., 2017. Developing bidding and offering curves of a price-maker energy storage facility based on robust optimization. *IEEE Transactions on Smart Grid*, 10, 1 (2017), 650–660.

Shaloudegi, K.; Madinehi, N.; Hosseinian, S.; and Abyaneh, H. A., 2012. A novel policy for locational marginal price calculation in distribution systems based on loss reduction allocation using game theory. *IEEE transactions on power systems*, 27, 2 (2012), 811–820.

Sharma, K. C.; Bhakar, R.; Tiwari, H.; and Chawda, S., 2017. Scenario based uncertainty modeling of electricity market prices. In *2017 6th International Conference on Computer Applications In Electrical Engineering-Recent Advances (CERA)*, 164–168. IEEE.

Shiina, T. and Birge, J. R., 2004. Stochastic unit commitment problem. *International Transactions in Operational Research*, 11, 1 (2004), 19–32.

Sierksma, G. and Zwols, Y., 2015. *Linear and integer optimization: theory and practice*. CRC Press.

Souza, S. M.; Gil, M.; Sumaili, J.; Madureira, A. G.; and Lopes, J. P., 2016. Operation scheduling of prosumer with renewable energy sources and storage devices. In *2016 13th International Conference on the European Energy Market (EEM)*, 1–5. IEEE.

Srikantha, P. and Mallick, M., 2020. Hidden convexities in decentralized coordination for the distribution networks. *IEEE Transactions on Power Systems*, (2020).

Sun, K. and Sun, X. A., 2021. A two-level admm algorithm for ac opf with global convergence guarantees. *IEEE Transactions on Power Systems*, 36, 6 (2021), 5271–5281.

Świerczyński, M.; Stroe, D. I.; Stan, A. I.; and Teodorescu, R., 2013. Primary frequency regulation with li-ion battery energy storage system: A case study for denmark. In *ECCE Asia Downunder (ECCE Asia), 2013 IEEE*, 487–492. IEEE.

Thorbergsson, E.; Knap, V.; Swierczynski, M.; Stroe, D.; and Teodorescu, R., 2013. Primary frequency regulation with li-ion battery based energy storage system-evaluation and comparison of different control strategies. In *Proc. 35th Int. Telecommun. Energy Conf.'Smart Power and Efficiency'(INTELEC)*, 178–183.

Tsai, C.-H., 2021. Operating reserves in the three most windy us power markets: A technical review. *Renewable and Sustainable Energy Reviews*, 135 (2021), 110190.

Tsai, S.-C.; Tseng, Y.-H.; and Chang, T.-H., 2017. Communication-efficient distributed demand response: A randomized admm approach. *IEEE Transactions on Smart Grid*, 8, 3 (2017), 1085–1095.

Ulbig, A.; Rullan, T.; Koch, S.; and Ferrucci, F., 2016. Assessment of aggregated impacts of prosumer behaviour. (2016).

Ulbig, A. et al., 2022. A stakeholder-oriented multi-criteria optimization model for decentral multi-energy systems. Technical report, arXiv. org.

Vatandoust, B.; Ahmadian, A.; Golka, M.; Elkamel, A.; Almansoori, A.; and Ghaljehei, M., 2018. Risk-averse optimal bidding of electric vehicles and energy storage aggregator in day-ahead frequency regulation market. *IEEE Transactions on Power Systems*, (2018).

Vayá, M. G. and Andersson, G., 2014. Optimal bidding strategy of a plug-in electric vehicle aggregator in day-ahead electricity markets under uncertainty. *IEEE Transactions on Power Systems*, 30, 5 (2014), 2375–2385.

Wang, J.; Shahidehpour, M.; and Li, Z., 2008. Security-constrained unit commitment with volatile wind power generation. *IEEE Transactions on Power Systems*, 23, 3 (2008), 1319–1327.

Wang, Q.; Guan, Y.; and Wang, J., 2011. A chance-constrained two-stage stochastic program for unit commitment with uncertain wind power output. *IEEE transactions on power systems*, 27, 1 (2011), 206–215.

Wang, Y.; Liang, H.; and Dinavahi, V., 2018. Two-stage stochastic demand response in smart grid considering random appliance usage patterns. *IET Generation, Transmission & Distribution*, 12, 18 (2018), 4163–4171.

Wang, Y.; Yin, W.; and Zeng, J., 2019. Global convergence of admm in nonconvex nonsmooth optimization. *Journal of Scientific Computing*, 78, 1 (2019), 29–63.

Wang, Z. and Wang, S., 2013. Grid power peak shaving and valley filling using vehicle-to-grid systems. *IEEE Transactions on Power Delivery*, 28, 3 (2013), 1822–1829. doi:10.1109/TPWRD.2013.2264497.

Weidlich, A.; Künzel, T.; and Klumpp, F., 2018. Bidding strategies for flexible and inflexible generation in a power market simulation model: Model description and findings. In *Proceedings of the Ninth International Conference on Future Energy Systems*, 532–537.

Wu, D.; Yang, T.; Stoorvogel, A. A.; and Stoustrup, J., 2016. Distributed optimal coordination for distributed energy resources in power systems. *IEEE Transactions on Automation Science and Engineering*, 14, 2 (2016), 414–424.

Xu, B.; Oudalov, A.; Poland, J.; Ulbig, A.; and Andersson, G., 2014. Bess control strategies for participating in grid frequency regulation. *IFAC Proceedings Volumes*, 47, 3 (2014), 4024–4029.

Xu, B.; Shi, Y.; Kirschen, D. S.; and Zhang, B., 2018. Optimal battery participation in frequency regulation markets. *IEEE Transactions on Power Systems*, 33, 6 (2018), 6715–6725.

Yan, R.; Saha, T. K.; Bai, F.; Gu, H.; et al., 2018. The anatomy of the 2016 south australia blackout: A catastrophic event in a high renewable network. *IEEE Transactions on Power Systems*, 33, 5 (2018), 5374–5388.

Yang, M.; Wang, Y.; Gao, S.; Zhang, Q.; Li, Z.; and Wang, D., 2021. A bidding model for virtual power plants to participate in demand response in the new power market environment. In *2021 International Conference on Power System Technology (POWERCON)*, 875–882. doi:10.1109/POWERCON53785.2021.9697757.

Yao, E.; Wong, V. W.; and Schober, R., 2018. Optimization of aggregate capacity of pevs for frequency regulation service in day-ahead market. *IEEE Transactions on Smart Grid*, 9, 4 (2018), 3519–3529.

Yuan, Z.; Hesamzadeh, M. R.; and Biggar, D. R., 2016. Distribution locational marginal pricing by convexified acopf and hierarchical dispatch. *IEEE Transactions on Smart Grid*, 9, 4 (2016), 3133–3142.

Zare, A.; Chung, C.; Zhan, J.; and Faried, S. O., 2018. A distributionally robust chance-constrained milp model for multistage distribution system planning with uncertain renewables and loads. *IEEE Transactions on Power Systems*, 33, 5 (2018), 5248–5262.

Zeng, S.; Kody, A.; Kim, Y.; Kim, K.; and Molzahn, D. K., 2022. A reinforcement learning approach to parameter selection for distributed optimal power flow. *Electric Power Systems Research*, 212 (2022), 108546.

Zhang, R. and Kwok, J., 2014. Asynchronous distributed admm for consensus optimization. In *International conference on machine learning*, 1701–1709. PMLR.

Zhang, Y.; Wang, L.; Ding, H.; Zhu, Y.; Hu, Q.; and Lv, Z., 2021a. An overview of virtual power plant prospects from the perspective of optimal scheduling, market bidding and transient analysis. In *2021 IEEE Sustainable Power and Energy Conference (iSPEC)*, 281–286. doi:10.1109/iSPEC53008.2021.9735631.

Zhang, Y.; Xu, D.; Yang, C.; Zhou, X.; Le, Y.; and Tang, J., 2021b. Economic analysis based on virtual power plant's optimal bidding strategy. In *2021 6th International Conference on Power and Renewable Energy (ICPRE)*, 1051–1056. IEEE.

Zhao, Q.; Shen, Y.; and Li, M., 2015. Control and bidding strategy for virtual power plants with renewable generation and inelastic demand in electricity markets. *IEEE Transactions on Sustainable Energy*, 7, 2 (2015), 562–575.

Zhu, D. and Zhang, Y.-J. A., 2019. Optimal coordinated control of multiple battery energy storage systems for primary frequency regulation. *IEEE Transactions on Power Systems*, 34, 1 (2019), 555–565.

Zhu, H. and Li, N., 2016. Asynchronous local voltage control in power distribution networks. In *2016 IEEE International Conference on Acoustics, Speech and Signal Processing (ICASSP)*, 3461–3465. IEEE.